This is to certify that the

thesis entitled

Measurement Of The Effect Of Water Activity On The Rate Of Lipid Oxidation At Constant Oxygen Concentration

presented by

Corey L. Berends

has been accepted towards fulfillment
of the requirements for

M.S. degree in Packaging

Major professor

Date 9/7/93

MEASUREMENT OF THE EFFECT OF WATER ACTIVITY ON THE RATE OF LIPID OXIDATION AT CONSTANT OXYGEN CONCENTRATION

By

Corey L. Berends

A THESIS

Submitted to
Michigan State University
in partial fulfillment of the requirements
for the degree of

MASTER OF SCIENCE

School of Packaging

1993

ABSTRACT

MEASUREMENT OF THE EFFECT OF WATER ACTIVITY ON THE RATE OF LIPID OXIDATION AT CONSTANT OXYGEN CONCENTRATIONS

By

Corey L. Berends

This study was performed to determine the effect of water activity (a_w) on the rate of lipid oxidation in a model food system, using hexanal as the index of oxidation. A continuous flow system was developed to maintain constant oxygen concentrations, water activity (a_w), temperature and light throughout the experiments. Rates showed a decrease as a_w increased, until the B.E.T. monolayer moisture content was reached, where the rates were at a minimum. Rates began to increase as a_w was increased above the a_w corresponding to the monolayer moisture content. The calculation of activation energy (E_a) by an Arrhenius plot showed the rates of hexanal increase were significantly dependent upon temperature, and could be reliably projected to other temperatures.

Dedicated to my parents, Dr. Ernest A. and Mary Jane Berends

ACKNOWLEDGMENTS

Dr. Theron Downes: For his professional advice, patience, understanding, and support while serving as my major advisor.

Dr. Jack Giacin: For his professional guidance, patience, and technical assistance while serving on my committee.

Dr. Rueben Hernandez: For his technical assistance in development of the system and analytical techniques while serving on my committee.

Dr. Ian Gray: For his professional advice and guidance while serving on my committee.

Dr. Heidi Hoojjat: For her technical assistance with analytical methods and instrumentation.

My parents and sisters: For their support and understanding.

Stacey Ann: For her support, patience and understanding.

TABLE OF CONTENTS

LIST OF FIGURES

LIST OF TABLES

NOMENCLATURE

a_o water activity (Eqn. 1)

a_1 constant (Eqns. 2, 3)

AU area units from gas chromatograph (Eqn. 16)

a_w water activity (Eqns. 4, 5, 6, 7, 8, 9, 10, 14)

b_o constant (Eqn. 1)

b_1 constant (Eqn. 2)

b constant (Eqns. 2, 3)

c_1 concentration of volatile compound (Eqn. 3)

c concentration of volatile compound (Eqns. 1, 2, 3)

C constant (Eqns. 9, 10)

°C degrees celcius

C.F. calibration factor (Eqn. 16)

E_a activation energy (Eqn. 19)

H_g micrograms of hexanal (Eqns. 16, 17, 18)

H_l hexanal concentration (micrograms/gram) in linoleic acid (Eqn. 18)

H_p hexanal concentration (micrograms/gram) in product model (Eqn. 17)

IMC initial moisture content (Eqns. 11, 12)

K constant (Eqns. 6, 7, 10)

L_w weight of linoleic acid (Eqn. 18)

M_m, m_1 monolayer moisture content (Eqns. 4, 5)

m water content (gH_2O/g dry) (Eqn. 4)

M_c chen predicted equilibrium moisture content (Eqn. 13)

M_{eq} empirical equilibrium moisture content (Eqns. 6, 7, 8, 9, 10, 12, 13, 14)

n constant (Eqn. 6)

P_f final product weight (Eqn. 12)

P_i initial product weight (Eqn. 12)

P_w product weight (Eqn. 17)

R gas constant (Eqn. 19)

t time (Eqns. 1, 2, 3)

t_b break point (Eqn. 3)

V_i injection volume (Eqn. 16)

V_s sample volume (Eqn. 16)

W_c weight change (Eqn. 11)

W_d weight of dry product (Eqn. 11)

W_m water content corresponding to saturation of all primary adsorption sites by one molecule of water (Eqn. 10)

INTRODUCTION

Lipid oxidation is one of the major causes of deterioration or spoilage in foods. Foods containing oils and fats can, in the presence of oxygen become unacceptable, effectively reducing product shelf-life (Nawar, 1985). Loss of acceptability and/or nutritional value often occurs because of the production of objectionable off-flavor and odor compounds, generally called rancid, from reactions involving oxygen absorption. The production of primary and secondary products (hydroperoxides, free radicals, endoperoxides, malonaldehyde, epoxides, alkanes, alkenes, hydrocarbons, alcohols, and acids) from lipid oxidation are possibly toxic to humans (Ajuyah et al., 1993). The factors which affect the rate of oxygen uptake by food products, such as oxygen concentration, light, temperature, and water activity (a_w) are important for process and product development, packaging and storage (Quast and Karel, 1972).

The effect of headspace oxygen concentration on the rate of lipid oxidation has been well documented (Koelsch et al. 1991; Labuza, 1971). Removal of oxygen from the headspace of a package to create a vacuum or replacing headspace air with nitrogen are verified approaches to extending the induction period of lipid oxidation and prolonging product

shelf-life. However, eliminating oxygen is difficult due to air trapped in internal cavities of a product, package defects (seal integrity, pinholing), and the inability of modern machinery to completely remove oxygen at reasonable rates of production. Even if the concentration of oxygen could be maintained at low levels of approximately 1% or lower, Tamsma et al. (1964) found that for certain products, oxygen concentrations lower than 1% can have a marked effect on the quality of the product (Quast and Karel, 1972).

Temperature and light will increase the rate at which fatty acids are oxidized. Light can be removed with packaging, and temperature is a function of the storage environment and/or processing conditions.

Water activity, defined as the partial pressure of water above a sample divided by the vapor pressure of pure water at the same temperature, has a decisive effect on the oxidative stability of low-moisture foods. Several researchers (Labuza et al.,1969, 1971; Quast and Karel, 1972) have studied the effect of a_w on the rate of oxygen uptake using an oxygen depletion system, called the Warburg apparatus. In this system, rates were not constant due to fluctuating oxygen concentrations. Labuza et al. (1969) found that water exerts a protective effect for dehydrated foods. The rate of oxidation was high at very low a_w and as a_w increased, the rate of oxidation decreased until it reached a minimum, usually between 0.3 and 0.4 a_w. The water content corresponding to this a_w is called the

monolayer moisture content, describing the amount of water needed to form a monolayer over the accessible, highly polar groups of dry matter (Fennema, 1985). The monolayer value provides a good estimate of the water content providing maximum stability for a dry product. The rate of lipid oxidation then begins to increase as the a_w continues to increase above 0.5. Thus, controlling a_w offers a viable approach to stalling the effects of lipid oxidation (Fennema, 1985).

With the knowledge of the rate of lipid oxidation at low oxygen concentrations (1.2%), as provided by Koelsch et al. (1991), accurate knowledge of how the rate is affected by water activity in a dynamic system of constant oxygen concentration is essential in determining the stability of unsaturated fatty acids in a low-moisture food product.

The objectives of this study were to:

1. Develop a continuous flow system to promote lipid oxidation of a product model conditioned to a constant moisture content.
2. Develop a freeze-dried product model using linoleic acid as the oxidizable substrate.
3. Test the system at a variety of constant water activities, using hexanal as the index of oxidation.
4. Determine the rate of lipid oxidation as a function of a_w.

LITERATURE REVIEW

Mechanism of Lipid Oxidation

Karel (1981), Labuza (1971), and Nawar (1985) have discussed the mechanism of lipid oxidation in detail. A brief description of the general scheme follows. Lipid oxidation can occur by both enzymatic and non-enzymatic mechanisms, and is often autocatalytic, meaning the oxidation products themselves catalyze the reaction (Karel, 1981). Oxidation can be catalyzed by autocatalytic reaction products, metal ions, hydroperoxide decomposition or the enzyme lipoxygenase. Metal ions decrease the induction period and reduce the activation energy of the initiation step. Several metal reactions are possible including catalyst decomposition, activation of molecular oxygen possibly to singlet oxygen, and direct radical initiation with substrate. Hydrolysis of the ester bonds in lipids by lipases (lipolysis), results in the liberation of free fatty acids. Free fatty acids are more susceptible to oxidation than fatty acids esterified to glycerol (Nawar, 1985). Autoxidation, considered the main reaction involved in oxidative deterioration of lipids, focuses on a free-radical mechanism. The rate of reaction is affected by water activity (Labuza, 1971; Karel and Yong, 1981), oxygen concentration, temperature (Quast and Karel, 1972), and light.

Autoxidation, the reaction of unsaturated fatty acids

with molecular oxygen, is commonly divided into three stages: initiation, propagation, and termination. Initiation begins with the abstraction of a proton, requiring a high activation energy of 35 kal/mole (Nawar, 1985). Hydrogen atoms, alpha to a carbon-carbon double bond are labile and can easily be removed by a non-enzymatic catalyst. This forms an allylic free radical, forming a resonating structure. Monomolecular decomposition in the initiation stage occurs with the rate proportional to the square root of the extent of oxidation (Karel and Yong, 1972).

The propagation stage begins as molecular oxygen is consumed rapidly by reacting directly with the allylic free radical to form a hydroperoxy radical. The hydroperoxy abstracts a hydrogen atom from another unsaturated fatty acid chain to form an unstable hydroperoxide. The abstraction of the hydrogen atom from the fatty acid creates another free radical to react with oxygen, speeding up the rate of oxidation, and quickly increasing the hydroperoxide concentration. Hydroperoxides are then decomposed to give an aldehyde and an ester, among other compounds. Bimolecular decomposition of hydroperoxides occurs with the rate proportional to peroxide concentration.

In the last stage of autoxidation, termination, allylic free radicals can react in many different ways forming non-radical products which can no longer react with molecular oxygen. The various breakdown products vary widely in their

chemical and physical properties and how they impact flavor. The schematic of lipid oxidation is displayed in Figure 1.

initiation	RH + oxygen + initiator ----> R′+ H
propagation	R′+ oxygen ----> ROO′----> ROOH + R′
termination	R′+ R′----> R-R, non-radical
	ROO′+ ROO′----> ROOR + oxygen, non-radical
	R′+ ROO′----> ROOR, non-radical

Figure 1: Autoxidation Reaction Schematic

Singlet Oxidation

It is also possible for initiation to occur via a reaction of singlet oxygen with C=C bonds in RH and ROOH. Singlet oxygen can be formed through photo-chemical reactions in the presence of a sensitizer (Labuza, 1971). Plant and tissue pigments such as chlorophyll, pheophytin, and myoglobin can act as sensitizers. Trace metals, high temperatures, and UV light have been postulated as possible initiators. Dulog (1964) found the initial rate of autoxidation initiated by singlet state oxygen was at least 10^5 to 10^6 times slower than for monomolecular decomposition at 25°C (Labuza, 1971). Therefore, initiation by singlet oxygen would show long induction periods, especially under conditions protected from UV light. The singlet state oxygen is more electrophilic than triplet state oxygen, reacting approximately 1500 times faster than triplet oxygen with moieties of high electron density, such as C=C bonds.

Hydroperoxides will then cleave to initiate conventional free radical chain reactions (Nawar, 1985).

Formation of hydroperoxides by singlet oxygen proceeds via mechanisms that are different than for free radical autoxidation. Since oxygen is inserted at the ends of the double bond, linoleate produces 9-, 10-, 12-, and 13-hydroperoxides instead of 9-, and 13- from free radical autoxidation. There is general agreement that once the initial hydroperoxides are formed, the free radical chain reaction prevails as the main mechanism. Thus, giving formation of products based on free radical autoxidation (Nawar, 1985).

Breakdown of Linoleic Acid

In linoleic acid the double bonds are located at the 9,12-carbon positions. The most labile hydrogen atom on the 11-carbon is removed and a conjugated free radical structure is formed at the 13- or 9-carbon position in its resonating form.

Hydroperoxides are decomposed to form a number of secondary products, one of which is the saturated aldehyde, hexanal. The 1,4-pentadiene structure of linoleic acid is more susceptible to oxidation (by a factor of 20) than the propene system of oleate. Other secondary products of linoleic acid include 2,4-decadienal, nonanal, and pentane.

2,4-Decadienal and nonanal can be further decomposed to form hexanal, pentane, and various other products (Fennema, 1985).

Kinetics of Lipid Oxidation

Rate of reaction is not a direct function of the degree of unsaturation, but increases rapidly as the number of double bonds increase. The increased rate is due to the sensitivity created by the methyl group between two double bonds. The activated bond once attacked forms a conjugated system which allows for resonance of the free radical and the myriad of products formed. In conditions where oxygen is not limiting, it is assumed that initially all the oxygen reacted is in the form of peroxides. Once the first hydroperoxides are produced, the chain reaction takes over. As each oxygen molecular reacts, one peroxide molecule, [ROOH], is formed (Koelsch et al., 1991).

Monomolecular Rate Period

The monomolecular decomposition of peroxides into free radicals occurs by the time many foods go into storage. A plot of the rate of oxidation vs. square root of the extent should give a straight line up to the point where either the substrate concentration decreases significantly or the peroxides decompose into secondary products (Labuza, 1971). The rate of oxidation for high levels of oxygen in the

headspace, is dependent upon substrate concentration, and independent of oxygen concentration (Labuza, 1971). The breakdown of peroxides is monomolecular, therefore the rate of hexanal production is directly proportional to the peroxide level. This assumes the rate of formation of hexanal to be much faster than the rate of its disappearance, during lipid oxidation (Koelsch et al., 1991).

Bimolecular Decomposition

After monomolecular decomposition where an unsaturated lipid has been oxidized, hydroperoxide concentration builds up to a point at which a change in the initiation mechanism occurs, and peroxides begin to decompose faster than produced. In this period, the rate is directly proportional to the extent of peroxide concentration, assuming the rate of hexanal formation is equivalent to peroxide concentration (Koelsch et al., 1991).

Hall et al. (1985) described the formation of oxidative products as zero order, first order, and so forth. A mathematical model was developed for the overall characterization of the formation of volatile fat oxidation products. It is generally accepted that the reaction has an initial linear phase (zero order), and gradually changes to an exponential phase. The point where the rate of oxidation changes from zero order to first order, the break point, describes the end of the initiation stage (induction period)

and the beginning of the propagation stage. Hall et al. (1985) used the following linear models to describe zero and first order kinetics:

zero order: $c = a_o + b_o t$ (1)

first order: $c = a_1 e^{b1t}$; $\log c = \log a_1 + b_1 t$ (2)

where c =concentration of the volatile compound
t =storage time

A special nonlinear model was developed for applications that includes both zero and first order kinetics (Hall et al., 1985):

$$c = c_1 = a_1 e^{b(t-tb)} \quad ; \; t > t_b \qquad (3)$$

where t_b =break point

Hall et al. (1985) found the nonlinear mixed model offered a better description of the kinetics of fat oxidation than do models for first of zero order kinetics taken separately.

Factors Influencing the Rate of Oxidation

Oxygen concentration, fatty acid composition, water activity, antioxidants, trace metals, temperature and light are factors capable of modifying the rate of lipid oxidation.

Oxygen Concentration

The partial pressure of oxygen in the headspace of a product-package system has a direct effect on the rate of oxidation. At high oxygen concentrations, where the supply of oxygen is unlimited, the rate of oxidation is independent of oxygen pressure, but at very low oxygen pressure the rate is approximately proportional to oxygen pressure (Nawar, 1985). As seen by Koelsch (1989), at low oxygen partial pressures (approximately 1.2%) the rate of reaction was much less than at higher oxygen concentrations (approximately 15.4%). After a certain time period, the rate of lipid oxidation begins to escalate exponentially. Koelsch found the additional time needed for the rate to reach the exponential stage for oxygen concentrations of 1.2% versus 15.4% was 523 hours.

The initiation stage of autoxidation cannot occur in the absence of oxygen. A product-package system could be vacuum packed or nitrogen flushed to remove oxygen from the headspace surrounding the product, preventing autoxidation from occurring. However, even with modern technology, lowering the oxygen concentration to 1% or less is rarely

achieved. If oxygen could be completely eliminated from the environment surrounding a product, cavities within the food product may contain oxygen and this residual internal oxygen can initiate oxidation (Koelsch, 1989). Inadequate packaging, such as an inferior barrier, defective seals, damaged package, or pinholing, could allow oxygen to enter the package and initiate oxidation.

Fatty Acid Composition

Foods contain a mixture of fatty acids that significantly change the food's susceptibility to oxidation (Nawar, 1985). The number, position, and geometry of double bonds of the fatty acids present has a marked effect on the rate of oxidation. Cis or trans configurations, and conjugated double bonds affect the reactivity of the fatty acid. Free fatty acids oxidize at a greater rate than when esterified to a glycerol (Nawar, 1985).

Pro-oxidant Effects

Transition metals, such as copper, cobalt, iron, manganese and nickel have major pro-oxidant effects on the rate of autoxidation. At very low levels of approximately 0.1 ppm, they work to decrease the induction period and increase the rate of oxidation. Trace metals are naturally present in all food tissues, and in most edible oils which come from the soil (Nawar, 1985). Metal ions could also originate from the package (Strasburg, 1992).

Water Activity

The effect of water activity (a_w) on the rate of lipid oxidation has been well documented (Karel and Yong, 1981; Labuza, 1972; Quast and Karel,1972). In dehydrated food systems, water is a major factor in lipid oxidation. Starting at very low a_w values, the rate of oxidation decreases as a_w is increased, until the rate of oxidation reaches a minimum, usually at (0.3-0.4a_w). Further addition of water results in increased rates of oxidation, until high a_w values (0.75-0.85) are reached, when oxidation again decreases. The effect of water activity on the chemical reactions in food systems is described by the "stability map" given in Figure 2, adopted from Labuza (1971).

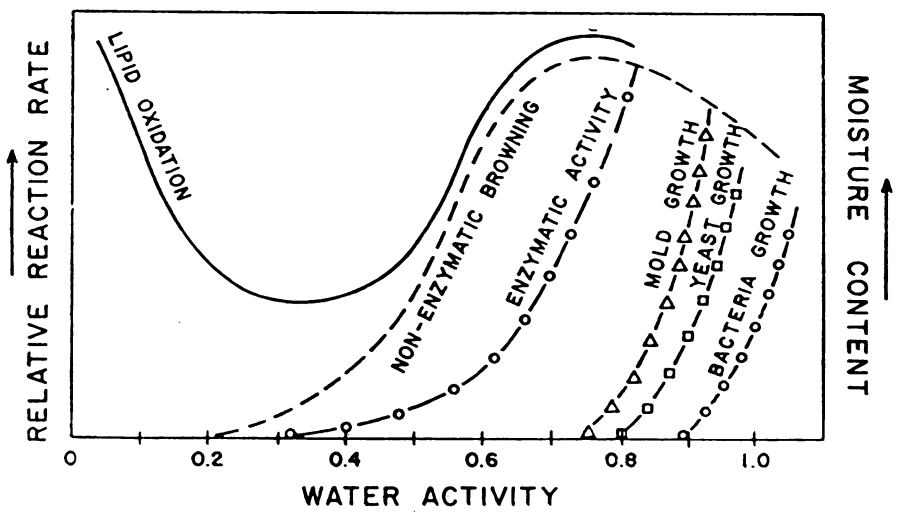

Fig. 2: Effect of Water Activity on the Rate of Chemical Reactions in Foods

The mechanisms by which water exerts its protective effect has been investigated by Labuza et al. (1966), Karel et al. (1967), Karel and Yong (1981). In the range of low a_w (0.0-0.4), water hydrogen-bonds to hydroperoxides produced during the free-radical chain reaction, protecting the hydroperoxides from decomposing, thereby slowing the rate of normal bimolecular decomposition. Water hydrates trace metal catalysts, inhibiting their ability to accelerate the initiation steps, primarily affecting the monomolecular rate period, and possibly decreasing bimolecular decomposition. The presence of water results in quenching of free radicals causing rapid loss, possibly through recombination reactions. Once water content is increased to a level greater than the monolayer coverage, resistance to diffusion decreases and solubilization becomes increasingly significant (Karel and Yong, 1981). At higher a_w values (0.5-0.6) water may accelerate oxidation by inducing swelling of the matrix, exposing additional catalytic sites, or solubilizing catalysts giving increased mobility. When water activity reaches values of 0.75-0.85, catalysts could be diluted retarding the rate of oxidation.

Water activity is a far better indicator of food perishability than water content. Various foods with the same water content vary greatly in perishability. Water associates with nonaqueous constituents with different intensities, contributing to this phenomenon. Water content is therefore not a reliable indicator of perishability

(Fennema, 1985). Water engaging in strong associations is less able to support degradative reactions, such as growth of microorganisms and hydrolytic chemical reactions. Water activity takes this into account. Although the measure of a_w to define food perishability is still not perfect, it correlates well to the rates of many degradative reactions (Fennema, 1985). The relationship between water content and a_w of a product can be described by an equilibrium sorption isotherm.

Monolayer Moisture Content

The moisture content corresponding to the minimum rate of oxidation for a product is called the monolayer value. Monolayer does not mean the coverage of all dry matter with a closely packed single-layer of molecules. Monolayer value is best described as the amount of water needed to form a monolayer over the accessible, highly polar groups of the dry matter (Fennema, 1985). The monolayer value provides a good estimate of the water content providing maximum stability for a dry product. Using the data from the low-moisture end of the isotherm, initial moisture content, and

the Brunauer, Emmett, and Teller (BET) equation (Brunauer, 1938), the monolayer value can easily be determined using the following equation:

$$a_w / m(1-a_w) = 1/m_1c + (c-1/m_1c)a_w \qquad (4)$$

where m = water content (g H_2O/g dry matter)
m_1 = monolayer value
c = constant

The BET equation is a useful compromise between theory and practice for multi-layer models. The equation fits all sigmoid sorption isotherms up to about a_w values of 0.40 (Van den Berg and Bruin, 1981). From this equation, a plot of $a_w/[m(1-a_w)]$ versus a_w, should yield a straight line. This plot, known as a BET plot, can be used to calculate the monolayer value using the following equation:

$$\text{Monolayer value} = 1/(\text{y-intercept}) + \text{slope} \qquad (5)$$

The monolayer water content will correspond to a specific a_w when applied to the products' sorption isotherm. Chen, Halsey, Henderson and GAB equations were generated to represent experimental water sorption isotherm data (Kirloskar, 1991). These equations, involving data manipulation and numerous constants, are selected based on the shape of the sorption isotherm plot. A plot of these

equations, written in their linear form, should yield a straight line. These equations are provided below:

Henderson equation:

$$\ln[-\ln(1-a_w)]=n\ln M_{eq}+\ln K \qquad (6)$$

where: a_w =water activity; M_{eq} =equilibrium moisture content; n and K are constants

Chen equation:

$$\ln(-\ln a_w)=K-aM_{eq} \qquad (7)$$

where: K =temperature dependent constant

Halsey equation:

$$a_w=\exp^{(-aw/Meq)} \qquad (8)$$

B.E.T. equation:

$$a_w/M_{eq}(1-a_w)=1/M_mC+a_w(C-1/M_mC) \qquad (9)$$

where: M_m =monolayer moisture content; C =constant related to the net heat of sorption

GAB equation:

$$M_{eq}=CK(a_w)W_m/(1-Ka_w)(1-Ka_w+CKa_w) \qquad (10)$$

where: W_m =water content corresponding to saturation of all primary adsorption sites by one molecule of water; C =Guggenheim constant; K= constant associated with the association of water

Antioxidation

Antioxidants are added to many types of foods, as well as packaging materials to extend the shelf-life to at least equal the normal distribution and marketing time of

foods. There are literally hundreds of compounds, both natural and synthetic, that possess antioxidant properties. However, their use in food is limited by health concerns and accompanying governmental regulations.

Antioxidants do not improve quality of the product or stop oxidation from occurring, but delay the onset or slow the rate of oxidation of autoxidizable materials. Antioxidants use various mechanisms to prolong the induction period of the autoxidation reaction, and generally function by interrupting the propagation of the free radical chain mechanism (Nawar, 1985). Phenols, such as butylated hydroxyanisole (BHA) and butylated hydroxytoluene (BHT), act as free radical chain stoppers by donating a hydrogen to a free radical (Labuza, 1971). BHA and BHT are typically used in conjunction with other primary antioxidants to achieve synergistic effects (Labuza, 1971). Tocopherols, naturally occurring antioxidants in vegetable oils, can survive oil processing in sufficient quantity to provide increased oxidative stability to the finished product (Nawar, 1985). Tocopherols, both natural and synthetic (alpha, gamma, delta, beta), act as free radical chain stoppers by donation of a proton. Chelating agents such as ethylene diaminetetraacetic acid (EDTA), citric acid, and phosphates function as free radical production preventors by tying up metal catalysts.

Substantial differences in effectiveness of various antioxidants are noted when used with different types of

oils or fat-containing foods. The different levels of effectiveness are due primarily to the differences in molecular structure between antioxidants. Therefore, selection of an antioxidant is product dependent. In addition to level of effectiveness, other factors such as ease of incorporation into the food, carry-through characteristics, sensitivity to pH, tendency to discolor or produce off-flavor, availability, and cost further complicate selection of an antioxidant (Nawar, 1985).

Analytical Techniques

Product Model

The matrix of a food product, product surface area, porosity, moisture content, and storage conditions could affect the ability of oxygen to reach oxidation-susceptible food components, influencing the rates of oxidation. Product models are often employed to reduce the variables involved in research. Flink (1971) as cited by Karel and Yong (1981) studied the influence of physical structure of freeze-dried emulsified systems on the oxidation behavior of the lipid component. He found that in freeze-dried emulsions where insoluble carbohydrates (ungelatinized starch granules and microcrystalline cellulose) were the matrix-forming solute, dried powders were formed with all the lipid component present on the surface. In systems where proteins were used as the matrix-forming solute, the

lipid was effectively encapsulated, with only small amounts of lipid present on the surface. Emulsions included a lipid (linoleic acid), water, nonvolatile solute-matrix former (microcrystalline cellulose), and an emulsifier. The insoluble carbohydrates were observed to have only surface lipid with no encapsulation and more uniformly distributed than with soluble carbohydrates. This uniformity would allow for all lipid components to be exposed to headspace oxygen. When surface lipid is exposed to air, it is readily oxidized, whereas encapsulated lipid is well protected and unavailable as a site for oxygen to react (Karel and Yong, 1981). Koelsch (1989) adapted a product model consisting of microcrystalline carboxymethyl cellulose, soybean oil, tween 20, and distilled water. The product proved to be consistent and uniform throughout oxidation studies.

Product models are used in research to remove inconsistent variables which could influence the outcome of an investigation. Kogashiwa (1980) and numerous other researchers employed product models to eliminate inconsistent variables and maintain control over product characteristics in repetitive oxidation studies (Koelsch, 1989).

Indices of Oxidation

No single method for measuring the extent of lipid oxidation can possibly measure all oxidative events at once, be equally useful at all stages of the oxidative process, be

applicable to all fats, all foods, or all conditions of processing (Nawar, 1985). Several methods, thiobarbituric acid test (TBA), peroxide value (PV), the Kreis test, and more recently gas chromatography, have been used to quantify the extent of lipid oxidation.

In the TBA test, one mole of malonaldehyde, an oxidation product of unsaturated systems, reacts with two moles of thiobarbituric acid in solution to give a pink color. The more absorbance in the liquid state, the higher the TBA value, corresponding to a more rancid flavor (Nawar, 1985). The drawback to this method is that malonaldehyde is a very small component of oxidation, and is a secondary product of polyunsaturated systems of only 3 or more double bonds such as linolenic acid, not linoleic or oleic. Linolenic only comprises a small amount of the total fatty acid concentration in most vegetable oils. Thus, TBA tests can only be used in measuring oxidation of linolenic acid. Malonaldehyde has been known to react with proteins in an oxidizing system giving abnormally low TBA values (Nawar, 1985). TBA reagent can also react with other food components (sugars and carbohydrates) besides malonaldehyde (Nawar, 1985). This method may be more accurately defined as TBARS (thiobarbituric acid-reactive substances) to compensate for these compounds which produce the characteristic pink chromagen (Kumor, 1986).

Peroxide Value (PV) is a measure of the ability of peroxide to liberate iodine from potassium iodide, or to

oxidize ferrous to ferric ions (Nawar, 1985). Peroxides are the reaction intermediates of autoxidation, which react to form secondary reaction products. This test could be useful in the initial stages where peroxides are formed faster than they are decomposed, but as oxidation proceeds, peroxides decompose at a faster rate than they are formed. Therefore, as rancidity increases, the peroxide value may be decreasing, giving a poor correlation to sensory evaluation. Quast and Karel (1972) found that in oxidation of potato chips, in most cases peroxide value increased in storage initially, then decreased to a level lower than the starting value. Correlations between this test and development of rancid flavors have been attempted, but are inconsistent (Quast and Karel, 1972).

One of the first tests used to measure the extent of lipid oxidation was the Kreis test, which involved measurement of a red color believed to result from the reaction of epihydrin aldehyde (an isomer of malonaldehyde) or other oxidation products with phloroglucinol. The problem was the characteristic color sometimes developed in fresh non-oxidized foods, giving inconsistent results (Nawar, 1985). The Kreis test and the Oxirane, a colorimetric method based on the reaction of the oxirane group with picric acid, require direct product analysis. In direct product studies, the product must be removed from the test environment for analysis. In a closed system, the test environment cannot be disturbed (Koelsch, 1989).

The above mentioned problems and inconsistencies with TBARs, PV, and direct product analysis led to the refining of chromatographic techniques to measure hexanal and other volatile derivatives. With the development of sensitive gas chromatograph (GC) instrumentation, the headspace technique as a measure of lipid oxidation has become widely accepted. Scholz and Ptak (1966) employed a direct injection technique in the analysis of cottonseed oil volatiles. They claimed peroxide values and rancid flavors and odors were not closely associated, and consequently chose gas chromatography for its correlation to the results obtained by flavor and odor testing panels.

Headspace isolation and concentration techniques have been developed to concentrate volatile vapors over an oxidizing product. Brinkman (1972) flushed simmering beef broth with purified nitrogen gas and collected flavor components in a porous polymer trap. Headspace trapping procedures feature a number of advantages such as small sample size (1-300g) needed, short preparation time, isolation and concentration of both low- and high boiling compounds, short sampling and analysis cycle, and reduced occurrence of artifacts (Sugisawa, 1981).

Adsorption polymers, which have a high affinity for, and reversible adsorption of, organic compounds are used for collection, concentration and subsequent GC analyses in a wide variety of applications. There are several polymer based traps used in headspace analysis of volatiles,

including Chromosorb, Porapak, and Tenax GC. Butler and Burke (1976) found Tenax GC to be good for high boiling components due to its high thermal stability and low retention volume. Good stability assures no volatiles will bleed from the trap onto the GC column during analysis, and complete regeneration of the porous polymer (Buckholz, 1980). Water vapor does not affect Tenax GC performance, which is an asset if quantifying lipid oxidation in a humidified system. Tenax GC can also be employed in the collection and desorption of volatiles of higher molecular weight. It is also excellent in adsorption of volatiles at room temperature and permits efficient desorption of the same volatiles at 200-300°C. Porous polymer traps can store collected volatiles for two weeks, and storage at 0 to 4°C or room temperature gave reproducible GC results (Sugisawa, 1981).

Analysis of hexanal via extraction from porous polymer traps has been adapted for use in products from fruit, vegetables, meats, and vegetable oils (Koelsch, 1989). When measuring the extent of lipid oxidation at constant oxygen concentrations, Koelsch used Tenax GC to isolate, concentrate, and quantify the amount of hexanal produced in the headspace of a test cell above oxidizing soybean oil. These 1/8 inch o.d. glass traps packed with the porous polymer can be inserted directly into the modified injection port of a gas chromatograph equipped with a flame ionization detector. If the GC injection port is incapable of

receiving a glass trap, the hexanal can be extracted by washing the Tenax GC with a solvent. Koelsch used HPLC grade 2-methylbutane, centrifuge, and then concentrated the solution into a septa seal vial. A syringe was then used for direct injection from the septa seal vial onto the GC column.

Hexanal

Hexanal is one of the major secondary oxidation products of linoleic acid (Frankel et al., 1981). Being a terminal product of oxidation, hexanal is less subject to further interaction with other food ingredients. Since linoleic acid comprises approximately 55% of the fatty acid content in soybean oil, and a large portion in many other vegetable oils, the accumulation of hexanal is an excellent indicator of the degree of rancidity in snack foods. Hallberg and Lingnert (1991), when boiling potato granules, claimed hexanal was the most abundant aldehyde formed. Fritsch and Gale (1977) used hexanal as a measure of rancidity in low fat foods, such as potatoes and soy products. When rancid odors were first noted, the hexanal concentration was found to be 5-10ppm. They found for these foods, a good prediction of the time required for rancidity at any temperature can be made from tests carried out at accelerated conditions. In foods whose fat contained an abundance of linoleic acid and less than 1ppm hexanal when fresh, an increase to 5ppm or more hexanal was found to

indicate significant deterioration in quality due to lipid oxidation (Fritsch and Gale, 1977). Jeon et al (1984) tested the susceptibility of potato chips to oxidation under various accelerated temperature conditions. Monitoring a sharp increase in n-hexanal was found to be a good index for accelerated stability testing.

In studying the correlation of flavor scores with instrumental measurement techniques, Goetz and Waltking (1990) found as the rate of flavor deterioration increased, the PV content decreased, and recommended that hexanal and pentane be used in predicting flavor scores. Being a stable end-product, the concentration of hexanal increases as a food product containing linoleic acid becomes increasingly rancid. Hexanal's relationship to flavor tests is not linear, but flavor tests are very subjective, and hexanal has proven to be a very effective indicator of off-flavor. With increased sensitivity of the gas chromatographic techniques, hexanal analysis is more reproducible, less time consuming, more simplistic, and provides a better relationship to sensory evaluation.

Apparatus

Quast and Karel (1972) adapted a closed system developed by Unbreit (1964), to determine the rate of oxygen uptake by an oxidizing product as a function of oxygen concentration and water activity. This system, the Warburg apparatus, measured the rate of oxygen uptake using mercury

filled manometers which determined the partial pressure within the flask. The equilibrium relative humidity and initial headspace oxygen concentration could be adjusted to the desired level within the Warburg flask. Measuring headspace oxygen concentration at regular time intervals, extent of oxidation and the rate of oxidation could be determined as a function of time. However, this was an oxygen depletion system, as oxygen was consumed by the oxidizing substrate the headspace oxygen concentration decreased. Quast and Karel (1972) tried to rectify the problem by periodically injecting a humidified nitrogen/oxygen mixture into the headspace of the flask. The oxygen concentration was still inconsistent between injections.

Hall et al (1985) adopted a dynamic headspace sampling procedure from Murray (1977). Helium carried volatile compounds to a Chromosorb 105 polymer, where adsorption took place.

Labuza et al (1971) adapted a model system from Maloney et al (1966) to analyze the effect of water on freeze-dried model systems. Freeze-dried samples were placed above saturated solutions of known water activity and allowed to equilibrate. Oxygen adsorption was measured using Warburg manometers.

A dynamic system to quantify lipid oxidation as a function of oxygen concentration was used by Koelsch (1989). A humidified nitrogen/oxygen mixture continuously flowed

into the headspace of a glass test cell containing an oxidizing product. Volatiles were trapped by Tenax GC and analyzed. Temperature was held constant at 23±2°C and light was eliminated.

METHODS

Product Model

A product model was developed to simulate a low moisture content, fatty acid-containing food product, such as a potato chip or other snack food. It was also important to have uniform thickness, density, moisture content, and surface area. Product model ingredients included linoleic acid (Eastman Kodak Co., Rochester, NY), used to provide the substrate for oxidation, distilled and deionized water, Tween 20 (Eastman Kodak Co., Rochester, NY), and microcrystalline cellulose (CMC PH101 Food Manufacturing Corp., Philadelphia, PA). These ingredients were mixed several times until the most uniform product in terms of moisture content and surface area was attained. Ingredients and uniformity of the mixture were based on similar models using soybean oil by Koelsch (1989). The final product model mixture giving the best overall characteristics is shown in Table 1.

Table 1
Product Model Ingredient Mixture
product ingredients (% wet basis)

Linoleic Acid	CMC	Tween 20	H_2O
9.34	24.40	0.02	66.24

H_2O is distilled and deionized
CMC is microcrystalline carboxymethyl cellulose

Linoleic acid, Tween 20 (used as an emulsifier), and distilled and deionized water were mixed at low speed in a domestic blender due to product density, and to prevent splashing and loss of product. Microcrystalline carboxymethyl cellulose was slowly added to liquid and mixed at medium speed. Once a uniform slurry was obtained, the mixture was poured evenly, one eighth inch thick into 150 x 15mm plastic petri dishes. Petri dishes were weighed and tared prior to adding product. Petri dish covers were immediately applied to cover product, and simultaneously weighed. Aluminum foil was wrapped around each dish which was placed in a cooler on dry ice for instantaneous freezing. Foil and covers were removed and product was placed in a laboratory freeze drier (Vitris Model II, Repp Industries Inc., Gardiner, NY). Freeze drier conditions were 100 micro torr at -50°C, with a platen temperature of -38°C. Frozen product was dried for 5 days (120 hours).

The vacuum was broken using air. Product was

immediately covered with petri dish covers, weighed, and wrapped in aluminum foil. Samples were then stored in a conventional freezer until being transferred to the test cell.

Initial Moisture Content

A vacuum oven method was used to determine the initial moisture content of the product model immediately after freeze-drying. The method is described in section 28 (Fats and Oils) of the Official Method of Analysis of the Association of Official Analytical Chemists (1975). This technique was used by Koelsch (1989) for a similar product model. The product was weighed into tared aluminum weighing dishes and placed in the oven. The vacuum oven conditions were set at 30 mmHg and 100°C for six hours. The temperature setting was then lowered to 23±2°C for 2 hours to allow for equilibration. Dishes were removed and weighed. The average of triplicate results was used to determine initial moisture content.

Sorption Isotherm

A sorption isotherm was developed to determine the Equilibrium Moisture Content (EMC) of the product model at specific water activities (Aw). Isotherm data were obtained gravimetrically by measuring product weight change over a two week period. Salt solutions were developed using the procedure described in Hygrodynamics Technical Bulletin No.5

(Creating and Maintaining Humidities by Salt Solutions) and placed in eight tightly sealed recloseable plastic buckets, creating constant relative humidity environments. The buckets were allowed to equilibrate for a two week period before testing began. The humidities inside the buckets were monitored by hygrometers placed in a rubber hole stopper and mounted in the plastic lid. Product was taken immediately from the petri dish and weighed on an analytical balance into tared aluminum weighing dishes. Three aluminum dishes of product were then placed into each storage container controlled at a specific relative humidity. After each week, dishes were weighed until a constant weight was obtained. All humidity conditions inside storage containers remained constant. Temperature in the storage area was measured at 23±2°C. All experiments were performed in triplicate.

Apparatus

System Design

A dynamic system of constant relative humidity and oxygen concentration was designed to quantify the rate of lipid oxidation. This system was adapted from an earlier study by Koelsch (1989) in which lipid oxidation experiments were performed. The system was developed to allow for the rate of oxidation to be a function of oxygen concentration and water activity (Aw). The study was conducted at an

ambient temperature of 23±2°C, accelerated temperatures of 40 and 66°C, and in the absence of light. Higher temperatures act to increase the rate of reaction (Jeon et al., 1984). Light accelerates the oxidation reaction and is difficult to control so it was eliminated to reduce the number of variables.

A system of gas washing bottles, glass rotameters (0 to 60 scale Cole Parmer, Chicago, Ill.), and glass test cells, were connected by one-eighth inch copper tubing using swagelok fittings (Crawford Fitting Co., Solon, Ohio). Two tanks were utilized, a nitrogen tank (Tn) and air tank (Ta). The nitrogen tank was split into two streams. The purity of the nitrogen tank was tested by withdrawing several samples and injecting them into the Headspace Oxygen Analyzer. The oxygen concentration of the nitrogen tank was found to be less than a 2 parts per million. One stream (R_2) was bubbled through H_2O in a gas washing bottle and humidified. The humidified nitrogen was then reconnected with the pure nitrogen stream (R_1) to provide a humidified source of nitrogen (R_3). The air tank was similarly split into two streams, one of which was bubbled through H_2O (R_{11}) and reconnected with pure air (R_{12}) to provide a humidified source of air (R_4), monitored by an hygrometer. A vent (R_{10}) served as a pressure release on the humidified air stream. The air stream (R_4) was then diluted with the nitrogen gas stream (R_3), providing a mixture of air and nitrogen. An exhaust valve (R_5) was used following the dilution to adjust

the mixture to the desired concentrations and control the rate of flow for the nitrogen/air mixture (R_6). A second dilution could then be made with the humidified nitrogen stream (R_7) if the oxygen concentration in the humidified N_2/air stream (R_6) needed to be adjusted. The final mixture of humidified N_2/air (R_9) goes through an hygrometer to monitor Aw, before moving on to the test cell. This stream was then split to send equivalent flow through each glass cell. A valve on each stream monitored flow to both the equilibration and test cells. When equilibration was taking place, flow to the test cell could be ceased, allowing for the oxygen concentration to be stabilized in the equilibration cell without oxidizing the product in the test cell. This also allowed for the product to be humidified to the correct Aw, before being exposed to oxygen. The test cell was wrapped in aluminum foil to protect the product model from being exposed to light. In the accelerated temperature studies (40 and 66°C) the test cell was placed in a hot water bath, held at constant temperature. A schematic of the system is given in Figure 3. Figure 4 represents the system prepared for accelerated temperature studies.

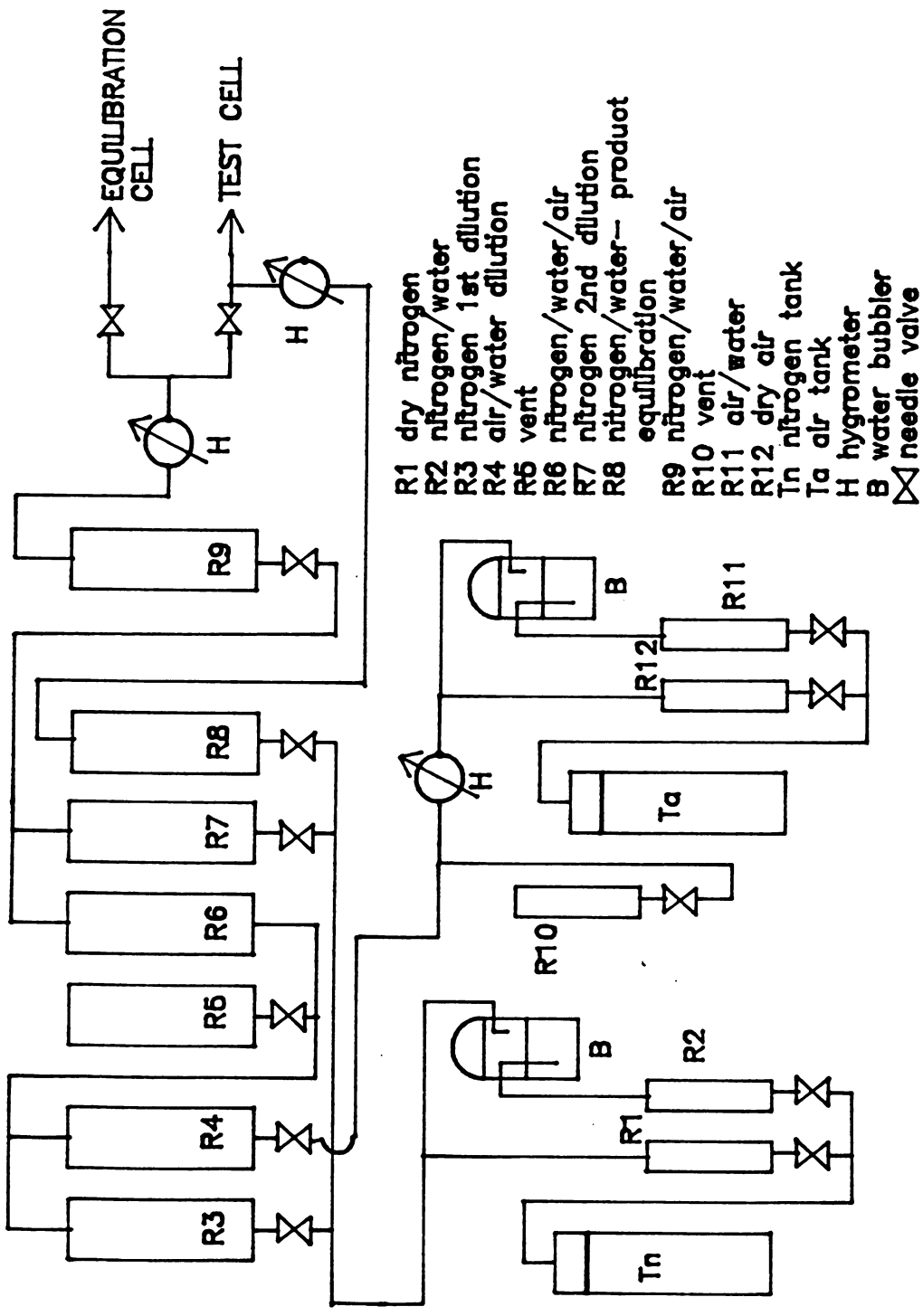

Fig. 3: System for the Measurement of Lipid Oxidation at Constant Water Activity, Temperature, and Oxygen Concentrations

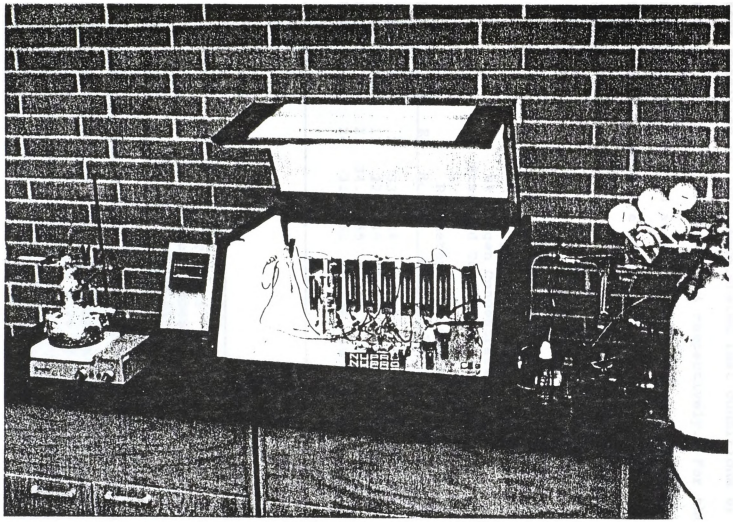

Fig. 4: System Prepared for Accelerated Temperature Studies

For the experiments conducted at 8% oxygen concentration, the flow rates for each of the rotameters at the standard test condition of 23°C, accelerated test conditions of 40 and 66°C are given in Tables 2-4 respectively. For the experiments conducted at an oxygen concentration of 1.5% and accelerated temperature of 66°C, the rotameter settings are given in Table 5.

Table 2
8% Oxygen Concentration
Standard Conditions (23°C)

	Rotameter Settings (ml/min)											
a_w	R_1	R_2	R_3	R_4	R_5	R_6	R_7	R_8	R_9	R_{10}	R_{11}	R_{12}
0.069	33.5	2	33	46	40	35	0	25	38.5	20	2	36
0.20	32.5	11	22	45	41	37	9	36	41	24	13	40
0.32	42	21	34.5	55	48	42.5	0	34	44	30	22	41
0.49	19	24	31	52	44	34	10	35	41	37.5	29	34

Table 3
8% Oxygen Concentration
Accelerated Conditions (40°C)

	Rotameter Settings (ml/min)											
a_w	R_1	R_2	R_3	R_4	R_5	R_6	R_7	R_8	R_9	R_{10}	R_{11}	R_{12}
0.081	30	3	25	30	31	28	0	9	31	24	3	29
0.24	25	8	24	30	29	26	0	10	28	26	10	28

Table 4
8% Oxygen Concentration
Accelerated Conditions (66°C)

	Rotameter Settings (ml/min)											
a_w	R_1	R_2	R_3	R_4	R_5	R_6	R_7	R_8	R_9	R_{10}	R_{11}	R_{12}
0.062	35	2	30	40	39	35	0	24	42	18	2	35
0.26	30	9	29	34	34	31	0	10	32	22.5	9	26

Table 5
1.5% Oxygen Concentration
Accelerated Conditions (66°C)

	Rotameter Settings (ml/min)											
a_w	R_1	R_2	R_3	R_4	R_5	R_6	R_7	R_8	R_9	R_{10}	R_{11}	R_{12}
0.08	30	3	30.5	5	21	20	0	14	20	40	3	31
0.21	35	12	39	5	26	23	0	4	23	41	12.5	35
0.30	36	16	31	5	21	18.5	0	13	20	40	17	37
0.53	19	23	27	4.5	20	15.5	0	13	25	40	21	20

Test Cell and Equilibration Cell Design

Two glass cells designed by Koelsch (1989) were utilized to contain the product model during the experiments. A 135ml pyrex glass 40/50 gas washing bottle, modified by the Chemistry Dept. Glass Blowing Shop at Michigan State University, allowed for continuous headspace sampling (Figure 5). The cells were designed to ensure that oxygen concentration was constant during the oxidation process. This was accomplished by continuously flowing the

N_2/air gas mixture through the cell.

The glass test cells were designed with one inlet port in the base and two outlet ports in the removable head section. One outlet port was a multi-purpose port which allowed for headspace sampling of oxygen concentration. Using a syringe, a headspace extraction could be made through tygon tubing attached to the port. The oxygen concentration was determined using a 3500 Headspace Oxygen Analyzer (Illinois Instruments, Inc.). Calibration data for the Headspace Oxygen Analyzer are given in Appendix A. The second port was divided into two outlets equipped with ball and socket joints, allowing for attachment of Tenax traps. A three-way stop cock controlled the gas flow from one outlet port to the other, thus enabling continuous sampling of volatiles. When tests were in progress, the multi-purpose port remained closed to force all flow through the sampling port. The three-way valve opened for flow into one outlet port at a time, allowing flow to be switched to the other outlet at a specified time.

An equilibration cell was used to monitor oxygen concentration. Flow was switched from the equilibration cell to the test cell containing the product once the oxygen concentration was constant as indicated by repetitive headspace samples analyzed by the Headspace Oxygen Analyzer. The hygrometer connected to the humidified air stream (R_4) before it was mixed with the humidified N_2 stream (R_3) to ensure that the test cell and equilibration cell had

equivalent a_w. A pure air stream would dilute the humidity of the N_2 stream, creating a humidity difference between the test cell and equilibration cell. The test cell was designed to allow the product model to equilibrate to the moisture content for a chosen a_w, the same a_w as in the equilibration cell. Adjusting the humidity of the air and N_2 streams would create a common humidity environment within the two cells. The test cell was humidified by directly intercepting the humidified N_2 stream between R_3 and R_7, and reattaching after the valve, allowing flow to the test cell, controlled by a rotameter (R_8).

The cells were allowed to equilibrate for twelve hours before the product was added to the test cell. After twelve hours the a_w inside the test cell was constant, fluctuating less than 0.01. The oxygen concentration and a_w inside the equilibration cell were also constant, with oxygen concentration varying less than 0.1%. The product was weighed and placed in base of the test cell, one-eigth inch below the inlet port.

Once the product was in equilibrium with the test cell environment, the valve leading to the test cell could be opened and flow to the equilibration cell could be closed. Oxidation will now be dependent upon moisture content of the product and oxygen concentration, unaffected by possible adsorption or desorption by the product. This was noted as time zero. After each experiment the test cell was washed and placed in a 100°C oven for 12 hours.

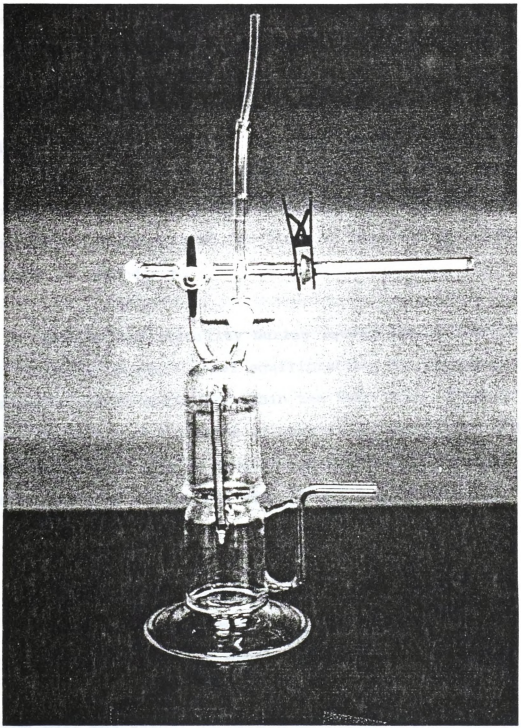

Fig. 5: Test Cell

Product Model Equilibration

The time required for the product model to reach equilibration within the specific humidity environment of the test cell, was determined gravimetrically. This ensured the moisture within the product had become constant before being exposed to oxygen. The product was taken from petri dishes, placed in a tared aluminum dish, and weighed on an analytical balance. The product weight was determined periodically until a constant weight was reached. This procedure was performed for 0.076 a_w and 0.43 a_w, with data given in Appendix A.

Hexanal Detectability During Equilibration Process

During product model equilibration (24 hours) to the specific water activity within the test cell, a Tenax trap was attached to determine if production of hexanal occurred before time zero. No hexanal was detected by the gas chromatograph during the equilibration period.

Headspace Sampling and Extract Analysis

Sorption of Volatiles

With the multi-purpose port closed, flow from the test cell is forced through the sampling port, out through one of the ball and socket joints, and into the Tenax trap where volatiles are sorbed. The glass traps were filled with 0.38±0.02 grams of Tenax (35/60 mesh), and glass wool was

applied at either end of the tube to prevent spilling of Tenax. The traps are glass tubes approximately 7 cm in length and 6 mm inside diameter. On the end of each trap is the socket end of the ball and socket joint between the trap and the test cell. A spring-loaded clamp was used to hold the joint tight to inhibit leakage of volatiles. At specific time intervals, flow through the cell was switched to an alternative Tenax trap. The removed trap could then be analyzed for sorbed hexanal using the following extraction method.

Extraction and Concentration Procedure

A 0.5 microliter injection of HPLC grade 2-methylbutane (Aldrich Chemical Co., Milwaukee, Wis.) was made into the gas chromatograph to ensure its purity before it was used to wash the hexanal from the glass traps. The Tenax tubes were placed into a single hole cork stopper that was placed into the end of a 5 ml graduated centrifuge tube. Using disposable glass pipettes, 1 ml of 2-methylbutane (isopentane) was pipetted into the socket end of the Tenax tube. The centrifuge tube was then placed in a centrifuge to accelerate the extraction of hexanal from the Tenax. The centrifuge (International Equipment Co., Boston, Mass.) was set at 750 rpm for 2 minutes, forcing solvent containing hexanal, to the bottom of the graduated centrifuge tube. A 1.0-1.5 ml aliquot of isopentane was pipetted into the Tenax tube and it was centrifuged again. Approximately 2 ml of

extractant remained. Nitrogen was used to concentrate the hexanal by evaporating the extractant to a volume of 0.5 ml. This enabled trace amounts of hexanal to be detected by the gas chromatograph. Contents of the centrifuge tube were quickly pipetted into a 1.5 ml Pierce (Rockford,Ill.) septa seal vials. After hexanal was removed, Tenax traps were rinsed with isopentane, centrifuged, and baked in 100°C oven for 12 hours. At the end of each test for a specific a_w, glass traps were washed, filled with new Tenax and conditioned.

Percent Recovery of Hexanal from Tenax GC and Concentration Technique

To determine if loss of hexanal occurs from the Tenax GC during the extraction and concentration processes, a recovery study was performed. Three solutions of hexanal (3.34, 8.34, 16.68ppm) were developed and tested in triplicate to determine percent recovery.

A 1 ml aliquot of the 3.34 parts per million hexanal solution with 2-methylbutane was injected into the top of the glass tube containing Tenax GC. Two milliliters of 2-methylbutane was washed through the Tenax GC with the aid of a centrifuge. The extract in the centrifuge tube was then concentrated to 1.0 ml under nitrogen. A 0.7 microliter aliquot of the extract was injected into the programmed gas chromatograph, and the average area response of three injections determined percent recovery of hexanal from Tenax

GC. This procedure was performed again for the 8.34 and 16.68 parts per million solutions.

Gas Chromatography

A 10 microliter syringe (Hamilton Co., Reno, Nv.) was placed in a freezer to cool. 0.7 microliter aliquots of extractant were injected with the cooled syringe into a 5890 Hewlett Packard gas chromatograph equipped with dual flame ionization detectors (FID). Standard solutions of hexanal in dichloromethane were made prior to injection of samples in 2-methylbutane to ensure consistency of gas chromatographic response. Volatile separation took place in a bonded Carbowax 20M column (Supelco Inc., Bellefonte, Pa.). A Hewlett Packard 3392A integrator was interfaced with the gas chromatograph. The conditions of the gas chromatograph were programmed at an initial temperature of 40°C for 1 minute followed by heating at a rate of 5 degrees/minute increase until the temperature reached 150°C. The final temperature was held for 10 minutes. Injection port temperature was set at 200°C, and the detector temperature was 250°C.

Gas Chromatograph Calibration Procedure

The solutions used in the calibration procedure were hexanal (density 0.834g/ml) and dichloromethane (used due to low boiling point of 2-methylbutane). Volumetric flasks used for the procedure were washed, rinsed with

dichloromethane and dried in a conditioned 100°C air oven. While the flasks were dried, the purity of the dichloromethane solvent was evaluated using the GC. The GC conditions were programmed to an initial temperature of 40°C for ten minutes followed by programming at a rate of 2 degrees per minute until a final temperature of 150°C was reached and held for 10 minutes. The injection port temperature was held at 200°C and helium flow rate was 2.2 cubic centimeters per minute. The detector temperature was 250°C. The range and attenuation setting were 2 and 0 respectively.

Three 0.7 microliter injections, with a 10 microliter syringe, of dichloromethane were made into the GC. No peaks near the retention time of hexanal were evident. After one hour in the oven, flasks were taken out and cooled to room temperature, at which time the flasks could be labeled with their appropriate concentrations.

1. 5 microliters of hexanal were added to 50ml of dichloromethane in a 50ml volumetric flask providing an initial solution with a hexanal concentration of 83.4ppm.

   (0.834g/ml)(0.005ml/50ml)(1E+06)= 83.4ppm

2. 1ml of the 83.4 parts per million solution was added to 25ml of dicholoromethane in a 25ml volumetric flask.

   (83.4ppm)(1ml/25ml)= 3.34ppm

3. 1ml of the 83.4 parts per million solution was added to 10ml of dichloromethane in a 10ml volumetric flask.

   (83.4ppm)(1ml/10ml)= 8.34ppm

4. 2ml of the 83.4 parts per million solution was added to 10ml of dichloromethane in a 25ml volumetric flask.

(83.4ppm)(2ml/10ml)= 16.68ppm

5. 10ml of the 83.4 parts per million solution was added to 25ml of dichloromethane in a 50ml volumetric flask.

(83.4ppm)(10ml/25ml)= 33.36ppm

Three 0.7 microliter injections from each flask were made into the gas chromatograph, using the same syringe (10microliter syringe from Hamilton Company, Reno, Nevada) for all the injections. After each injection the syringe was washed with dichloromethane and acetone, and heated in a 100°C oven for 15 minutes to remove all traces of solvent. The results from the three injections at each concentration were averaged and values plotted. Hexanal calibration curve data and plot are given in Appendix B.

RESULTS AND DISCUSSION

Product Model

The initial moisture content was calculated and an equilibrium sorption isotherm was developed to determine the relationship between a_w and the product model. Using the product composition information, the weight in grams (dry basis) of linoleic acid that was placed in the base of the test cell for each experimental condition was determined. The product weight (wet basis) in a chosen petri dish was multiplied by the % weight (wet basis) of linoleic acid in the product model, giving the weight in grams (wet basis) of linoleic acid. It was assumed that the weight of linoleic acid remained constant during the freeze-drying process. Therefore, the weight in grams of linoleic acid is equivalent for the wet and dry basis. The weight of linoleic (dry basis) was then divided by the calculated dry product weight in the petri dish after freeze-drying to give the % weight (dry basis) for linoleic acid. The % weight on a dry basis for linoleic acid was then multiplied by the weight of product in the test cell to determine the weight in grams of linoleic acid used as the oxidizing substrate. Table 6 gives an example for the determination of the weight in grams (dry basis) of linoleic acid placed in the test cell.

Table 6
Weight % of Linoleic Acid in Product Model

	Product Model (grams)	Linoleic Acid % Weight	Linoleic Acid Weight (grams)
Wet Weight	22.21	9.3373	2.0738
Dry Weight	7.320	28.3306	2.0738
Test Weight	3.051	28.3306	0.8643*

*Weight of Linoleic Acid in Test Cell

The B.E.T. monolayer value was calculated using sorption isotherm empirical data.

Initial Moisture Content

The initial moisture content was determined using the following equation:

$$IMC = (Wc/Wd)*100 \qquad (11)$$

where: Wc =weight change (grams)
Wd =weight of dry product (grams)

Initial moisture content was 4.45 $gH_2O/100g$ dry product. Data and calculations are in Appendix C.

Equilibrium Sorption Isotherm

From the constant weight (average of triplicate weighings) that was obtained in each of the relative humidity conditions, the equilibrium moisture content was calculated according to the following equation:

$$EMC = [P_f\ (1+IMC)/P_i]-1\ *100 \qquad (12)$$

where: P_f =final product weight
P_i =initial product weight
EMC =equilibrium moisture content
IMC =initial moisture content

Data and calculations for the sorption isotherm are in Appendix C. Equilibrium moisture contents at the eight relative humidity environments are in Table 7.

Table 7
Equilibrium Moisture Contents at Each Water Activity

Water Activity	Equilibrium Moisture Content
0.12	4.8480
0.23	5.6429
0.31	8.1673
0.40	9.2370
0.50	10.8467
0.63	11.6522
0.82	16.6239

A summary of the experimental sorption isotherm data is shown in Figure 6.

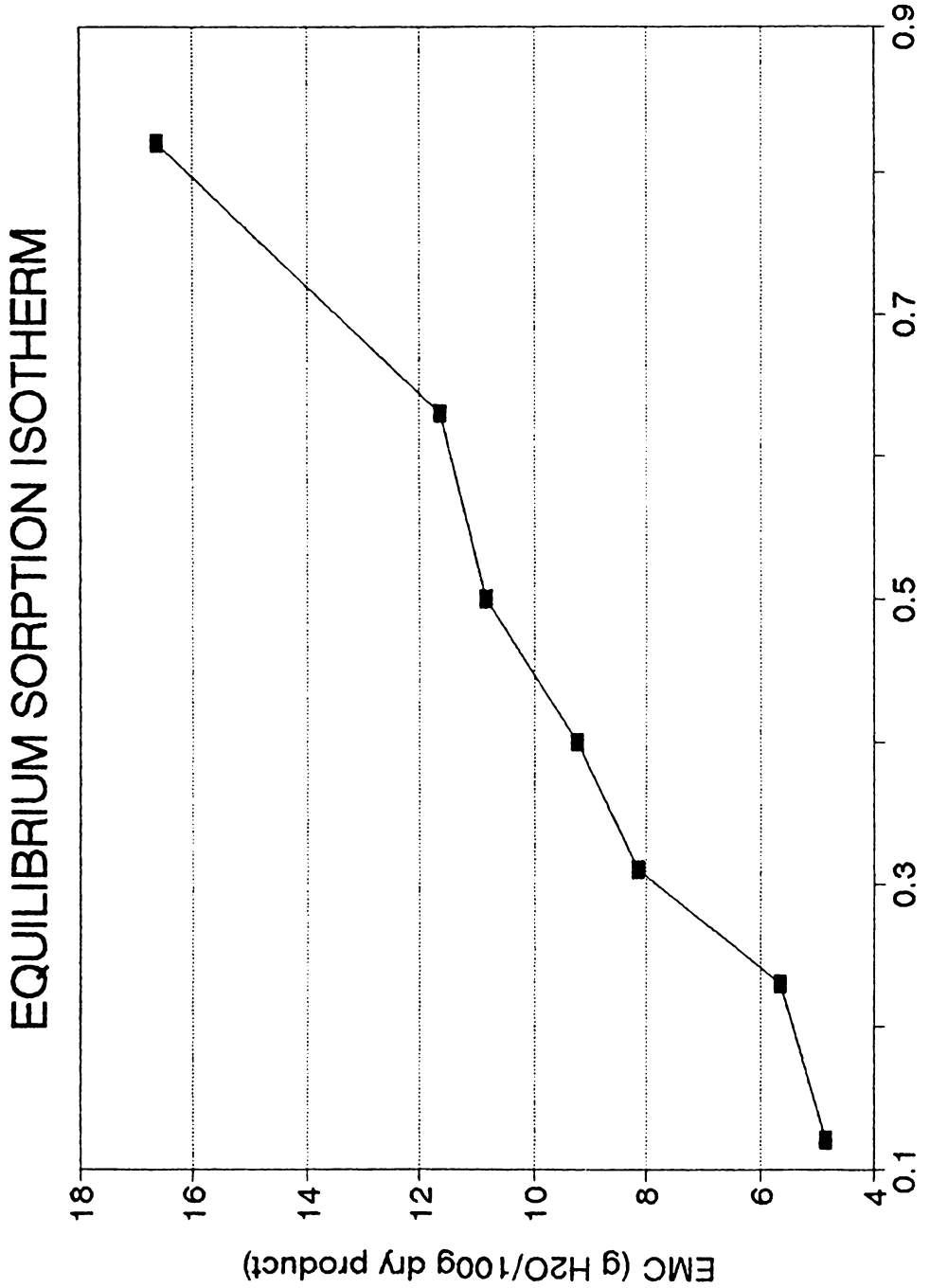

Fig. 6: Relationship Between Water Activity and Equilibrium Moisture Content

Using Mathematical Models to Predict Product Model Moisture Content at Specific Water Activities

The equilibrium sorption isotherm describes the water sorption or desorption characteristics of the product model. The configuration of the curve is a function of these sorption properties of the product. The resultant curve is usually sigmoidal in shape, and can be described by the Chen, Halsey, Henderson, B.E.T. and GAB equations among others. From the equilibrium sorption isotherm data, these mathematical models described a linear relationship between water activity and the product moisture content.

Using Quattro Pro 4.0, a statistical analysis was performed for each model and the corresponding correlation coefficient was calculated. The correlation coefficient estimated the degree of fit between the predicted mathematical models and the experimental sorption isotherm. The constants in each model were calculated from the linearized form of the equations allowing for determination of the water activity at any product moisture content. The resultant linearized form and correlation coefficients of the four equations are listed in Table 8.

Table 8
Linearized Mathematical Models to Predict Water Activity from Product Moisture Content and Corresponding Correlation Coefficients

Mathematical Model	Linearized Equation	Correlation Coefficient
Henderson	$\ln[-\ln(1-a_w)]=n\ln M_{eq}+\ln K$	0.969
Chen	$\ln(-\ln a_w)=K-aM_{eq}$	0.980
Halsey	$a_w=\exp^{(-a/Meq)}$	0.927
B.E.T.	$a_w/M_{eq}(1-a_w)=1/M_mC+a_w(C-1/M_mC)$	0.942
GAB	$M_{eq}=C(K)(a_w)(W_m)/(1-Ka_w)(1-Ka_w+CKa_w)$	0.893

The x- and y-axis calculations and regression formulas generated from the mathematical models are given in Appendix D. The Chen equation gave the highest correlation (0.980) to the experimental equilibrium sorption isotherm data. The linear regression data for the Chen model is given in Table 9 and plot shown in Figure 7. The predicted equilibrium sorption isotherm values using the Chen model versus the experimental values are given in Table 10.

Table 9
Linear Regression Data and Linearized Chen Mathematical Model

Water Activity	X-axis M_{eq}	Y-axis $\ln(-\ln a_w)$
0.82	16.6239	-1.61721
0.63	11.6522	-0.77211
0.50	10.8467	-0.36651
0.40	9.2370	-0.08742
0.31	8.1673	0.15801
0.23	5.6429	0.38504
0.12	4.8480	0.75154

Line Equation: $\ln(-\ln a_w) = 1.656111 - 0.196088(M_{eq})$
Correlation Coefficient: 0.980

Table 10
Chen Model Predicted versus Empirical Equilibrium Product Moisture Content Values

Water Activity	Experimental M_{eq}	Predicted M_{eq}	% Diff.
0.82	16.6239	16.6931	0.42
0.63	11.6522	12.3833	6.27
0.50	10.8467	10.3149	-4.90
0.40	9.2370	8.8916	-3.74
0.31	8.1673	7.6399	-6.46
0.23	5.6429	6.4821	14.9
0.12	4.8480	4.6131	-4.85

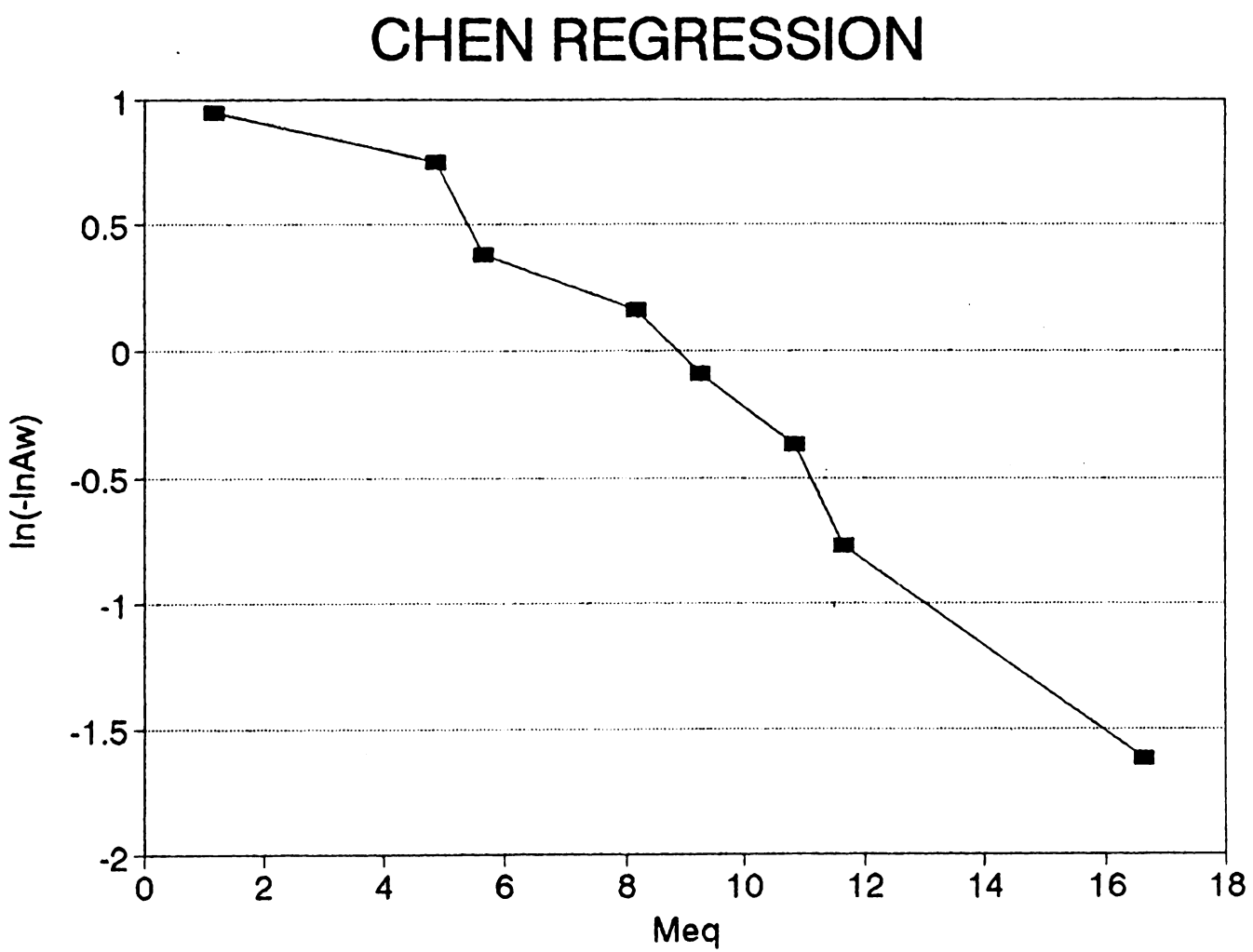

Fig. 7: Linear Regression of Chen Mathematical Model to Predict Water Activity from Product Moisture Content

The total error in estimating the product model moisture content from the Chen regression model was determined by the following equation:

$$\text{error of estimation} = \text{sum}\ [\ln(M_c) - \ln(M_{eq})]^2 \qquad (13)$$

where: M_c =Chen predicted equilibrium moisture content
M_{eq} =Empirical equilibrium moisture content

The sum of the squares error of estimation for the Chen linearized regression equation, $\ln(-\ln a_w)$ as a function of equilibrium moisture content, was 0.03385.

Brunauer, Emmett, and Teller Monolayer Value

Using the data from the low-moisture end ($0.05-0.4a_w$) of the equilibrium sorption isotherm and the B.E.T equation, the monolayer value was determined. The B.E.T. plot of a_w (x-axis) versus $a_w/M_{eq}(1-a_w)$ (y-axis) shown in Figure 8, yielded the linear regression equation:

$$a_w/M_{eq}(1-a_w) = 0.012856 + a_w(0.147944) \qquad (14)$$

Calculated x- and y-axis values for the B.E.T plot are given in Table 11.

Table 11
B.E.T. Regression Plot Values for the Low-Moisture End of the Sorption Isotherm for Determining Monolayer Value

Water Activity	X-axis a_w	Y-axis $a_w/M_{eq}(1-a_w)$
0.40	0.40	0.072
0.31	0.31	0.055
0.23	0.23	0.052
0.12	0.12	0.028

Using the slope and y-intercept values from the B.E.T. regression equation, the monolayer moisture content was determined using the following formula:

$$\text{Monolayer Value} = 1/(\text{y-intercept} + \text{slope}) \qquad (15)$$

The monolayer value was calculated to be 6.2189 $gH_2O/100g$ dry product. Using the Chen equation, which best described the product sorption isotherm data, the a_w corresponding to this value was calculated to be 0.2204.

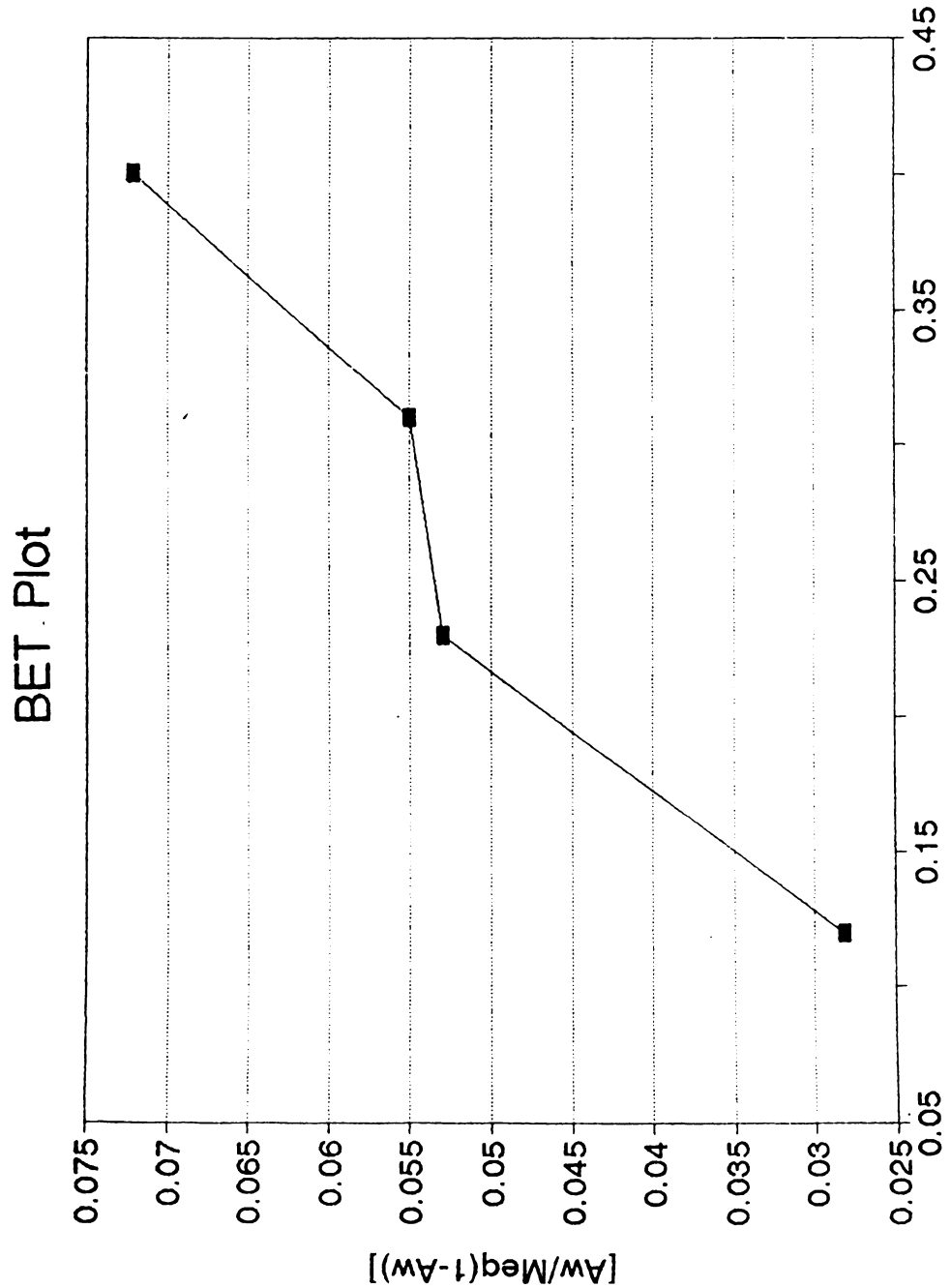

Fig. 8: Brunauer, Emmett and Teller Plot for Determining Monolayer Value

Data Collection and Analysis of Headspace Sampling

Headspace Sampling of Volatiles

Tenax traps, containing sorbed volatiles, were removed at random time intervals for analysis. Sampling frequency was a function of oxygen concentration and temperature conditions. The rate of sampling increased as hexanal began to be produced exponentially.

For experiments under ambient temperature conditions (23°C) at 7.98% oxygen concentration, samples were continuously taken (approximately every 30 hours) for about 280 hours. Sample times were rounded off at 30 minute intervals allowing for a maximum possible sampling error of 15 minutes.

Accelerated temperature experiments (40 and 66°C) had a sampling frequency of approximately 30-90 minutes after the initial 3-5 hour induction period. The experiments ran approximately 12-16 hours at 66°C and 40-50 hours at 40°C, dependent upon oxygen concentration. Sample times were rounded off to 1 minute.

Hexanal Data and Quantification

The hexanal data, collected and calculated, is reported in Appendix E on programmed Quattro Pro 4.0 spreadsheets. Using gas chromatography, area units of hexanal were obtained at each time interval in triplicate. The averaged area units were then used to quantify hexanal concentration (micrograms per gram linoleic acid) as a function of the product model and

linoleic acid. Total grams of hexanal were quantified with the following equation:

$$H_g = AU\ (C.F.)\ (V_s)/V_i \qquad (16)$$

where: H_g =micrograms of hexanal
AU =area units from gas chromatography
C.F. =calibration factor
V_s =sample volume
V_i =injection volume

A range setting of 2 or 4 for the gas chromatograph (range setting was 2 for calibration procedure) was used for the analysis. Increases in the range setting by 2 decreased the area units by a factor of 4. If a range setting of 4 was used, the area units were multiplied by 4. Concentration of hexanal in the product model is given in micrograms of hexanal per gram of product (300E-06 = 300 parts per million = 300 micrograms per gram). Dividing grams of hexanal (h_g) by the product weight, concentration of hexanal (weight/weight) can be determined, as described by the following equation:

$$H_p = H_g/P_w \qquad (17)$$

where: H_p =hexanal concentration (micrograms/gram) in product model
P_w =product weight (grams)

The concentration of hexanal per grams of linoleic acid is determined by the following equation:

$$H_l = H_g / L_w \qquad (18)$$

where: H_l =micrograms of hexanal per gram of linoleic acid
L_w =linoleic acid (grams)

Percent Recovery of Hexanal from Tenax GC

The percent recovery of hexanal from the Tenax GC was determined to be 80.3%. The data and calculations are given in Appendix F.

Rate of Oxidation at Constant Water Activity, Temperature and Oxygen Concentrations

Experimental Data Analysis Using a First Order Rate Expression

The experimental data of hexanal concentration (micrograms/gram of linoleic acid) versus time (hours) gives the configuration of an exponential plot and can be described by a first order expression. The natural log (ln) of hexanal concentration versus time was plotted and linear regression analysis performed that gave a simple linear equation (lny=a+bx). The linear equation was transformed into a first

order expression ($y=a^1e^{bx}$) as suggested by Hall et al (1985). A first order expression was used to fit each curve from time zero to the final time, with a correlation coefficient of at least 0.93. The first order equations for constant water activities at an oxygen concentration of 8% and temperature of 23°C are given in Table 12.

Zero Order Rate Expression

A zero order rate expression could not be utilized since accelerated tests (40 and 66°C) produced hexanal at a exponential rate over a very short time period. Using linear regression analysis, only the first two or three data points could be fitted to a correlation coefficient above 0.90.

Table 12
First Order Equations for 8% Oxygen Concentration and Water Activities of 0.069, 0.20, 0.32, 0.49 at 23°C

Water Activity	First Order Equation	Correlation Coefficient
0.069	$H_l = 2.05106 \exp[0.0210172(t)]$	0.934
0.20	$H_l = 1.58287 \exp[0.0183784(t)]$	0.979
0.32	$H_l = 1.49415 \exp[0.0189224(t)]$	0.959
0.49	$H_l = 1.59956 \exp[0.0204399(t)]$	0.975

H_l =micrograms of hexanal per gram of linoleic
t =time in hours

The plots of the experimental data (grams of Hexanal/ gram of Linoleic Acid) describing the effect of water activity (0.069, 0.20, 0.32, and 0.49a_w) on the rate of oxidation at a temperature of 23°C and oxygen concentration of 8% are given in Figures 9-12. Figure 13 represents the summary of these plots.

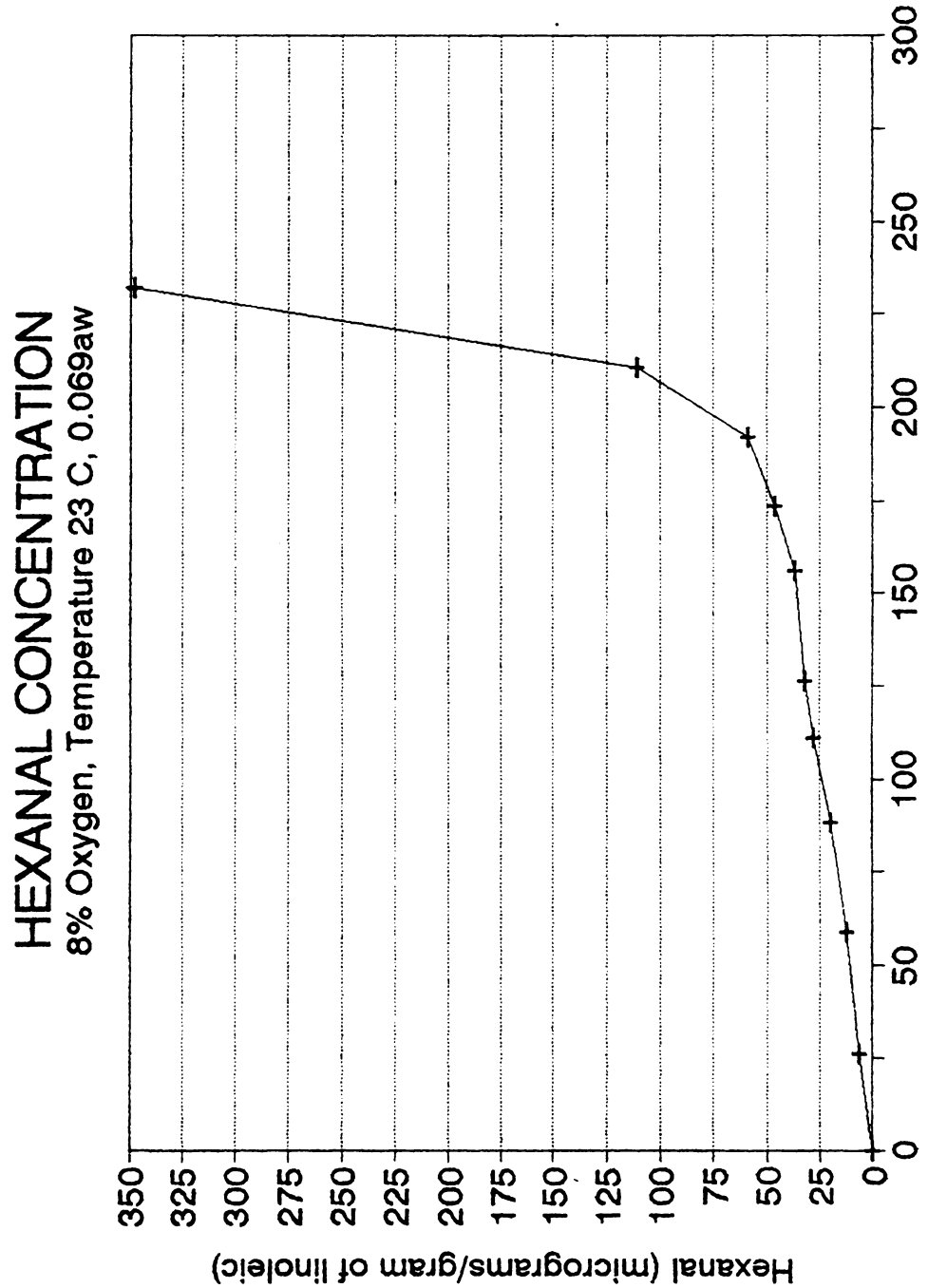

Fig. 9: Rate of Hexanal Formation at 23°C, 8% Oxygen Concentration and 0.069a_w

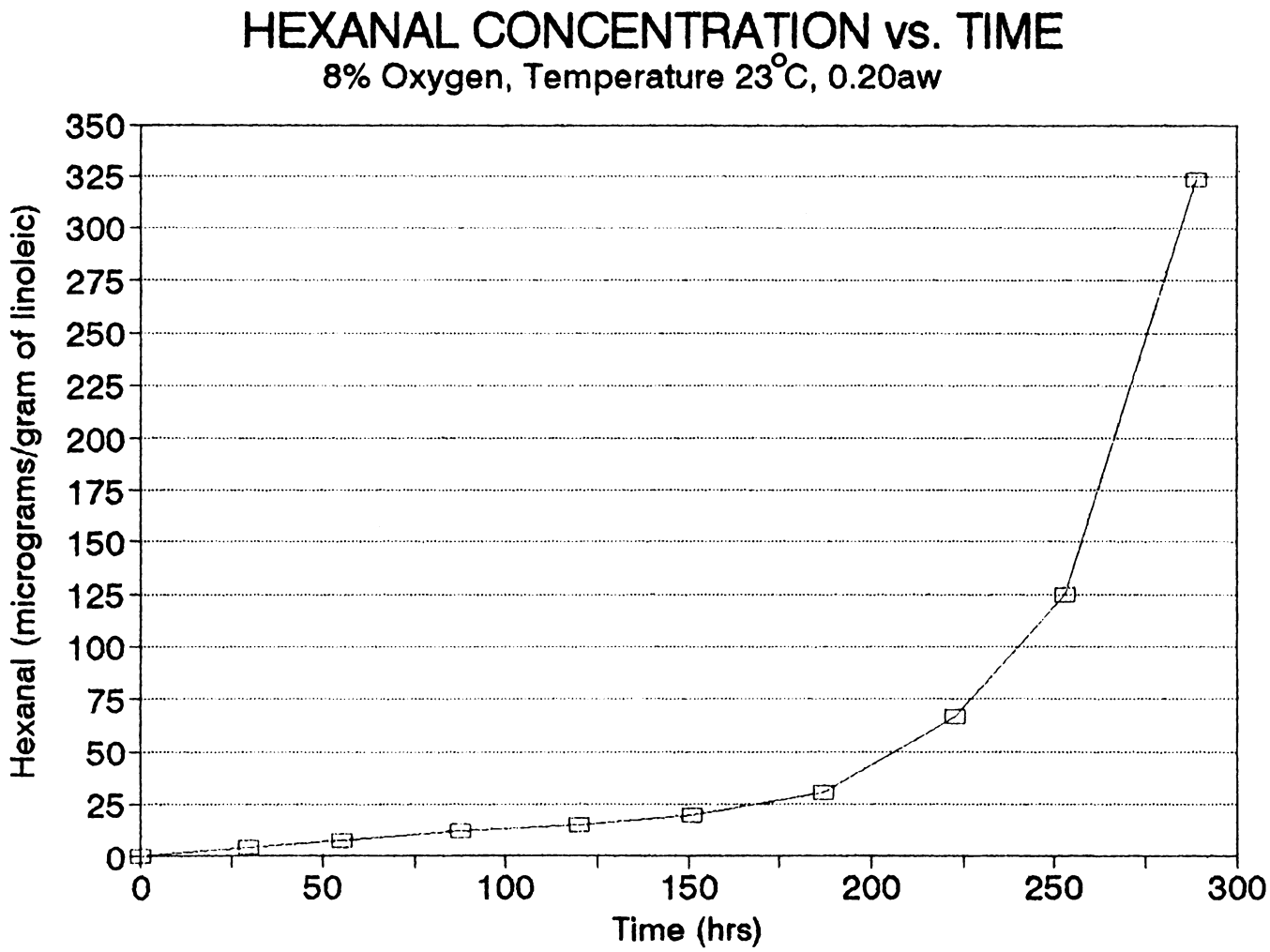

Fig. 10: Rate of Hexanal Formation at 23°C, 8% Oxygen Concentration and 0.20a_w

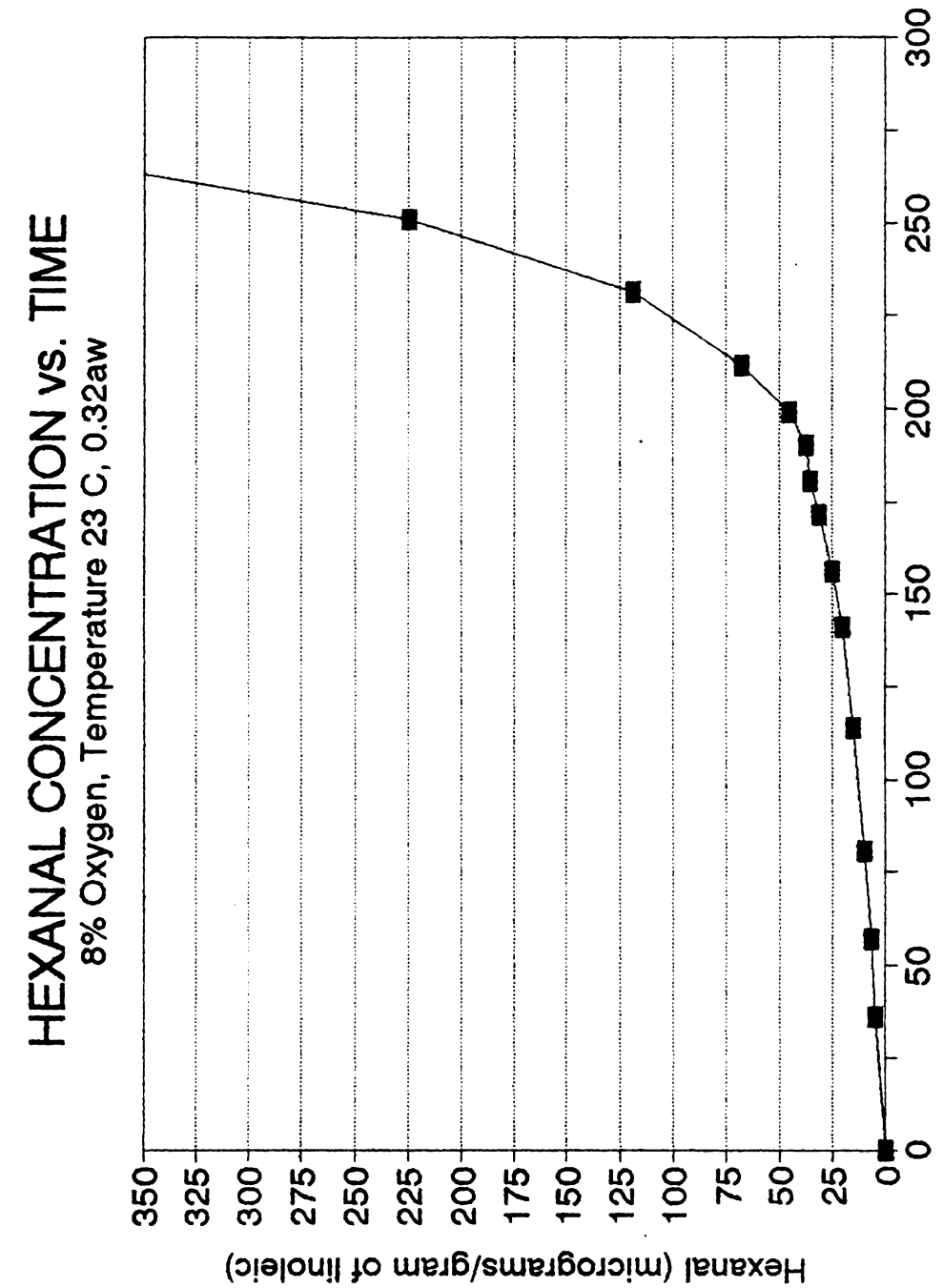

Fig. 11: Rate of Hexanal Formation at 23°C, 8% Oxygen Concentration and 0.32a_w

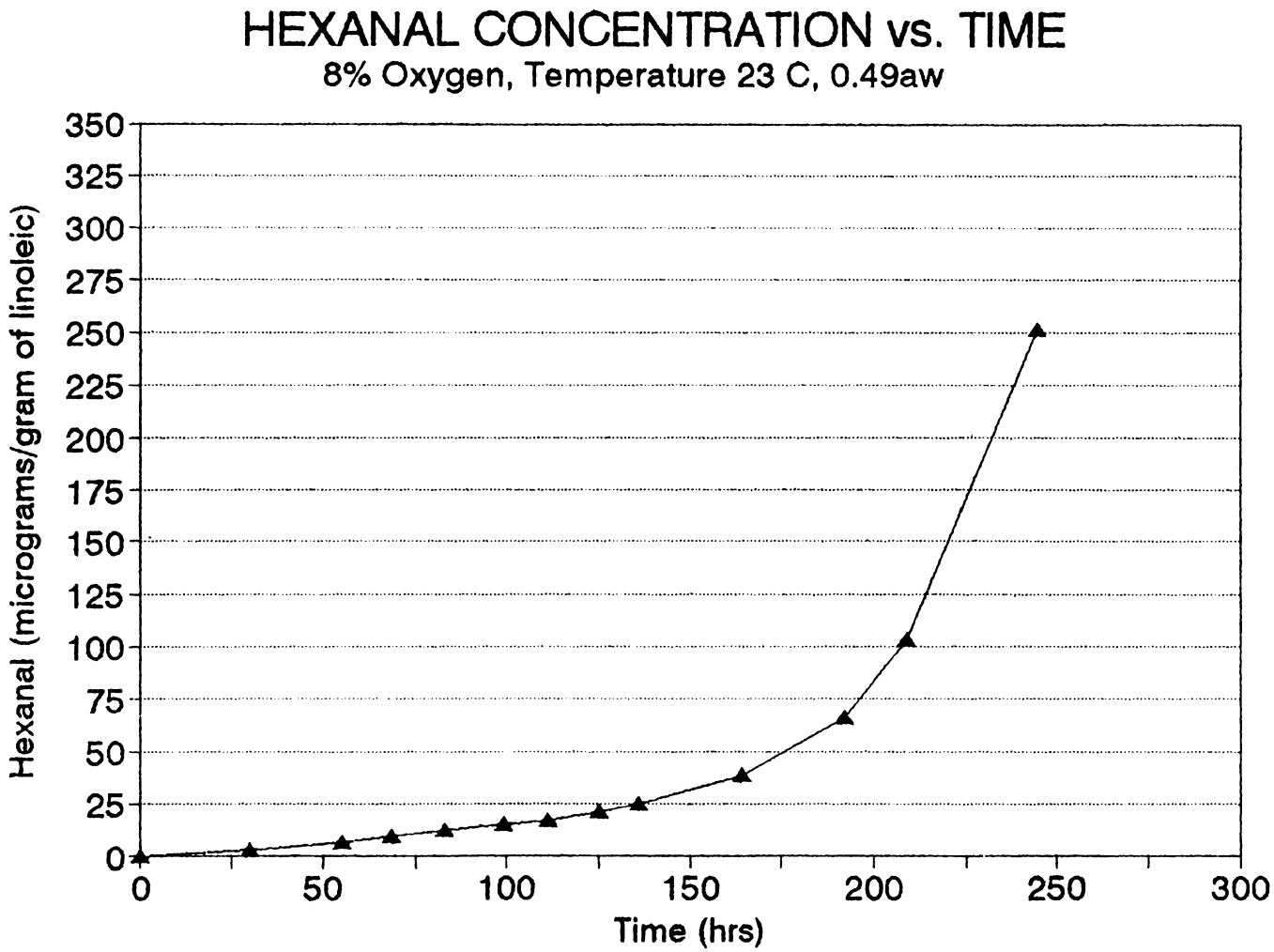

Fig. 12: Rate of Hexanal Formation at 23°C, 8% Oxygen Concentration and 0.49a_w

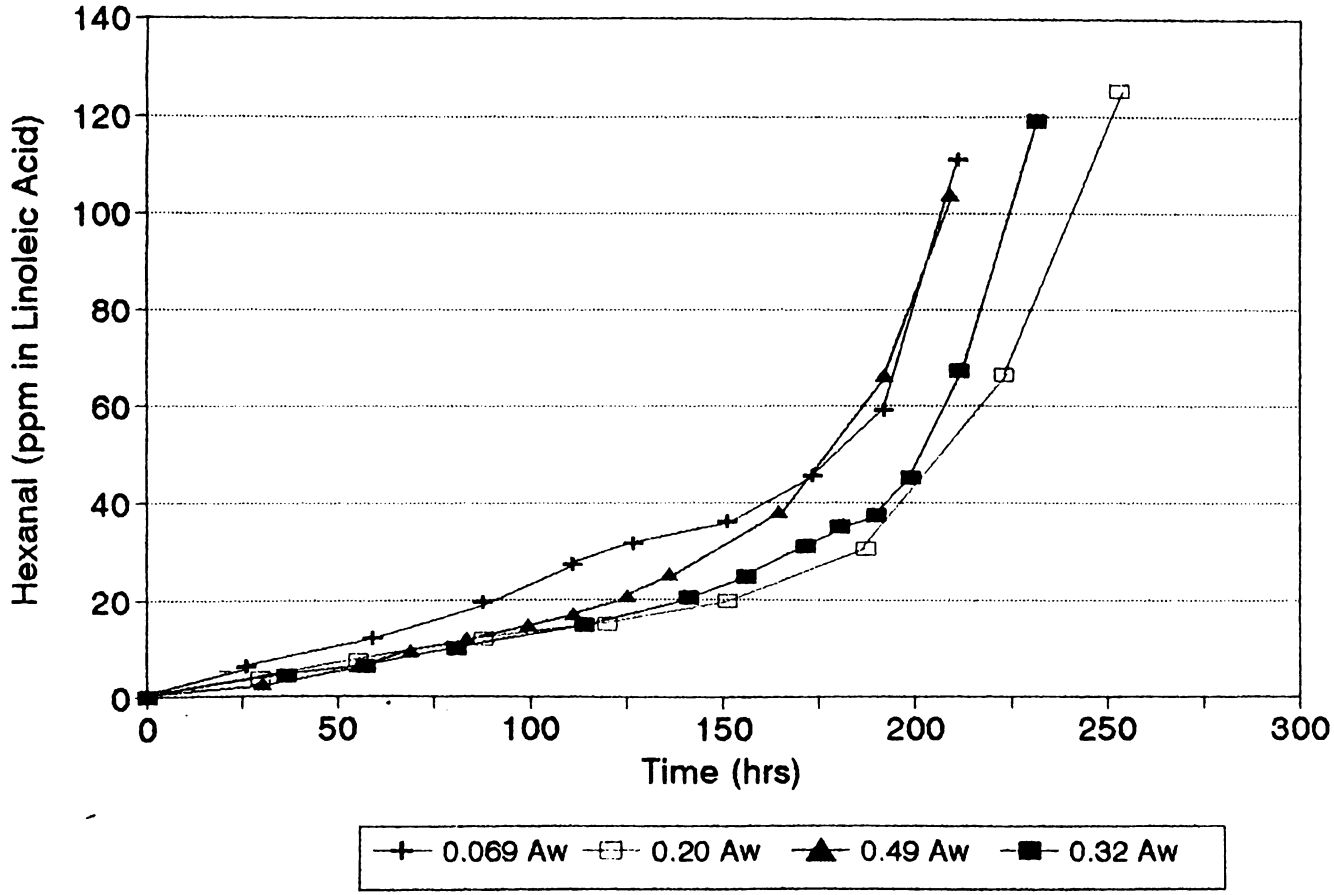

Fig. 13: Rate of Hexanal Formation at 23°C, 8% Oxygen Concentration and Four Levels of Water Activity

First Order equations describing experimental data at 40 and 66°C for 8% oxygen concentration at constant water activities are given in Tables 13-14.

Table 13
First Order Equations for 8% Oxygen Concentration and Water Activities of 0.072 and 0.24 at 40°C

Water Activity	First Order Equation	Correlation Coefficient
0.072	H_l =2.30659 exp[0.15033(t)]	0.963
0.24	H_l =2.52195 exp[0.112189(t)]	0.958

H_l =micrograms of hexanal per gram of linoleic
t =time in hours

Table 14
First Order Equations for 8% Oxygen Concentration and Water Activities of 0.062 at 66°C

Water Activity	First Order Equation	Correlation Coefficient
0.062	H_l =2.82474 exp[0.6980611(t)]	0.951
0.26	Hl =1.66522 exp[0.6885132(t)]	0.981

H_l =micrograms of hexanal per gram of linoleic
t =time in hours

Figures 14 and 15 graphically describe the effects of water activity (0.071 and 0.24a_w) on the rate of oxidation at a temperature of 40°C and oxygen concentration of 8%. Figure 16 gives a summary of these experimental results. Figures 17 and 18 show the results of the water activities 0.062 and 0.26 at 66°C and 8% oxygen concentration. These two curves are illustrated in Figure 19 for comparison.

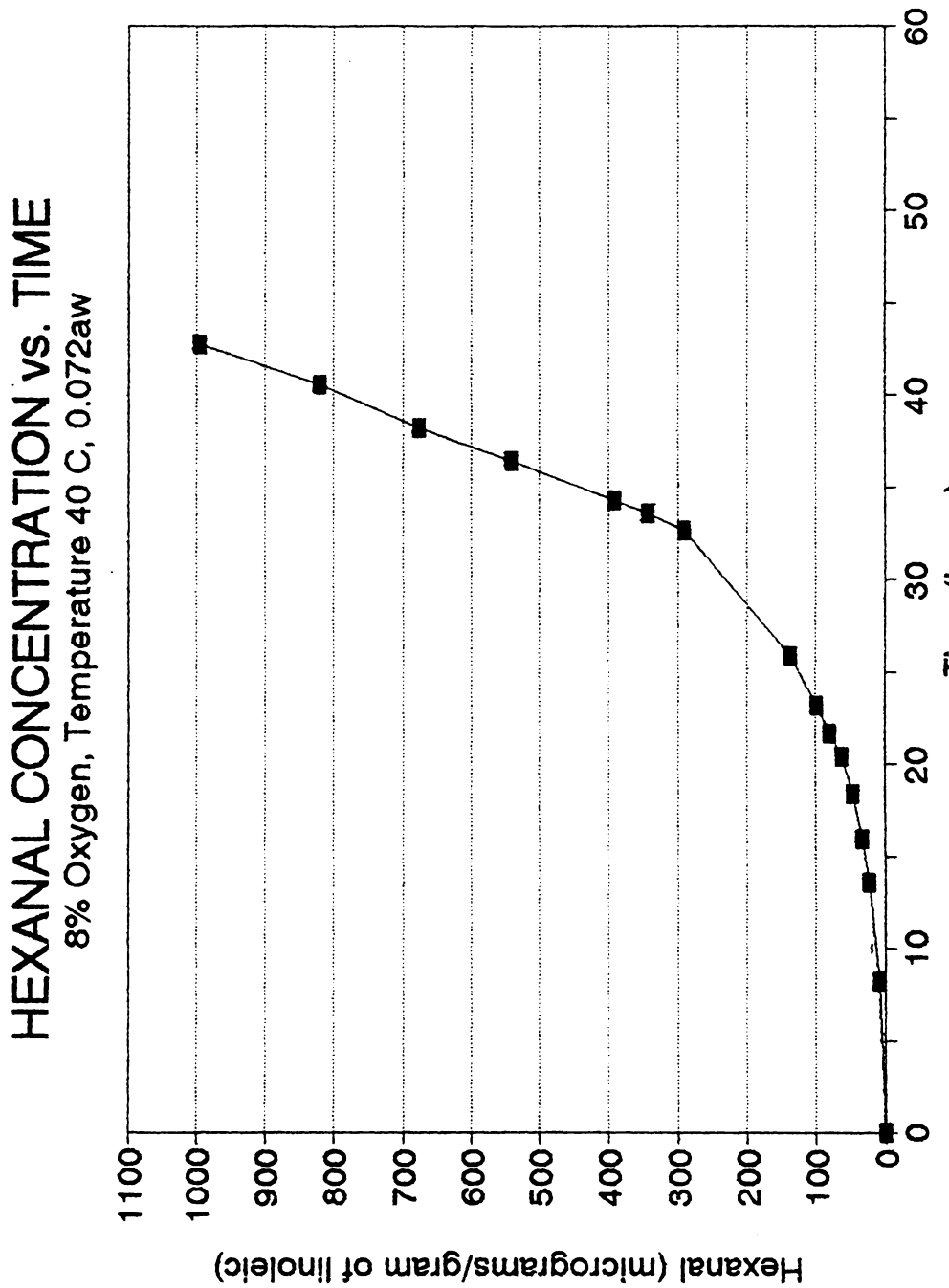

Fig. 14: Rate of Hexanal Formation at 40°C, 8% Oxygen Concentration and 0.072a_w

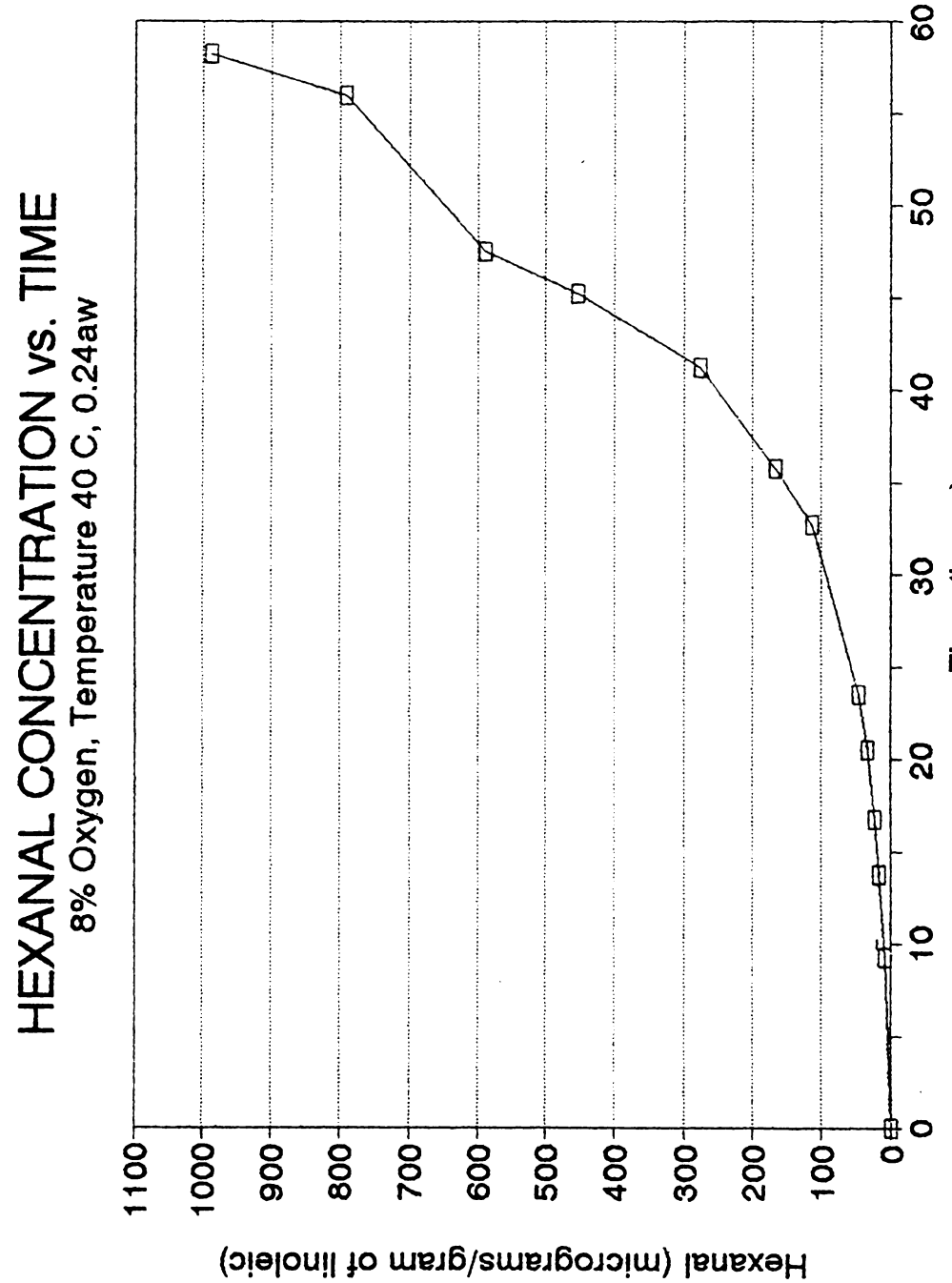

Fig. 15: Rate of Hexanal Formation at 40°C, 8% Oxygen Concentration and 0.24a_w

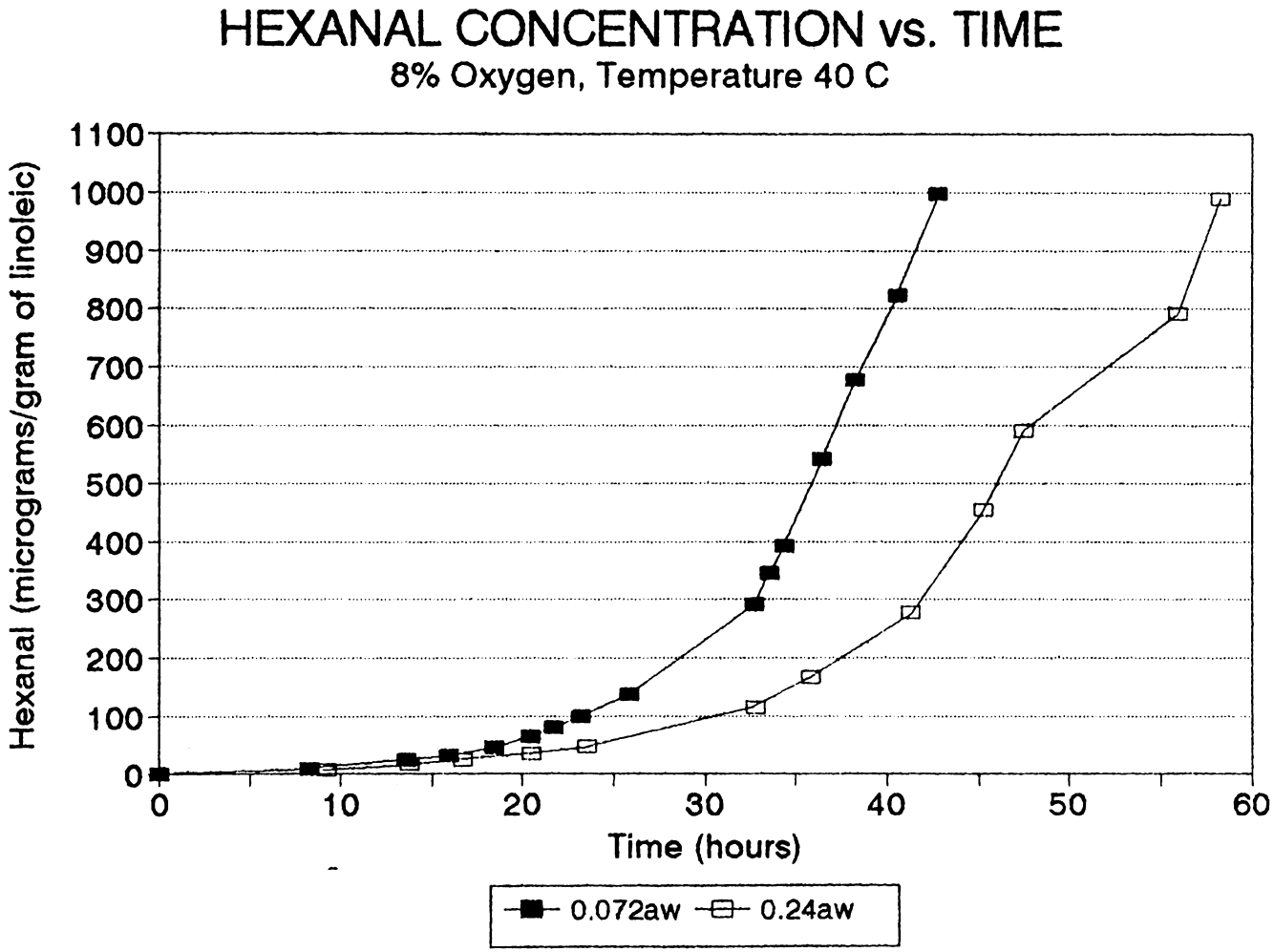

Fig. 16: Rate of Hexanal Formation at 40°C, 8% Oxygen Concentration and Two Levels of Water Activity

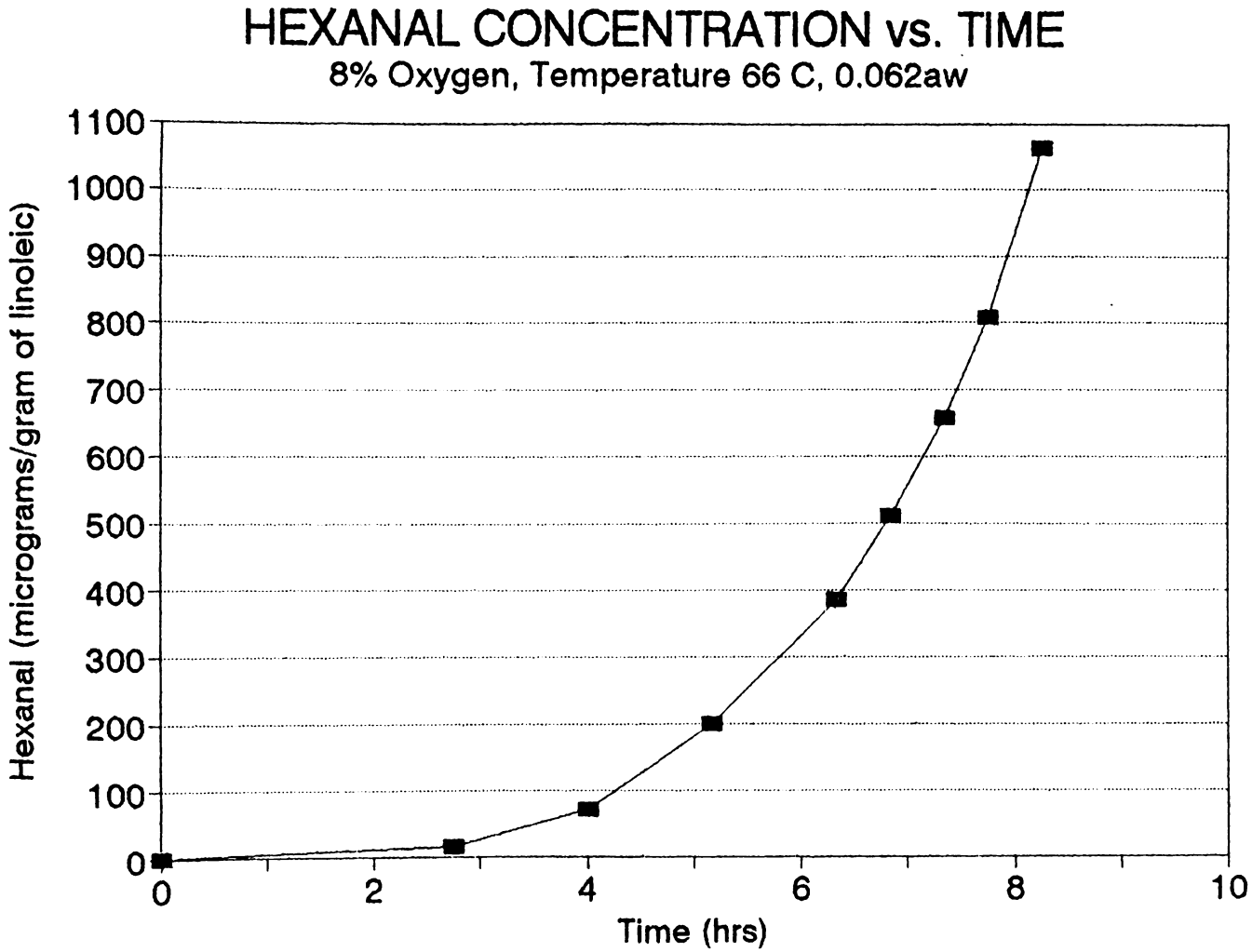

Fig. 17: Rate of Hexanal Formation at 66°C, 8% Oxygen Concentration and 0.062a_w

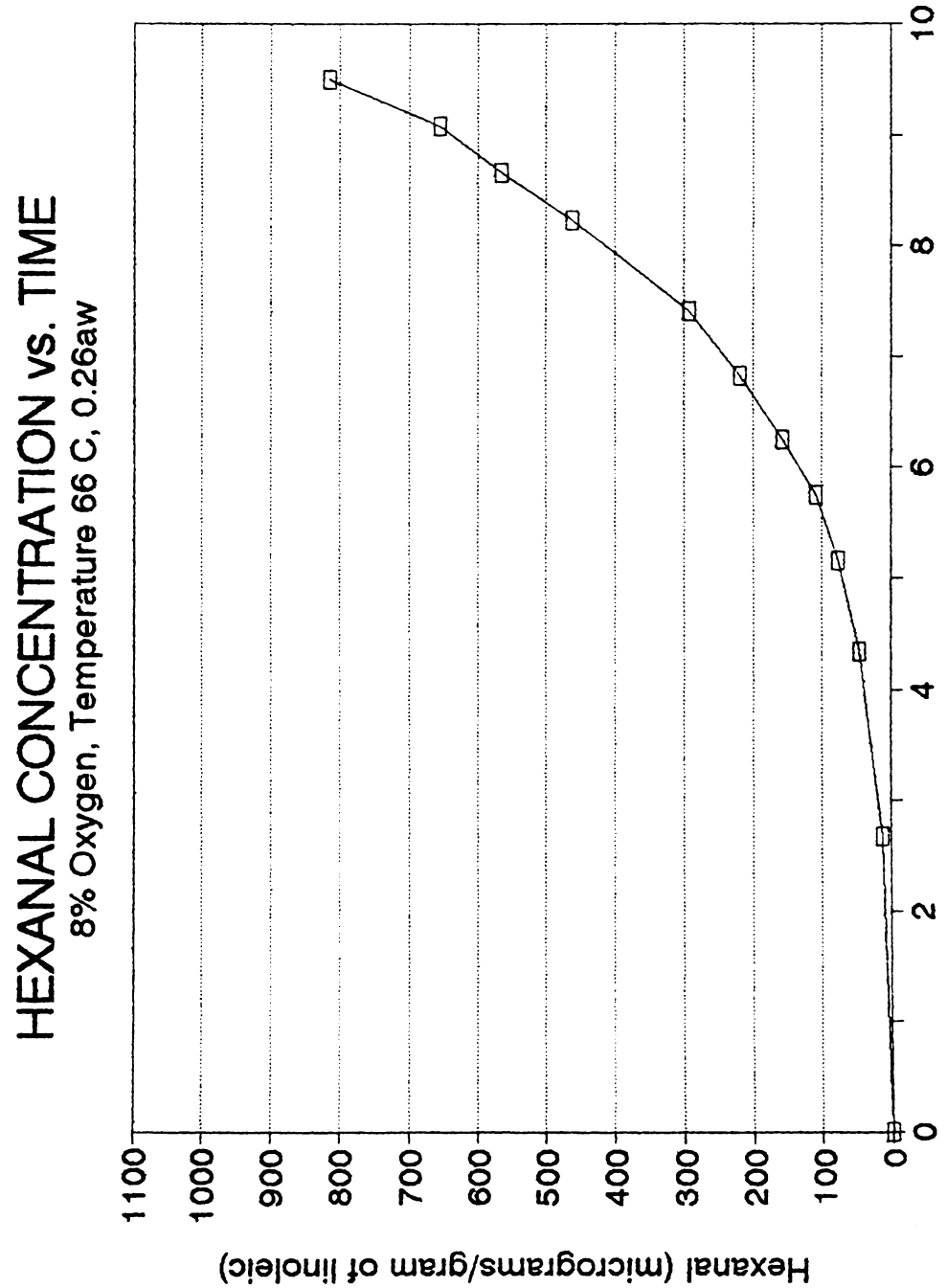

Fig. 18: Rate of Hexanal Formation at 66°C, 8% Oxygen Concentration and 0.26a_w

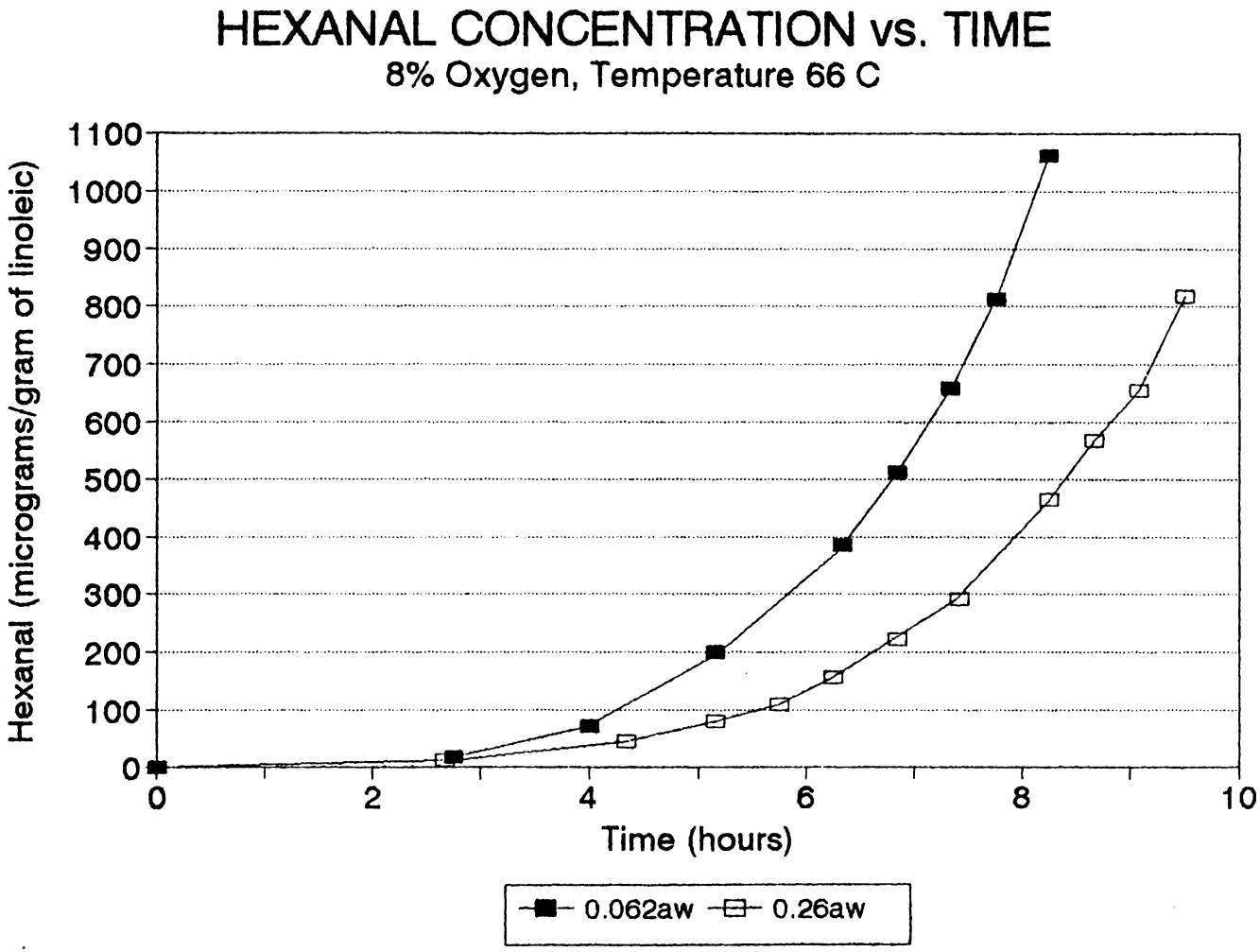

Fig. 19: Rate of Hexanal Formation at 66°C, 8% Oxygen Concentration and Two Levels of Water Activity

Table 15 gives the first order equations for each water activity at an oxygen concentration of 1.5% and a temperature of 66°C.

Table 15
First Order Equations for 1.51% Oxygen Concentration and Water Activities of 0.071, 0.21, 0.30, and 0.51 at 66°C

Water Activity	First Order Equation	Correlation Coefficient
0.071	H_l =2.56628 exp[0.5105221(t)]	0.941
0.21	H_l =2.29798 exp[0.4504038(t)]	0.954
0.30	H_l =3.00479 exp[0.4548029(t)]	0.931
0.53	H_l =2.28217 exp[0.5041664(t)]	0.951

H_l =micrograms of hexanal per gram of linoleic
t =time in hours

Figures 20-23 show the curves developed from the results of the experiments performed at an oxygen concentration of 1.5%, a temperature of 66°C and water activities of 0.071, 0.21, 0.30, and 0.53. The summary of the above curves is shown as a single plot in Figure 24.

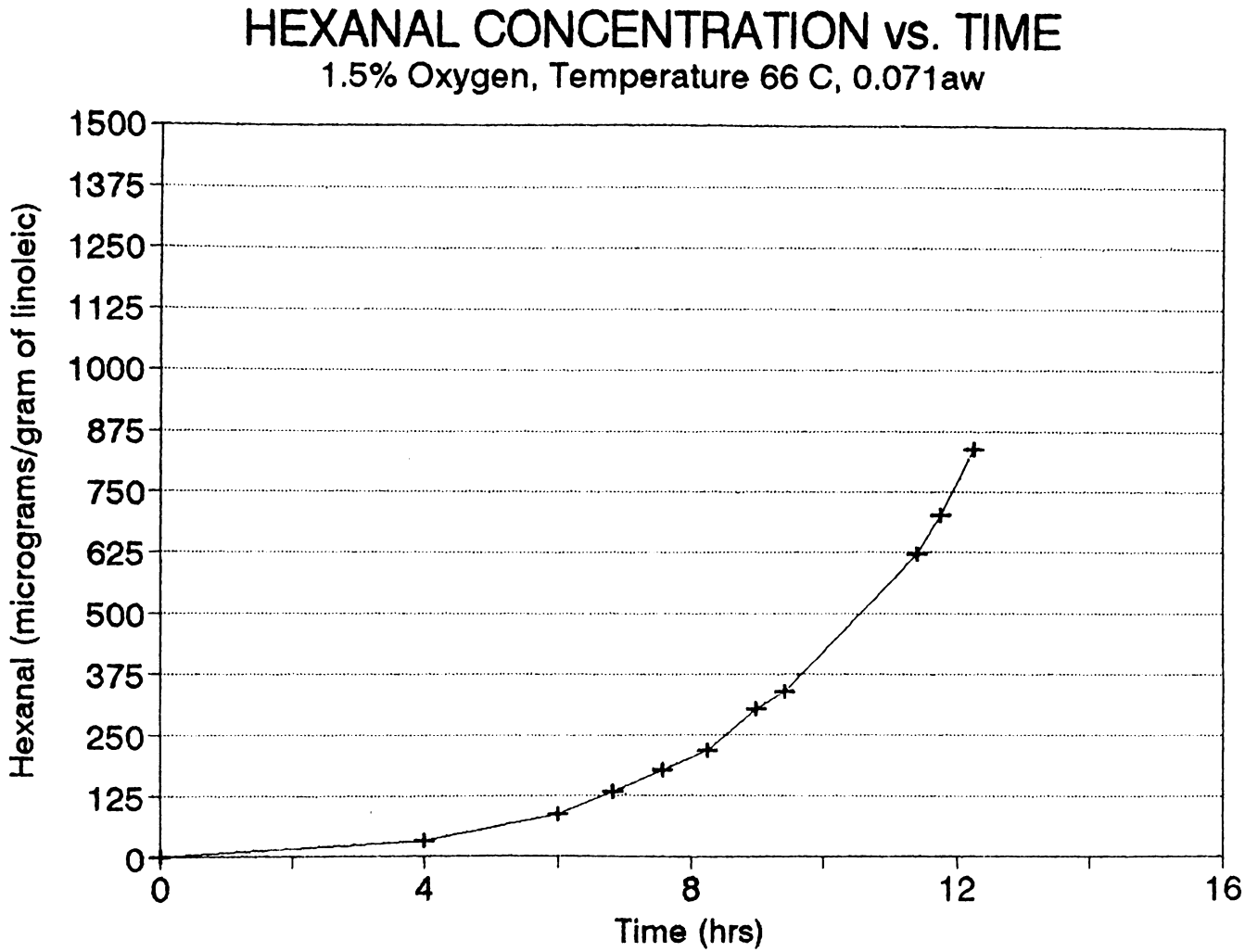

Fig. 20: Rate of Hexanal Formation at 66°C, 1.5% Oxygen Concentration and 0.071a_w

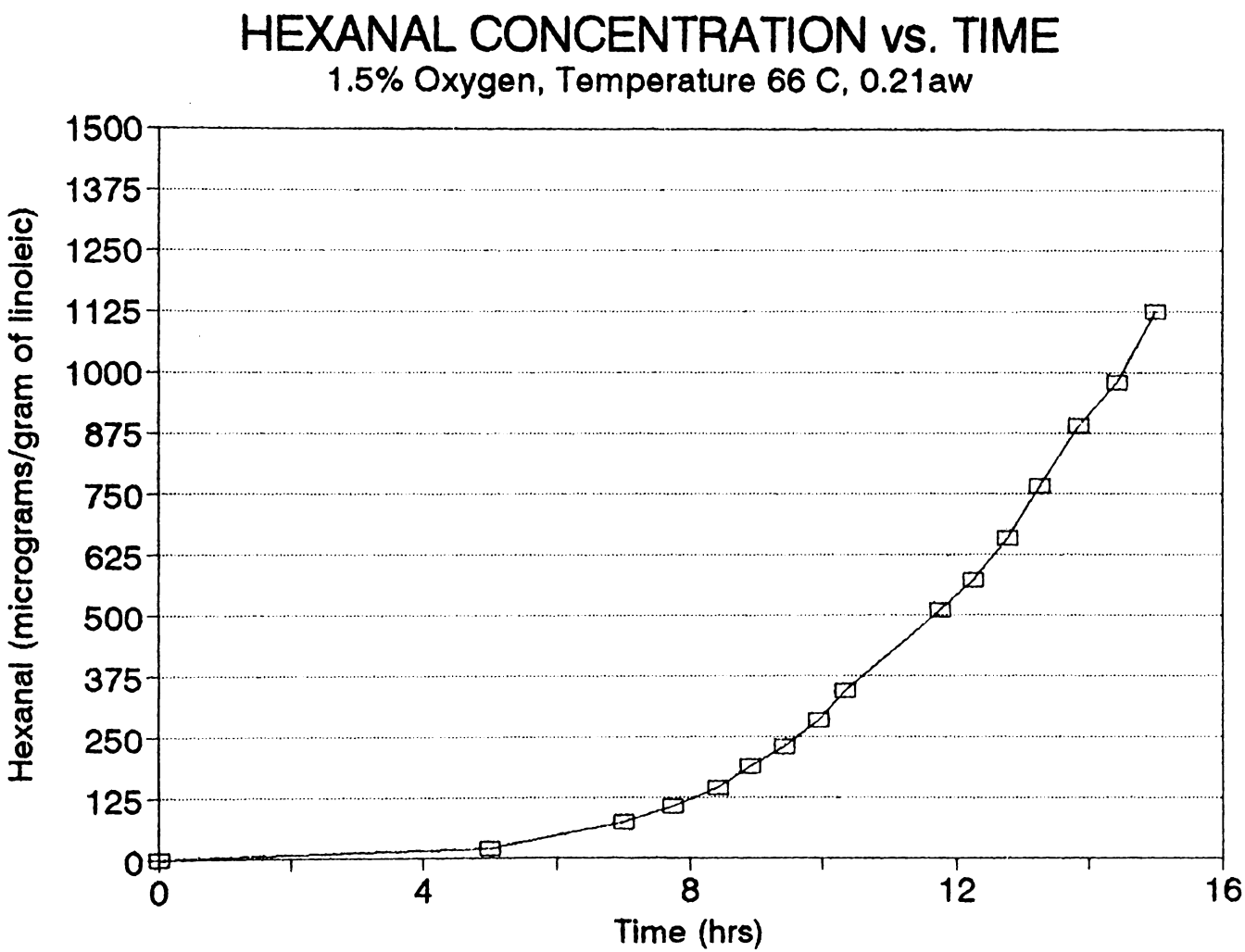

Fig. 21: Rate of Hexanal Formation at 66°C, 1.5% Oxygen Concentration and 0.21a_w

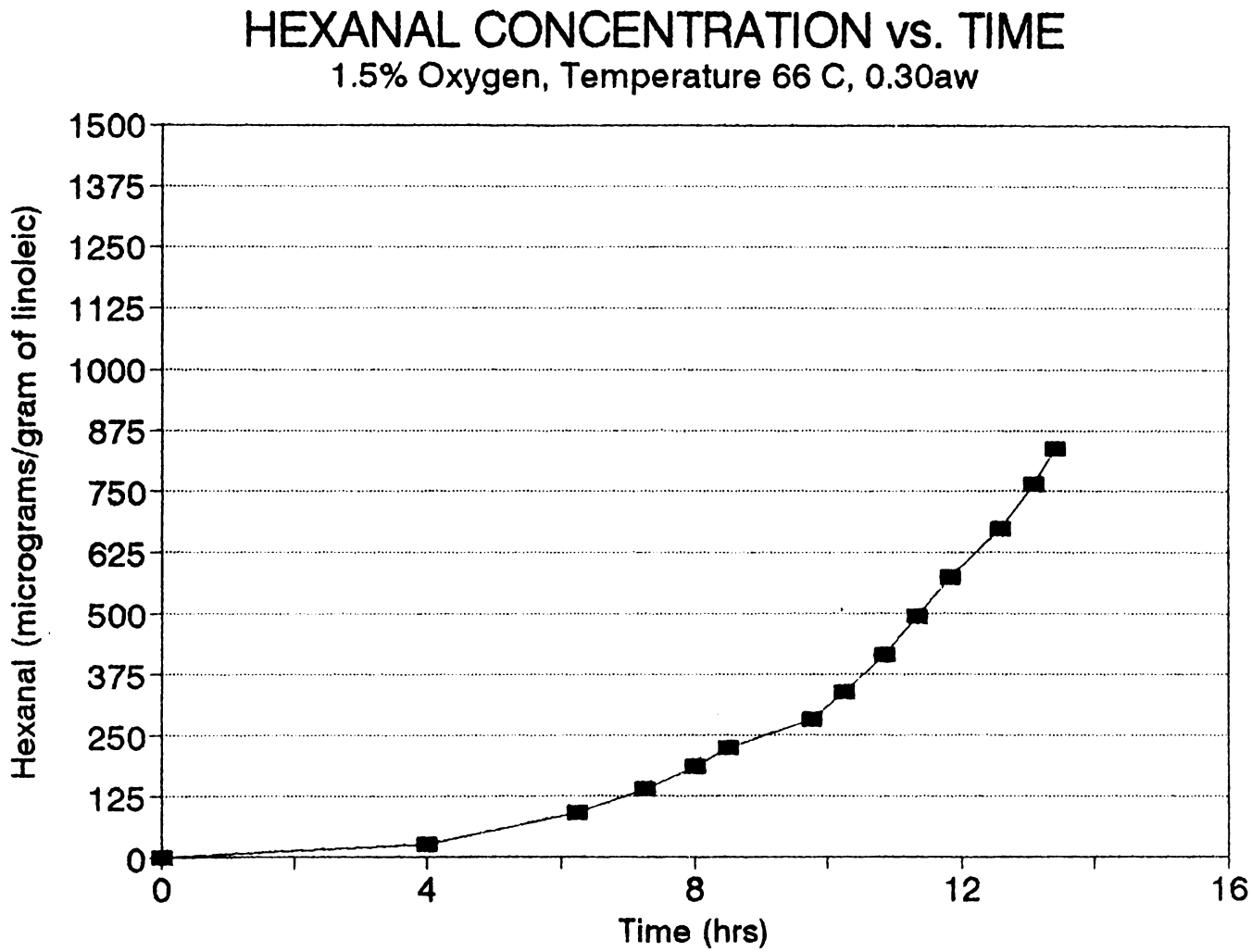

Fig. 22: Rate of Hexanal Formation at 66°C, 1.5% Oxygen Concentration and 0.30a_w

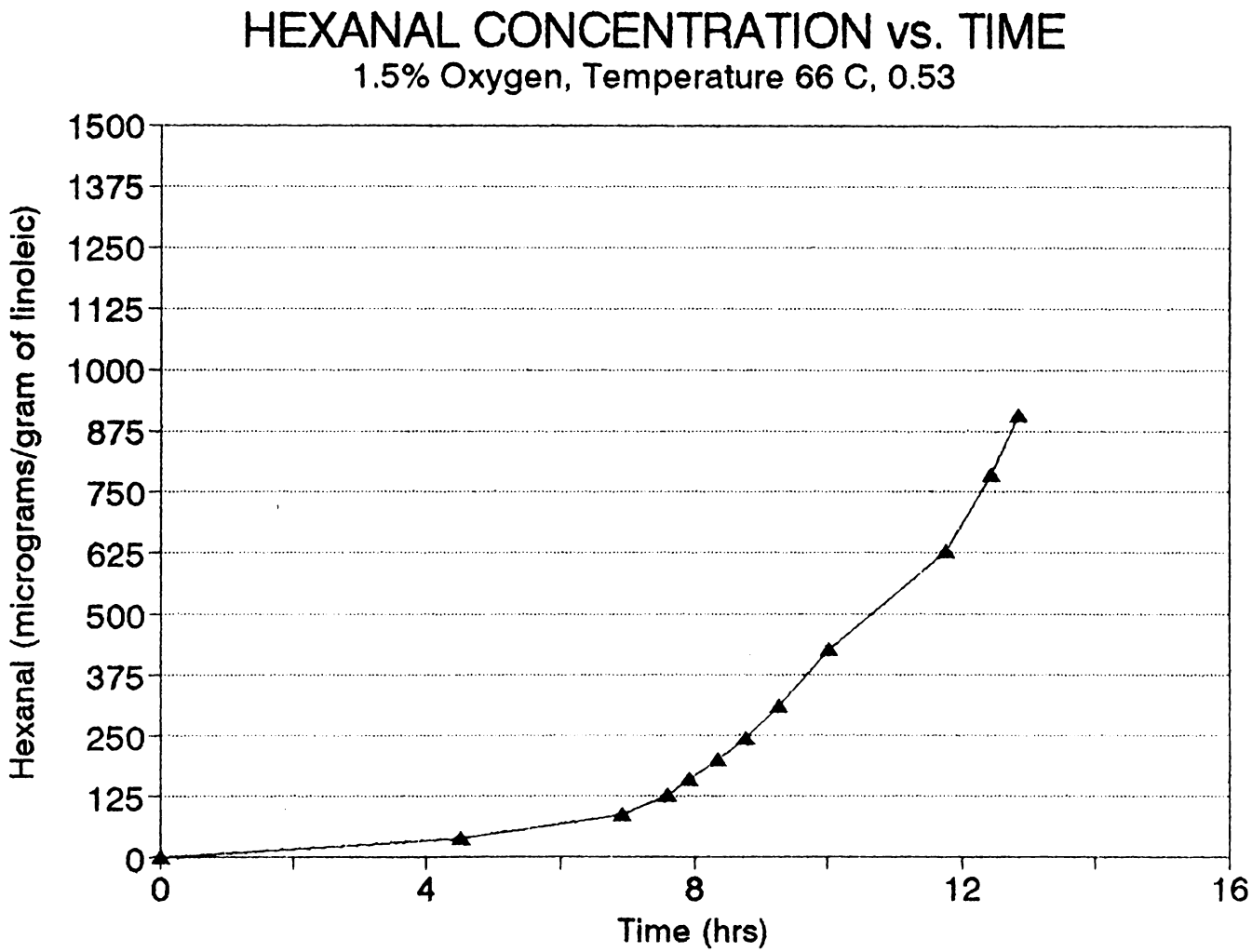

Fig. 23: Rate of Hexanal Formation at 66°C, 1.5% Oxygen Concentration and 0.53a_w

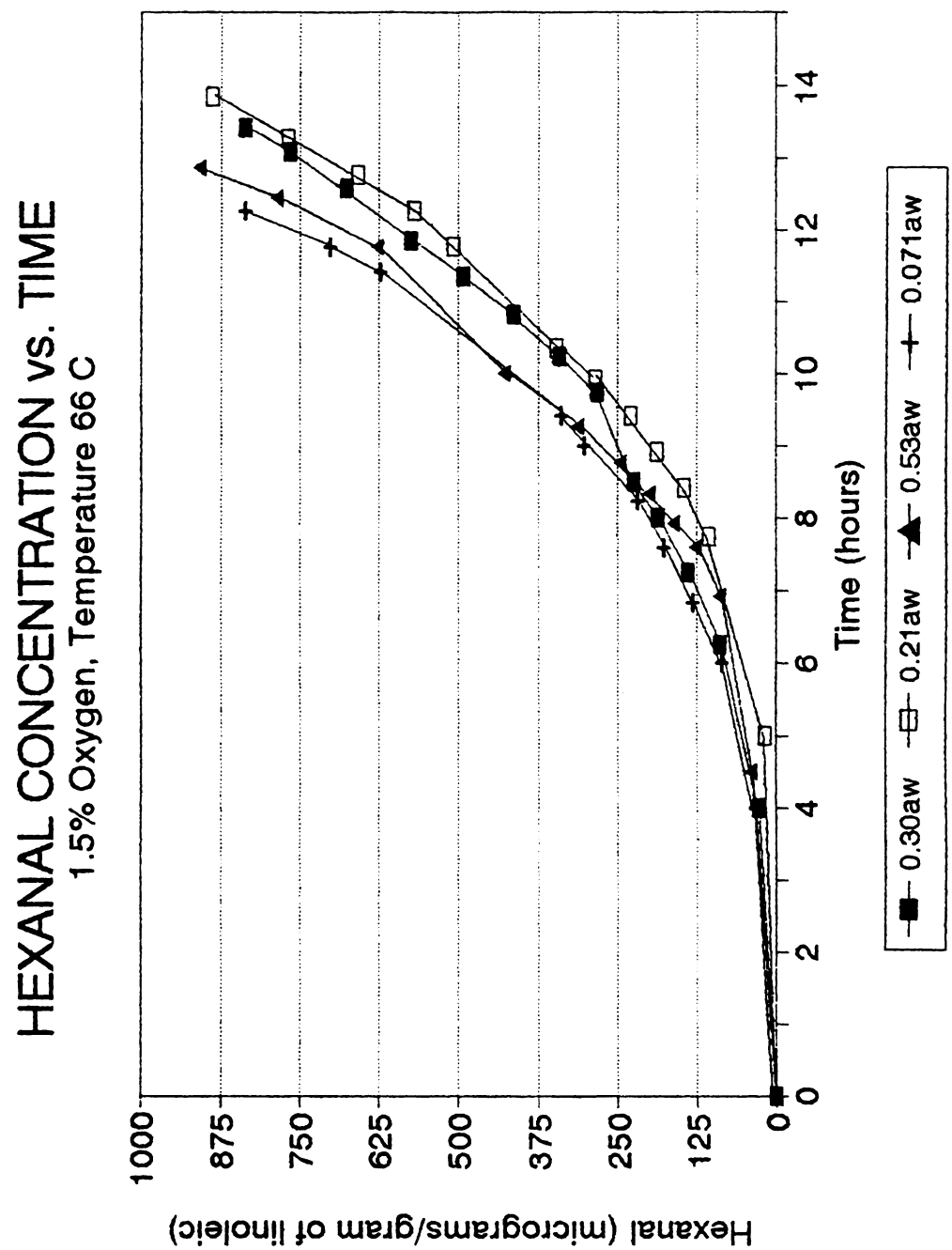

Fig. 24: Rate of Hexanal Formation at 66°C, 1.5% Oxygen Concentration and Four Levels of Water Activity

Determination of Hexanal Concentration at Specific Time Intervals

Hexanal concentration was calculated at several time intervals to compare experimental results. Hexanal concentration was determined using the first order rate expressions derived from the experimental data figures. This was used as a reference to compare the amount of hexanal (micrograms/gram) produced at each constant water activity under the same oxygen and temperature conditions. Tables 16-18 give the predicted hexanal concentration values for experiments conducted at 8% oxygen concentration under temperatures of 23, 40, and 66°C, respectively. Table 19 gives the predicted hexanal values for the experiment performed at 1.5% oxygen concentration and a temperature of 66°C.

Table 16
Predicted Hexanal Concentration Values Using First Order Rate Equations at an Oxygen Concentration of 8% and Temperature of 23°C

	Time (hours)			
Water Activity	50	100	150	200
	Hexanal (micrograms/gram)			
0.069	5.866	16.778	47.987	137.249
0.20	3.967	9.945	24.928	62.484
0.32	3.849	9.912	25.531	65.761
0.49	4.444	12.350	34.319	95.364

Table 17
Predicted Hexanal Concentration Values Using First Order Rate Equations at an Oxygen Concentration of 8% and Temperature of 40°C

	Time (hours)			
Water Activity	10	20	30	40
	Hexanal (micrograms/gram)			
0.072	10.371	46.635	209.698	942.627
0.24	7.744	23.779	73.017	224.212

Table 18
Predicted Hexanal Concentration Values Using First Order Rate Equations at an Oxygen Concentration of 8% and Temperature of 66°C

	Time (hours)			
Water Activity	2	4	6	8
	Hexanal (micrograms/gram)			
0.062	11.410	46.093	186.192	752.126
0.26	6.599	26.154	103.651	410.782

Table 19
Predicted Hexanal Concentration Values Using First Order Rate Equations at an Oxygen Concentration of 1.5% and Temperature of 66°C

Water Activity	Time (hours) 3	6	9	12
	Hexanal (micrograms/gram)			
0.071	11.870	54.904	253.954	1174.646
0.21	8.875	34.276	132.378	511.258
0.30	11.759	46.017	180.085	704.749
0.53	10.356	47.998	213.283	967.894

The predicted hexanal concentrations at the specific time intervals are represented as bar graphs. Figures 25-27 show the summary of predicted hexanal concentrations using the first order rate expressions for experiments performed under a oxygen concentration of 8% and temperatures of 23, 40, 66°C, respectively. The predicted data for 1.5% oxygen concentration at 66°C is given in Figure 28.

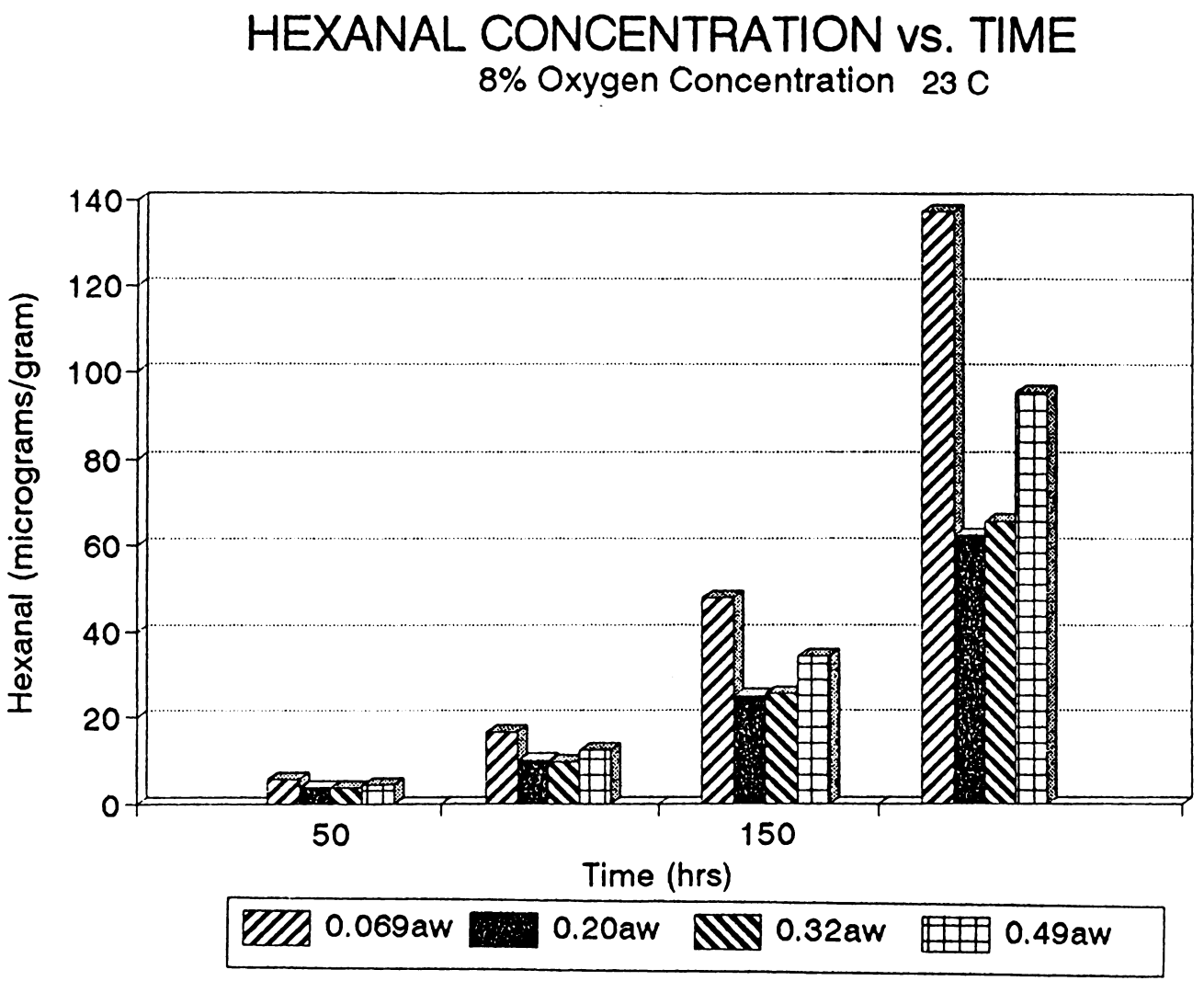

Fig. 25. Predicted Hexanal Concentrations at Specific Time Intervals Using First Order Expressions

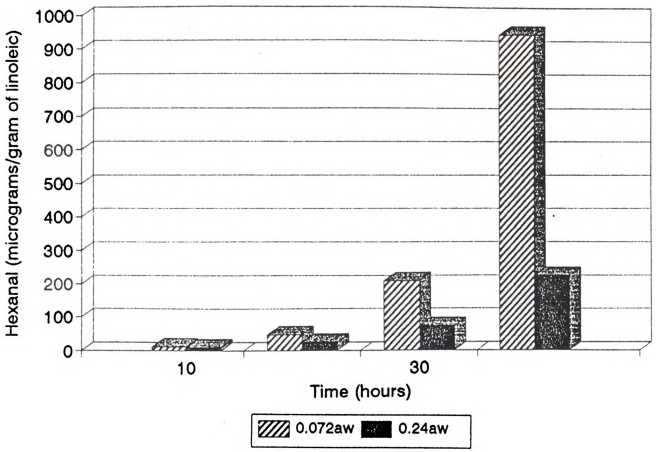

Fig. 26: Predicted Hexanal Concentrations at Specific Time Intervals Using First Order Expressions

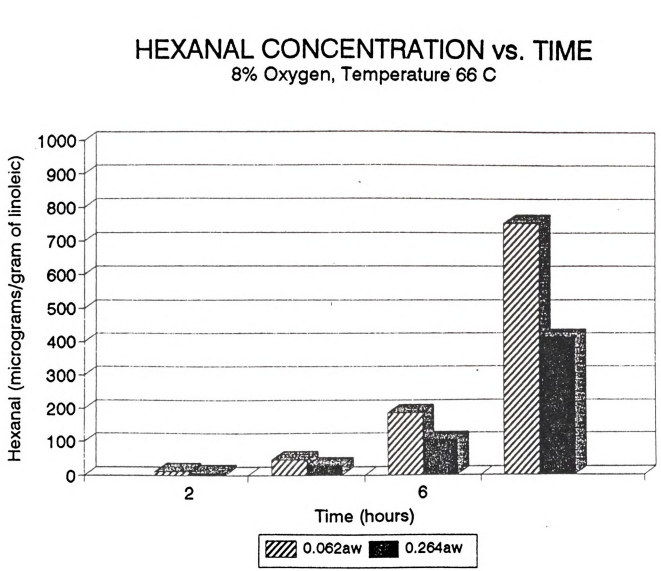

Fig. 27: Predicted Hexanal Concentrations at Specific Time Intervals Using First Order Expressions

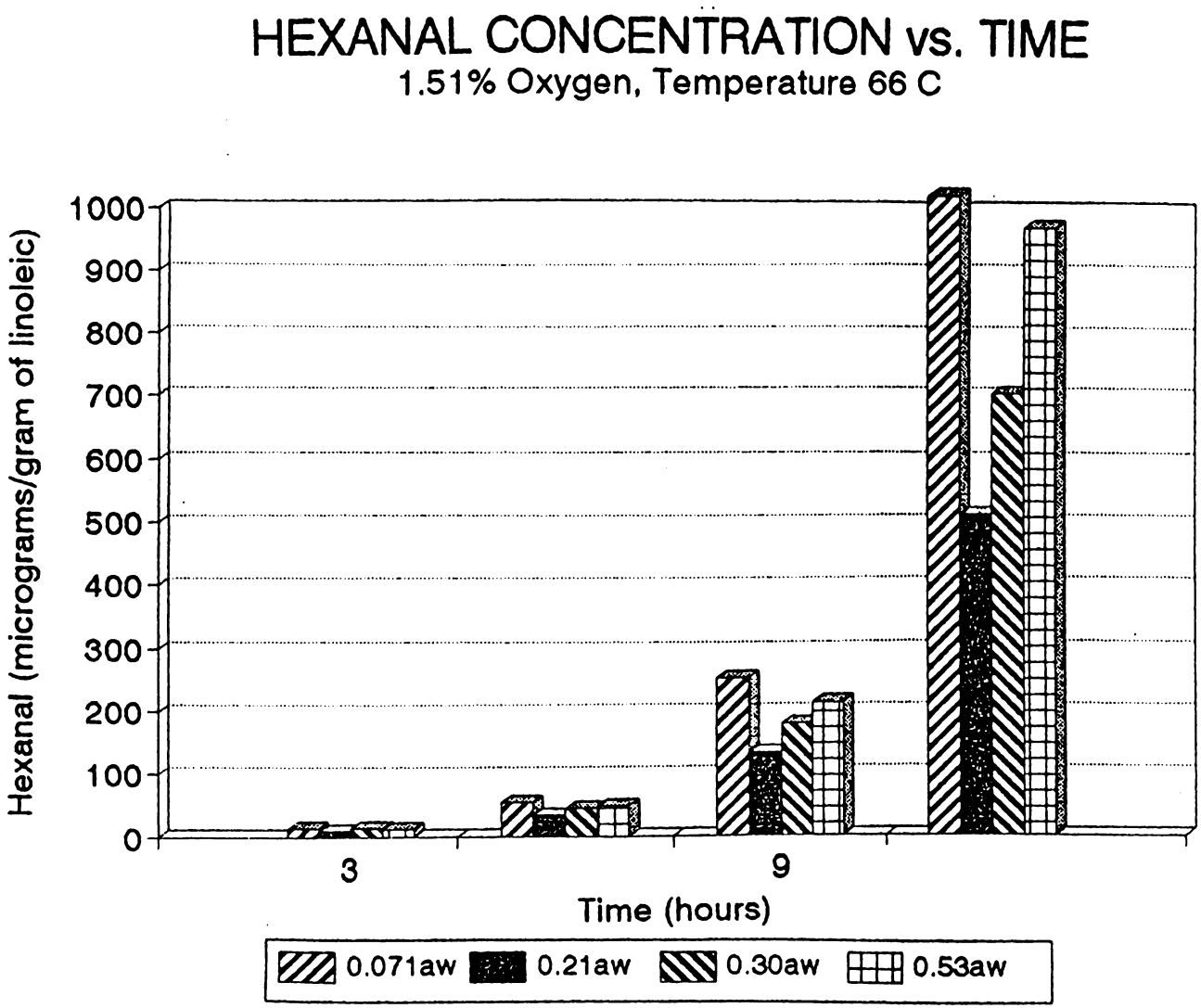

Fig. 28: Predicted Hexanal Concentrations at Specific Time Intervals Using First Order Expressions

Effect of Temperature on the Rate of Lipid Oxidation

A comparison of rate constants for lipid oxidation at three temperatures (23, 40 and 66°C) and at two different water activity ranges (0.06-0.07a_w and 0.2-0.26a_w) for an oxygen concentration of 8% was made by constructing an Arrhenius plot (Figure 29). When the ln of the rate constants (slope of the first order equations) were plotted against 1/T, where T is degrees Kelvin, straight lines were obtained. From the straight lines of the Arrhenius plot, activation energy (E_a) was calculated using the following equation:

$$Ea = slope * R \qquad (19)$$

where: R =gas constant (1.98 cal/deg-mole)

Activation energy was 15.9 kcal/mole for the low water activity range (0.06-0.07) and 16.6 kcal/mole for the intermediate water activity range (0.2-0.26). These results are consistent with the activation energy (19 kcal/mole) calculated from the studies performed by Berger (1971) on the oxygen uptake of potato chips as cited by Quast and Karel (1972). These results show that a small change in temperature can have a significant effect on the rate of lipid oxidation. Therefore, ambient temperatures could be used for accelerated stability tests. These plots also gave high correlation coefficients, showing that good prediction of the time required for the onset of rancidity can be

determined at any temperature.

The lower activation energy (15.9 kcal/deg) at the low water activity range compared to the higher activation energy (16.6 kcal/deg) at the moderate water activity range suggests that the oxidation reaction is thermodynamically more difficult at a water activity near the B.E.T. monolayer value. This difference in activation energies of approximately 700 cal/deg could be due to energies needed to disrupt hydrogen bonding, exposing reactive sites for oxygen near the B.E.T. monolayer moisture content. The experimental data and calculations are given in Appendix G.

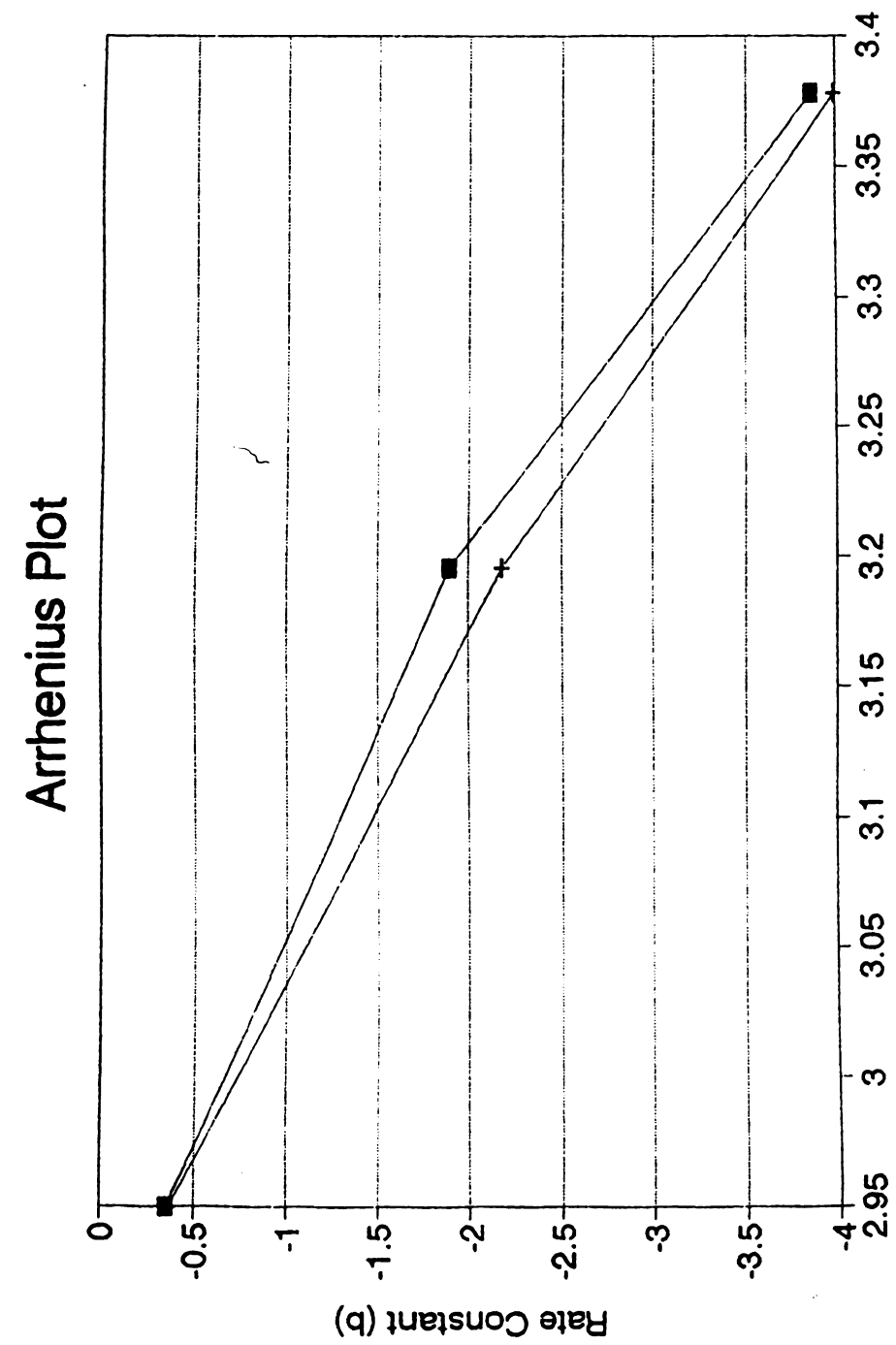

Fig. 29: Arrhenius Plot of Reaction Rate b vs. Inverse Absolute Temperature at 23, 40 and 66°C and Two Different a_w Ranges (0.06-0.07 and 0.2-0.26)

Effect of Water Activity on the Rate of Lipid Oxidation

The first order rate expressions ($y=a_1e^{bx}$; where y is hexanal concentration; x is time; a is the y-intercept; b is the slope), derived from the experimental data figures of hexanal concentration versus time, described the rates of oxidation. The slope (b) of the first order rate equation was used to describe the rate of oxidation at each experimental condition. A plot of the rate of oxidation (y-axis; first order rate equations) versus water activity (x-axis) was developed to show the effects of water activity on the rate of lipid oxidation. Tables 20-23 give the plot data for the rates of lipid oxidation for an oxygen concentration of 8% and temperatures of 23, 40 and 66°C, respectively.

Table 20
Rate of Oxidation Versus Water Activity at 8% Oxygen Concentration and 23°C

Water Activity	Rate of Oxidation
0.069	0.0210
0.20	0.0183
0.32	0.0189
0.49	0.0204

Table 21
Rate of Oxidation Versus Water Activity at 8% Oxygen Concentration and 40°C

Water Activity	Rate of Oxidation
0.072	0.1503
0.24	0.1121

Table 22
Rate of Oxidation Versus Water Activity at 8% Oxygen Concentration and 66°C

Water Activity	Rate of Oxidation
0.062	0.6980
0.26	0.6885

Table 23
Rate of Oxidation Versus Water Activity at 1.5% Oxygen Concentration and 66°C

Water Activity	Rate of Oxidation
0.071	0.5105
0.21	0.4504
0.30	0.4548
0.53	0.5041

Figures 30-32 give a summary of the effect of water activity on the rate of lipid oxidation for an oxygen concentration of 8% and temperatures of 23, 40 and 66°C. Figure 33 shows the effect of water activity on the rate of lipid oxidation for an oxygen concentration of 1.5% and temperature of 66°C.

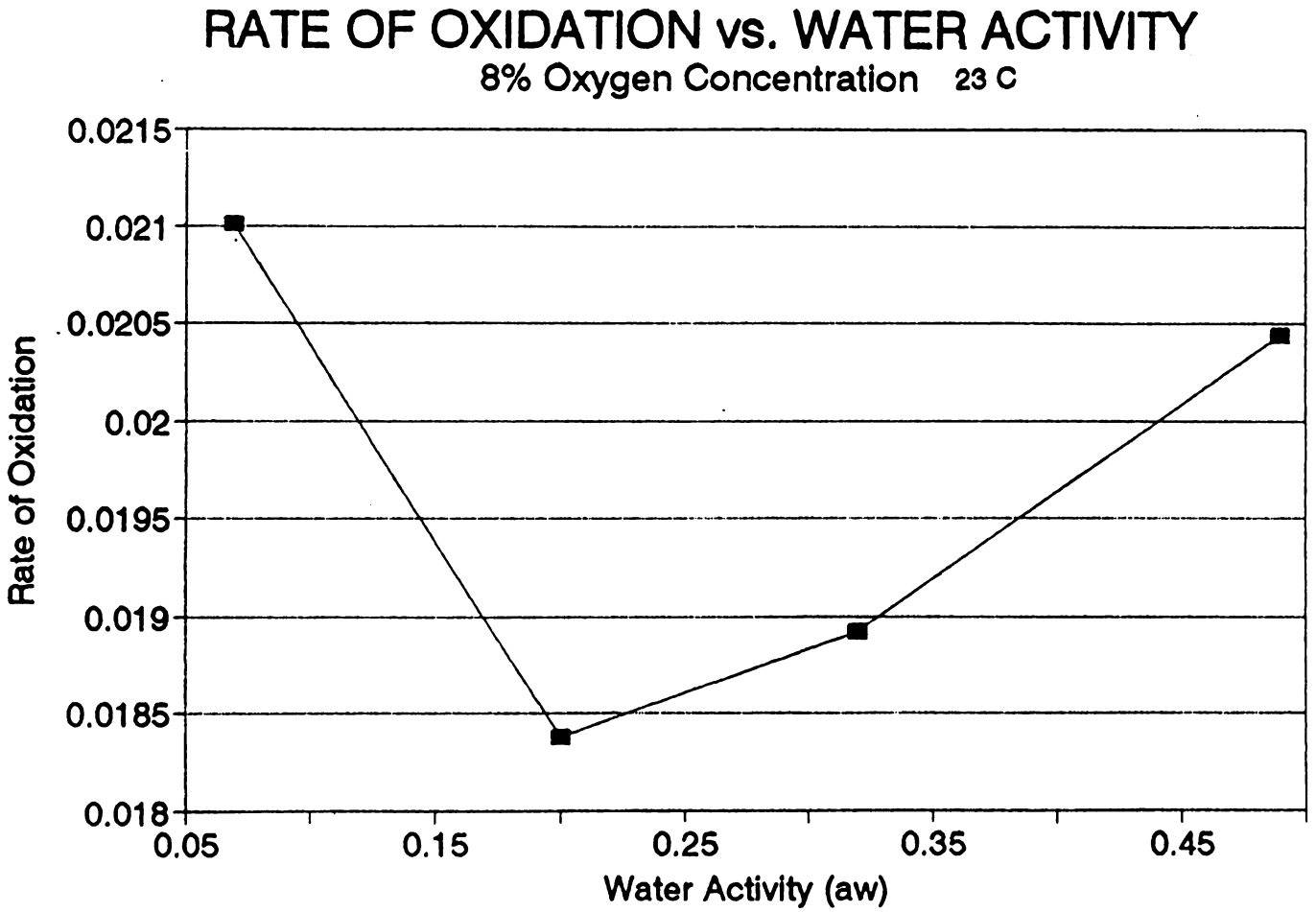

Fig. 30: Rate of Oxidation (slope of first order expression) as a Function of Water Activity

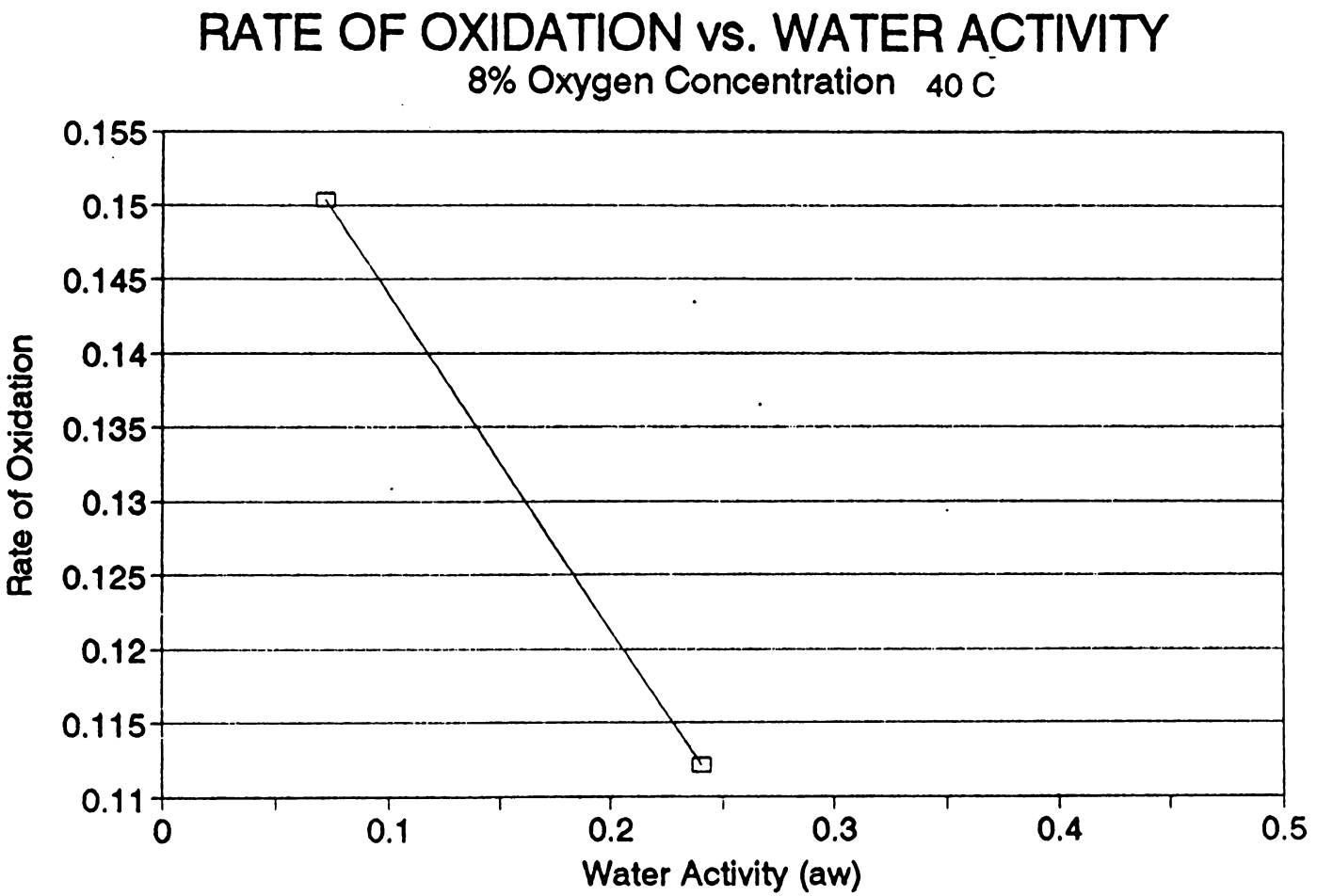

Fig. 31: Rate of Oxidation (slope of first order expression) as a Function of Water Activity

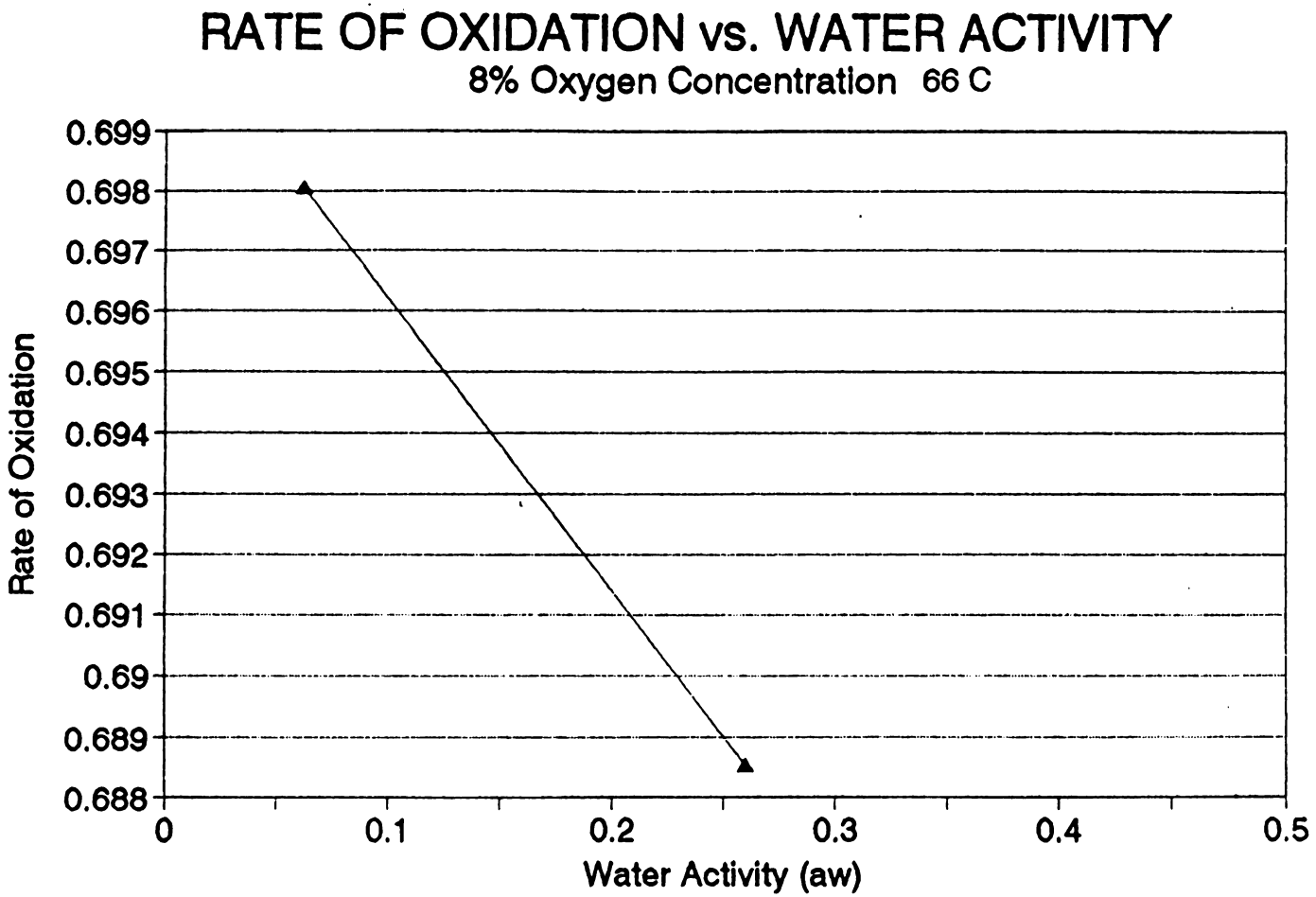

Fig. 32: Rate of Oxidation (slope of first order expression) as a Function of Water Activity

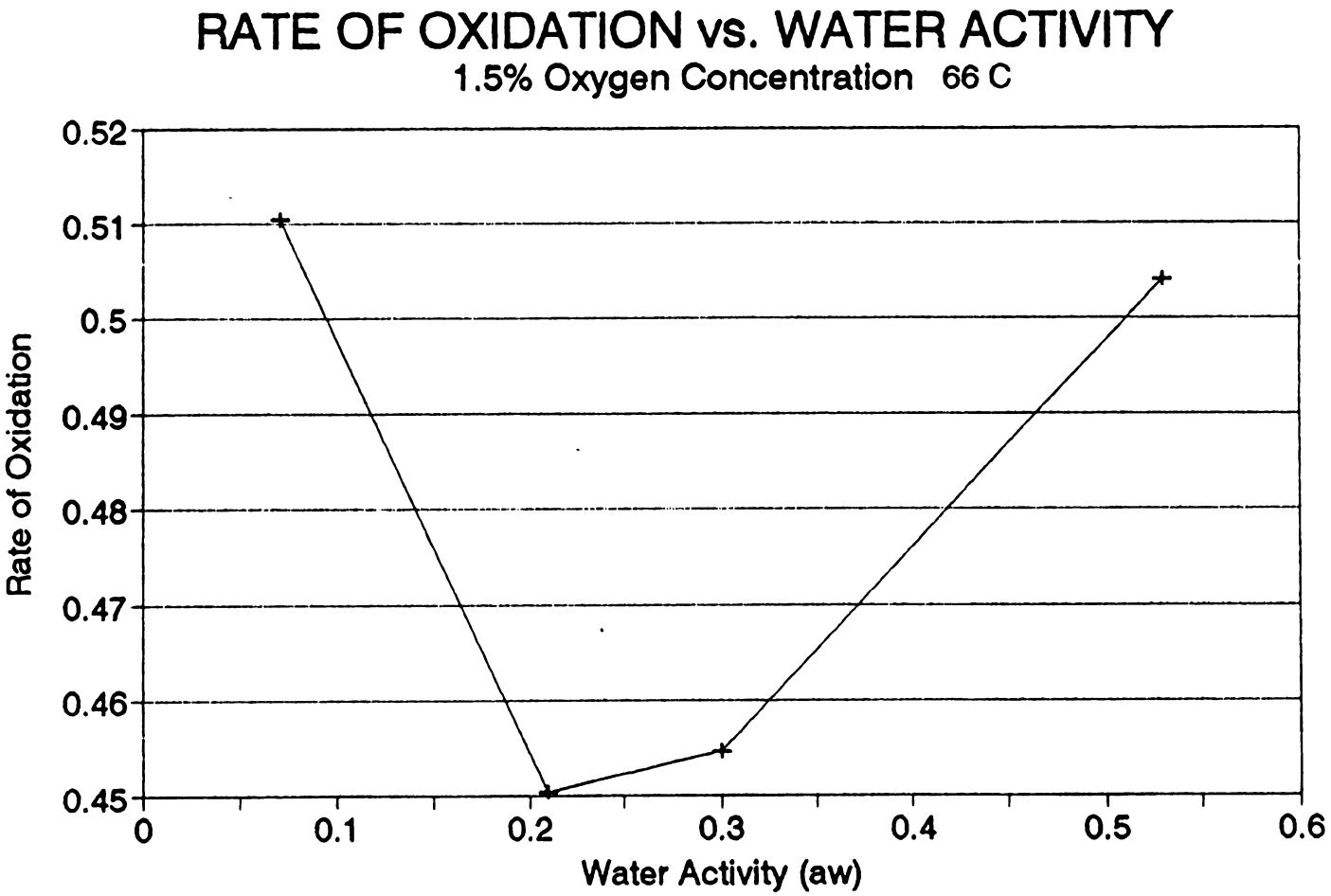

Fig. 33: Rate of Oxidation (slope of first order expression) as a Function of Water Activity

Product Shelf-Life Prediction

The shelf-life of the product model was determined by calculating the time for hexanal to reach a certain concentration. In a dehydrated food product containing substantial quantities of linoleic acid, a hexanal concentration of 5 -10 ppm was found to indicate a significant deterioration due to lipid oxidation (Fritsch and Gale, 1977). Attempting to predict shelf-life of a product as a function of a single off-flavor compound is presumptuous, however, hexanal can be a useful measurement for determining degrees of rancidity development in potato chips (Jeon and Bassette, 1984).

Since linoleic acid comprises approximately 50% of the fatty acid content in soybean oil and other vegetable oils used in processing compared with 100% of the fatty acid composition in this study, higher concentrations of hexanal were expected to signify rancidity development. Using the first order equations that describe hexanal concentration over time, the time to reach 10, 20 and 50 micrograms of hexanal/gram of linoleic acid were calculated as an index to the onset of rancidity development. Tables 24-26 give the shelf-life prediction data for an oxygen concentration of 8% and temperatures of 23, 40 and 66°C. The shelf-life prediction data for an oxygen concentration of 1.5% and temperature of 66°C is given in Table 27.

Table 24
Time to Reach a Hexanal Concentrations of 10, 20 and 50 micrograms/gram for an Oxygen Concentration of 8% and Temperature of 23°C

Water Activity	Time to Reach Concentration (hours) 10 mg/g	20 mg/g	50 mg/g
0.069	75	108	152
0.20	100	138	188
0.32	100	137	186
0.49	90	124	168

Table 25
Time to Reach a Hexanal Concentration of 10, 20 and 50 micrograms/gram for an Oxygen Concentration of 8% and Temperature of 40°C

Water Activity	Time to Reach Concentration (hours) 10 mg/g	20 mg/g	50 mg/g
0.072	10	14	20
0.24	12	18	27

Table 26
Time to Reach a Hexanal Concentration of 10, 20 and 50 micrograms/gram for an Oxygen Concentration of 8% and Temperature of 66°C

Water Activity	Time to Reach Concentration (hours) 10 mg/g	20 mg/g	50 mg/g
0.062	1.8	2.8	4.1
0.26	2.6	3.6	4.9

Table 27
Time to Reach a Hexanal Concentration of 10, 20 and 50 micrograms/gram for an Oxygen Concentration of 1.5% and Temperature of 66°C

Water Activity	Time to Reach Concentration (hours) 10 mg/g	20 mg/g	50 mg/g
0.071	2.7	4.0	5.8
0.21	3.3	4.8	6.8
0.30	2.6	4.2	6.2
0.53	2.9	4.3	6.1

Figures 34-36 give a graphical representation of the predicted time for the hexanal concentration to reach 10 micrograms/gram at each constant water activity, signifying the end of product shelf-life, for an oxygen concentration of 8% and temperatures of 23, 40 and 66°C, respectively. Figure 37 shows the summary of experimental data for shelf-life prediction at an oxygen concentration of 1.5% and temperature of 66°C.

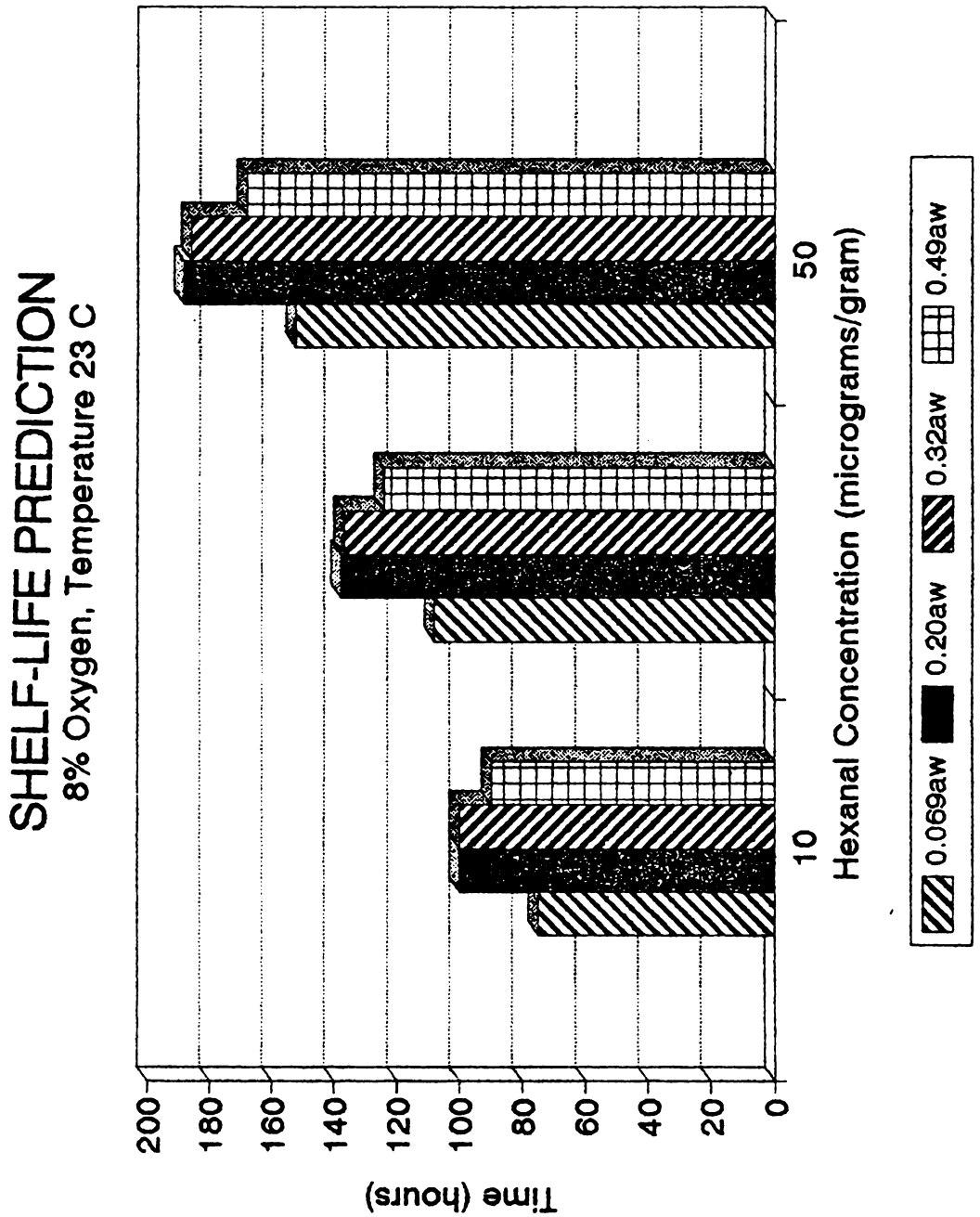

Fig. 34: Predicted Shelf-Life as a Function of Storage Time

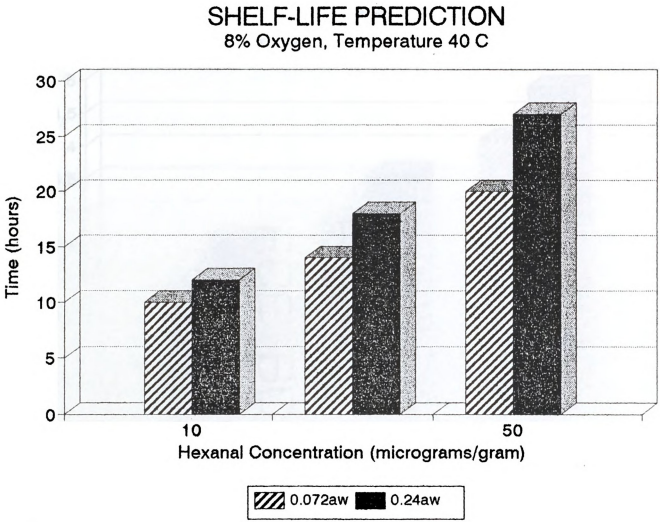

Fig. 35: Predicted Shelf-Life as a Function of Storage Time

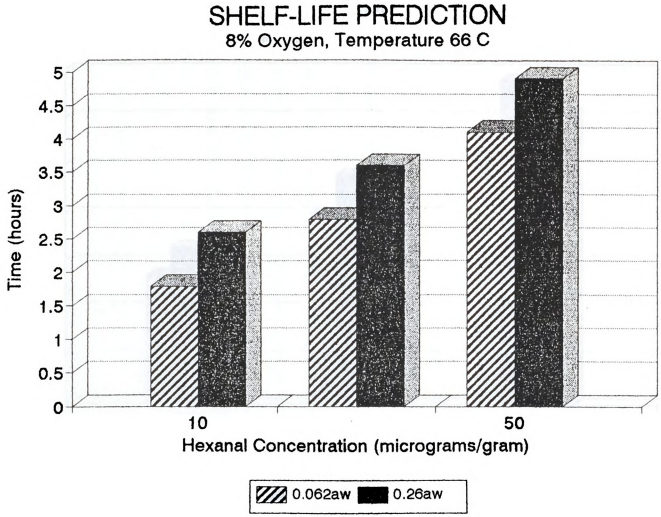

Fig. 36: Predicted Shelf-Life as a Function of Storage Time

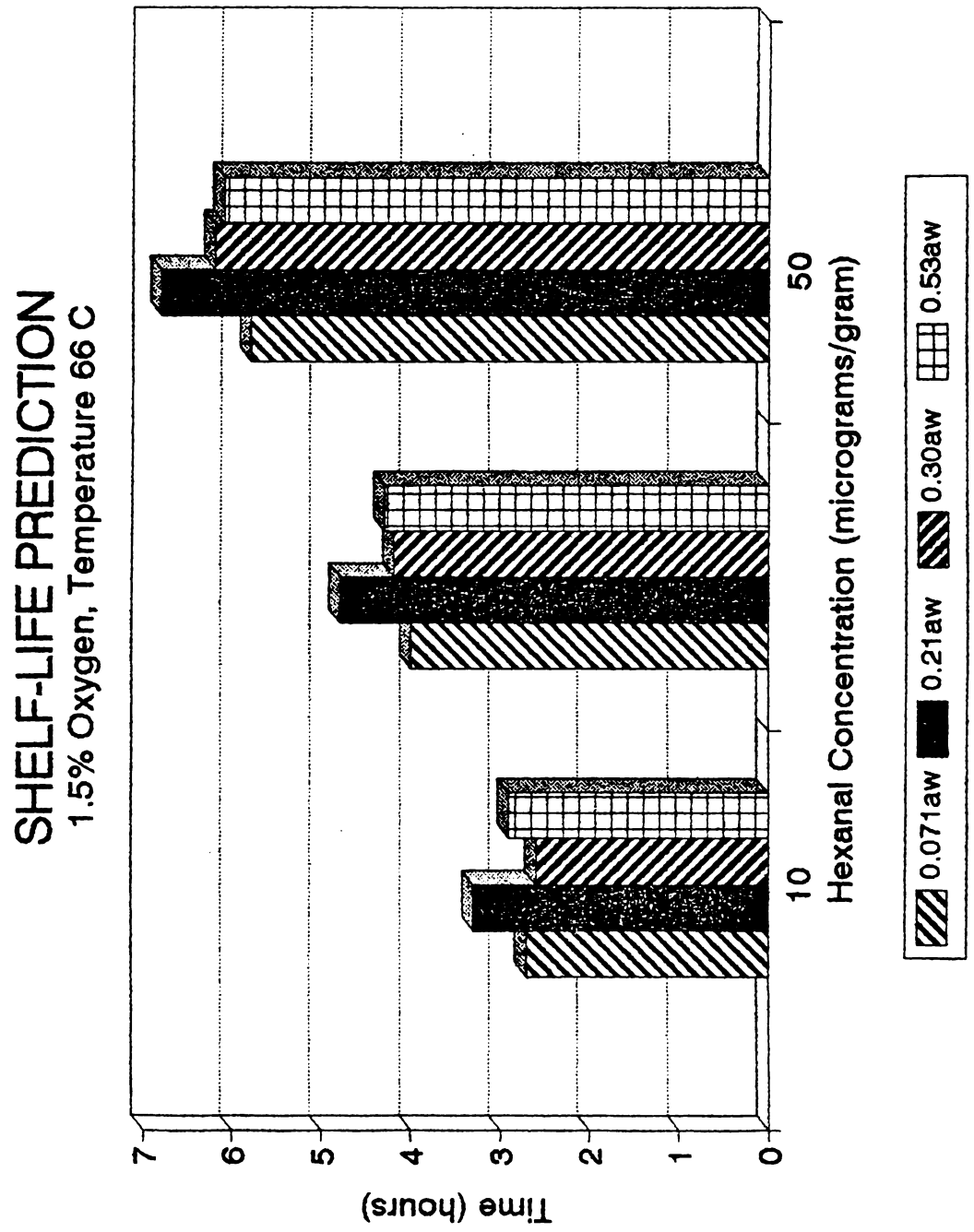

Fig. 37: Predicted Shelf-Life as a Function of Storage Time

Error Analysis

The errors associated with the experiments include both operator and instrumental errors, and are considered normal. Sampling frequencies for experiments at 23°C were rounded to the nearest 30 minutes. Therefore, a 15 minute maximum error is possible. The sampling frequency for experiments run under accelerated conditions of 40 and 66°C were 1 minute, giving minimal error. Error associated with concentrating the volume of extract to a 0.5 or 1 ml sample volume in the centrifuge tube is a result of misreading. Syringe error was a result of misreading the syringe calibrations and manufacturer error. The injection volume into the gas chromatograph could also vary due to leakage through the septa and loss due to evaporation of solvent. Retention time of hexanal could also vary due to carrier gas pressure and any variance between injection time and start time. The error associated with the area response of the integrator was due to the flame ionization detector.

SUMMARY AND CONCLUSIONS

The purpose of this study was to determine the effect of water activity on the rate of lipid oxidation in a model food product system. The product model developed contained linoleic acid as its oxidizing substrate. The system supplied a constant oxygen concentration, temperature, and humidity to the product in the absence of light. Hexanal was used to quantify the extent of lipid oxidation over time. First order reaction kinetics were used to describe the rate of lipid oxidation. Zero order kinetics could not be used due to the exponential rate at which hexanal was produced during the accelerated temperature experiments.

B.E.T. Monolayer Moisture Content

The B.E.T. monolayer value, is described as the moisture content which produces a monolayer coverage of water molecules over the highly reactive sites of the substrate, effectively retarding lipid oxidation. The determination of the monolayer value was imperative to this study, providing a good first estimate of the water content providing maximum stability to a dry product (Fennema, 1985). The B.E.T. monolayer value was calculated to be 6.2189 $gH_2O/100g$ dry product. The corresponding a_w, calculated using the Chen mathematical model which most accurately described the equilibrium sorption isotherm, was 0.22. The experiments in this study were organized in such

a way that water activity values below, above and equal to $0.22a_w$ were tested to determine their effect on the rate of oxidation.

Rate of Lipid Oxidation as a Function of Water Activity

Throughout all experiments, the water activity the product model was exposed to had a significant effect on the rate at which hexanal (micrograms/ gram of linoleic) was produced at constant oxygen concentrations. At low water activities, corresponding to a dry product, the greatest amount of hexanal was produced over time. As the water activity was increased, to a value close to the a_w corresponding to the monolayer value, the amount of hexanal produced over time decreased. The amount of hexanal produced over time again began to increase as water activity was increased above the monolayer value.

The amount of hexanal produced over time was also a function of temperature. As the temperature increased, the amount of hexanal produced over time increased. Experiments conducted at 40°C showed greater amounts of hexanal than experiments conducted at 23°C over the same time period and oxygen concentration of 8%. Experiments conducted at a temperature of 66°C and oxygen concentration of 8%, produced the greatest amount of hexanal over time.

The experimental data figures of hexanal concentration versus time took the shape of an exponential plot and were therefore fitted to a first order rate expression. The

first order equations for each water activity under constant temperature and oxygen concentration conditions described the rate of oxidation.

The experiments conducted at a temperature of 23°C and oxygen concentration of 8%, showed a high rate of oxidation at low water activities. As water activity was increased to near the monolayer value, oxidation decreased. When water activity was increased to a value close to 0.30, there was a slight increase in the rate of reaction, and as water activity increased further, the rate continued to increase. The accelerated experiments at 40 and 66°C for oxygen concentrations of 1.5 and 8%, showed a very similar trend to the experiment performed at 23°C in the rate of oxidation as a function of water activity.

Applicability of Results

There are several factors which determine the shelf-life of a food product containing a high % of oil, such as potato chips, water activity being one of them. Along with water activity, oxygen concentration, extent of oxidation, storage temperature, and light can significantly influence the rate at which lipid oxidation can occur. Significant research has been performed on the rate of lipid oxidation as a function of oxygen concentration (Koelsch, 1989; Labuza, 1971) and extent of oxidation (Quast and Karel, 1972). Various studies have also been aimed at the effect of temperature and light on the rate of oxidation (Jeon and

Bassette, 1984; Hallberg and Lingnert, 1991). These studies have shown that the headspace of a fatty acid food product, such as potato chips, must be flushed with an inert gas to secure any acceptable storage life. Quast and Karel (1972) have found that in a regular-sized package of potato chips, packaged at atmospheric oxygen concentration, the headspace oxygen is enough to cause oxygen uptake in excess of 3000 microliters O_2 STP/g. A significant increase in storage temperature could also increase the rate at which off-flavor or odor compounds are formed. Light can be excluded by packaging.

The results of this study show the significance of water activity and temperature on the rate of lipid oxidation. The water activity corresponding to the monolayer moisture content gave the slowest rate of oxidation for all temperature and oxygen concentration conditions, as compared to the dry product which showed the highest rate. The apparent shelf-life (time to reach 20 micrograms of hexanal/gram of linoleic acid) at a temperature of 23°C and oxygen concentration of 8% was approximately 22% longer for a a_w near the B.E.T. monolayer value (0.20) than for a low a_w (0.069). Temperature has a significant effect as can be seen by the activation energy. A small change in temperature could have a substantial effect on the rate of lipid oxidation. As can be seen by the Arrhenius plot (Figure 29) a good prediction of the rate can be made at any temperature.

In a modern manufacturing process, where meeting production quotas is contingent on line speeds, removing the headspace oxygen to create a vacuum or replacing it with an inert gas (nitrogen) to have a headspace environment in the absence of oxygen is extremely difficult. Usually, the manufacturer settles for an oxygen concentration greater than 1%. However, Tamsma et al. (1971) found that for certain products, even oxygen concentrations lower than 1% can have a marked effect on the quality on the product (Quast and Karel, 1972). By controlling the water activity inside the headspace, the product could be kept at a moisture content relatively close to that of the monolayer moisture content. Thus, if the oxygen concentration of the headspace can be held at an acceptable level, a_w could be a factor in reducing the rate of lipid oxidation, extending product storage life.

The experimental results showing the rate of lipid oxidation at constant a_w, oxygen concentration and temperature conditions could contribute to the future development of mathematical models for storage life prediction of oxygen sensitive products. By knowing product composition, the concentration of volatiles signifying the onset of rancidity, and by monitoring a_w as a function of package parameters and storage environment, and oxygen concentration as a function of processing conditions and the rate at which oxygen is absorbed by the product, the prediction of storage life by mathematical models could be

in the near future. The results of this study could be a valuable step toward extending the shelf-life of fatty acid food products. Future research in determining the effect of water activity on the rate of lipid oxidation at low oxygen concentrations under ambient temperature conditions is needed in order to make further contributions to the development of an accurate model for predicting product shelf-life.

APPENDICES

APPENDIX A
Calibration Data for 3500 Headspace Oxygen Analyzer and Product Model Equilibration Time Data

Table 28
Calibration Data for 3500 Headspace Oxygen Analyzer

Air Flow (ml/min)	Nitrogen Flow (ml/min)	Ratio	Calculated % Oxygen	Reading % Oxygen
60	0	1:0	20.4	20.4
60	60	1:1	10.2	9.89
30	60	1:2	5.1	5.04
20	60	1:3	3.4	3.31
15	60	1:4	2.55	2.55
10	60	1:6	1.7	1.91
5	60	1:12	0.85	1.11
0	60	0:1	0	1.51 ppm

Table 29
Product Model Equilibration Time

Aw	Initial Wt.	10 hours	15 hours	18 hours	24 hours
0.076	0.5380	0.5214	0.5207	0.5203	0.5204
0.43	0.6931	0.7038	0.7184	0.7263	0.7261

(all weights in grams)

APPENDIX B
Gas Chromatographic Calibration Procedure Data

Table 30
Hexanal Calibration Data

Sample	Grams of Hexanal Injected (E-09)	Area Response
1a	2.352	5789
1b	2.352	5622
1c	2.352	5701
Average		5704
2a	5.838	11608
2b	5.838	11688
2c	5.838	12038
Average		11778
3a	11.676	27191
3b	11.676	26456
3c	11.676	25104
Average		26250
4a	23.352	48624
4b	23.352	56379
4c	23.352	57801
Average		54268
5a	58.380	148340
5b	58.380	145310
5c	58.380	146280
Average		146643

Fig. 38: Chromatogram of Hexanal

APPENDIX C
Equilibrium Sorption Isotherm Data and Calculations

Table 31
Equilibrium Sorption Isotherm
($gH_2O/100g$ dry wt. product)

Aw	Dish Wt.	Initial Wt. Pi(-dish)	1st Week (-dish)	2nd Week Pf(-dish)	Moisture Gain(Mg)
0.12	1.3696	2.3254	2.3301	2.3379	0.0125
	1.3718	2.4922	2.4948	2.5031	0.0109
	1.3545	2.7333	2.7338	2.7378	0.0045
0.23	1.3663	3.3109	3.3289	3.3522	0.0413
	1.3328	3.9055	3.9235	3.9459	0.0404
0.31	1.3439	2.0559	2.0559	2.1302	0.0743
	1.3327	2.1303	2.1291	2.2072	0.0769
	1.3388	1.4612	1.4599	1.5116	0.0504
0.40	1.3695	1.8519	1.8745	1.9385	0.0866
	1.3632	1.8218	1.8428	1.9058	0.0840
	1.3248	1.0475	1.0582	1.0942	0.0467
0.50	1.3587	2.4618	2.6154	2.6178	0.1560
	1.3643	2.0941	2.2241	2.2242	0.1303
	1.3564	1.5749	1.6670	1.6664	0.0915
0.63	1.3617	1.6800	1.7938	1.7934	0.1134
	1.3530	2.4125	2.5782	2.5800	0.1675
	1.3582	1.2176	1.2980	1.3027	0.0851
0.82	1.3716	1.8004	1.9637	2.0147	0.2143
	1.3690	1.8132	1.9750	2.0268	0.2136
	1.3669	1.5906	1.7339	1.7700	0.1794

(all weights in grams)

Table 32
Equilibrium Sorption Isotherm
($gH_2O/100g$ dry wt. product)

Aw	Moisture Initial(Mi)	Dry Weight (Pd)	Moisture Total (MT)	EMC ($gH_2O/100g$ dry prdt)	EMC Mean
0.12	0.0991	2.2263	0.1116	5.0127	
	0.1062	2.3860	0.1171	4.9080	4.8480
	0.1165	2.6168	0.1210	4.6232	
0.23	0.1411	3.1698	0.1824	5.7541	5.6429
	0.1664	3.7391	0.2068	5.5317	
0.31	0.0876	1.9683	0.1619	8.2261	
	0.0908	2.0395	0.1677	8.2217	8.1673
	0.0623	1.3989	0.1127	8.0540	
0.40	0.0789	1.7730	0.1655	9.3356	
	0.0776	1.7442	0.1616	9.2673	9.2370
	0.0466	1.0029	0.0913	9.1079	
0.50	0.1049	2.3569	0.2609	11.0701	
	0.0892	2.0049	0.2195	10.9504	10.8467
	0.0671	1.5078	0.1586	10.5197	
0.63	0.0716	1.6084	0.1850	11.5017	
	0.1028	2.3097	0.2703	11.7033	11.6522
	0.0519	1.1657	0.1370	11.7515	
0.82	0.0767	1.7237	0.2910	16.8839	
	0.0773	1.7359	0.2909	16.7558	16.6239
	0.0678	1.5228	0.2472	16.2320	

(all weights in grams)

Table 33
Initial Moisture Content
($gH_2O/100g$ dry wt. product)

Dish Wt.	Initial Wt. Wi (-dish)	Final Wt. Wf (-dish)	% IMC ($gH_2O/100g$ dry prdt)	% IMC Mean
1.3248	2.3830	2.2657	5.1772	
1.3327	1.5517	1.5035	3.2059	4.4512
1.3328	1.5079	1.4365	4.9704	

(all weights in grams)

APPENDIX D
Halsey, Henderson and GAB Data and Mathematical Formulas

Table 34
Linear Regression Data and Linearized Halsey Mathematical Model

Water Activity	x-axis $\ln(M_{eq})$	y-axis $\ln(-\ln(a_w))$
0.82	2.8108	-1.6172
0.63	2.4555	-0.7721
0.5	2.3839	-0.3665
0.4	2.2232	-0.0874
0.31	2.1001	0.1580
0.23	1.7304	0.3850
0.12	1.5786	0.7515

Line Equation: $\ln(-\ln(a_w))=3.6820 - 1.7878(\ln(M_{eq}))$
Correlation Coefficient: 0.927

Table 35
Linear Regression Data and Linearized Henderson Mathematical Model

Water Activity	x-axis $\ln(M_{eq})$	y-axis $\ln(-\ln(1-a_w))$
0.82	2.8108	0.5393
0.63	2.4555	-0.0058
0.5	2.3839	-0.3665
0.4	2.2232	-0.6717
0.31	2.1001	-0.9914
0.23	1.7304	-1.3418
0.12	1.5786	-2.0570

Line Equation: $\ln(-\ln(1-a_w))=-5.0564 + 1.9957(\ln(M_{eq}))$
Correlation Coefficient: 0.969

Table 36
G.A.B. Formula Plot Data and Corresponding 2nd Degree Polynomial Equation

Water Activity	x-axis a_w	y-axis (a_w/M_{eq})
0.82	0.82	0.0493
0.63	0.63	0.0541
0.5	0.5	0.0461
0.4	0.4	0.0433
0.31	0.31	0.0380
0.23	0.23	0.0408
0.12	0.12	0.0248

Polynomial Equation: $a_w/M_{eq}=-0.074a_w^2 + 0.103a_w + 0.015$
Correlation Coefficient: 0.893

APPENDIX E
Experimental Hexanal Data and Calculations at Constant Water Activity, Temperature and Oxygen Concentrations

---

Table 37
Experimental Hexanal Data and Calculations for 8% Oxygen Concentration, 0.069 Water Activity, and 23°C (3.0283 grams of product)

Time (hours)	Sample Volume(ml)	Injection Vol. (microliters)	Area Response (AU)	GC Range
0	---	---	---	---
26	0.5	0.7	16784	2
59	0.5	0.7	17217	2
88.5	0.5	0.7	20365	2
111	0.5	0.7	22162	2
126.5	0.5	0.7	12439	2
156	0.5	0.7	12446	2
173.5	0.5	0.7	26843	2
192	0.5	0.7	37498	2
211	1.0	0.7	73948	2
232	1.0	0.7	83235	4
256	1.5	0.7	70228	4
268	1.5	0.7	66418	4

Time (hours)	Hexanal (grams)	Total Hexanal (grams)	Total Hexanal in Product (micrograms per gram)	Total Hexanal in Linoleic (micrograms per gram)
---	---	---	---	---
26	5.1061E-06	5.1061E-06	1.6861	5.9515
59	5.2378E-06	10.3438E-06	3.4157	12.0566
88.5	6.1955E-06	16.5393E-06	5.4616	19.2780
111	6.7422E-06	23.2815E-06	7.6880	27.1366
126.5	3.7842E-06	27.0657E-06	8.9376	31.5474
156	3.7864E-06	30.8519E-06	10.1879	35.9605
173.5	8.1662E-06	39.0181E-06	12.8845	45.4790
192	11.4077E-06	50.4258E-06	16.6515	58.7756
211	44.9931E-06	95.4189E-06	31.5091	111.2189
232	202.5750E-06	297.9943E-06	98.4031	347.3378
256	256.3780E-06	554.3722E-06	183.0638	606.1683
268	242.4690E-06	796.8410E-06	263.1315	928.7869

Table 38
Experimental Hexanal Data and Calculations for 8% Oxygen Concentration, 0.20 Water Activity, and 23°C (3.2974 grams of product)

Time (hours)	Sample Volume(ml)	Injection Vol. (microliters)	Area Response (AU)	GC Range
0	---	---	---	---
29.5	0.5	0.7	11203	2
55	0.5	0.7	11177	2
87.5	0.5	0.7	13593	2
120	0.5	0.7	9348	2
151	0.5	0.7	14988	2
187	0.5	0.7	33286	2
223	0.5	0.7	110483	2
253	0.5	0.7	179793	2
289	0.5	0.7	610367	2
319	0.5	0.7	1044057	2
341	0.5	0.7	305097	4
367	0.5	0.7	406055	4

Time (hours)	Hexanal (grams)	Total Hexanal (grams)	Total Hexanal in Product (micrograms per gram)	Total Hexanal in Linoleic
---	---			
29.5	3.4082E-06	3.4082E-06	1.03360	3.65229
55	3.4003E-06	6.8084E-06	2.06480	7.29612
87.5	4.1353E-06	10.9438E-06	3.31890	11.7272
120	2.8439E-06	13.7876E-06	4.18136	14.77512
151	4.5597E-06	18.3473E-06	5.56417	19.66137
187	10.1263E-06	28.4736E-06	8.63517	30.51296
223	33.6113E-06	62.0849E-06	18.82844	66.53160
253	54.6969E-06	116.7818E-06	35.41632	125.1460
289	185.6867E-06	302.4685E-06	91.72939	324.1322
319	317.6245E-06	620.0930E-06	188.0551	664.5059
341	371.2678E-06	991.3608E-06	300.6492	1062.365
367	494.1225E-06	1485.4830E-06	450.5014	1591.878

Table 39
Experimental Hexanal Data and Calculations for 8% Oxygen Concentration, 0.32 Water Activity, and 23°C (3.1236 grams of product)

Time (hours)	Sample Volume(ml)	Injection Vol. (microliters)	Area Response (AU)	GC Range
0	---	---	---	---
36	0.5	0.7	12330	2
57	0.5	0.7	5873	2
80.5	0.5	0.7	10474	2
114	0.5	0.7	13870	2
141	0.5	0.7	16237	2
156	0.5	0.7	13180	2
171.5	0.5	0.7	17989	2
180.5	0.5	0.7	11803	2
190	1.0	0.7	6717	2
199	1.0	0.7	23619	2
211.5	1.0	0.7	32231	2
231.5	1.0	0.7	75115	2
251	1.0	0.7	153890	2
279	1.0	0.7	108000	4

Time (hours)	Hexanal (grams)	Total Hexanal (grams)	Total Hexanal in Product (micrograms per gram)	Total Hexanal in Linoleic
---	---	---	---	---
36	3.7511E-06	3.7511E-06	1.2009	4.2278
57	1.7867E-06	5.5377E-06	1.7729	6.2416
80.5	3.1864E-06	8.7242E-06	2.7930	9.8331
114	4.2196E-06	12.9437E-06	4.1438	14.5890
141	4.9396E-06	17.8833E-06	5.7252	20.1564
156	4.0096E-06	21.8929E-06	7.0089	24.6757
171.5	5.4726E-06	27.3655E-06	8.7609	30.8439
180.5	3.5907E-06	30.9563E-06	9.9105	34.8911
190	2.0435E-06	32.9997E-06	10.5647	37.1943
199	7.1854E-06	40.1851E-06	12.8650	45.2930
211.5	19.6107E-06	59.7959E-06	19.1433	67.3964
231.5	45.7032E-06	105.4990E-06	33.7748	118.9088
251	93.6333E-06	199.1323E-06	63.7509	224.4437
279	262.8473E-06	461.9796E-06	147.8997	520.7012

Table 40
Experimental Hexanal Data and Calculations for 8% Oxygen Concentration, 0.49 Water Activity, and 23°C (3.3611 grams of product)

Time (hours)	Sample Volume(ml)	Injection Vol. (microliters)	Area Response (AU)	GC Range
0	---	---	---	---
30	0.5	0.7	7614	2
55	0.5	0.7	11832	2
68.5	0.5	0.7	9917	2
83	0.5	0.7	7309	2
99	0.5	0.7	8311	2
111	0.5	0.7	7407	2
125	0.5	0.7	11972	2
136	0.5	0.7	13255	2
164	0.5	0.7	42695	2
192	0.5	0.7	86673	2
209	0.5	0.7	108110	2
244.5	1.5	0.7	157730	2

Time (hours)	Hexanal (grams)	Total Hexanal (grams)	Total Hexanal in Product (micrograms per gram)	Total Hexanal in Linoleic (micrograms per gram)
---	---	---	---	---
30	2.3163E-06	2.3163E-06	0.6891	2.4280
55	3.6000E-06	5.9159E-06	1.7601	6.2011
68.5	3.0170E-06	8.9329E-06	2.6577	9.3636
83	2.2236E-06	11.1564E-06	3.3162	11.6944
99	2.5284E-06	13.6848E-06	4.0715	14.3448
111	2.2534E-06	15.9382E-06	4.7419	16.7068
125	3.6421E-06	19.5803E-06	5.8256	20.5246
136	4.0325E-06	23.6128E-06	7.0253	24.7515
164.5	12.9887E-06	36.3015E-06	10.8005	38.0521
192	26.3678E-06	62.9693E-06	18.7347	66.0060
209	32.8894E-06	95.8587E-06	28.5200	103.6263
244.5	143.9545E-06	239.8133E-06	71.3497	251.3787

Table 41
Experimental Hexanal Data and Calculations for 8% Oxygen Concentration, 0.072 Water Activity, and 40°C (2.9301 grams of product)

Time (hours)	Sample Volume(ml)	Injection Vol. (microliters)	Area Response (AU)	GC Range
0	---	---	---	---
8.25	1.0	0.7	10854	2
13.58	1.0	0.7	20067	2
15.91	1.0	0.7	3269	4
18.41	1.0	0.7	17096	2
20.41	1.0	0.7	24481	2
21.66	1.0	0.7	21381	2
23.16	1.0	0.7	26591	2
25.83	1.0	0.7	53009	2
32.66	1.0	0.7	52424	4
33.58	1.0	0.7	18440	4
34.33	1.0	0.7	16271	4
36.41	1.0	0.7	51040	4
38.24	1.0	0.7	45734	4
40.57	1.0	0.7	49607	4
42.82	1.0	0.7	59275	4

Time (hours)	Hexanal (grams)	Total Hexanal (grams)	Total Hexanal in Product (micrograms per gram)	Total Hexanal in Linoleic (micrograms per gram)
---	---	---	---	---
8.25	6.6040E-06	6.6040E-06	2.2538	7.9555
13.58	12.2096E-06	18.8136E-06	6.4208	22.6639
15.91	7.9560E-06	26.7696E-06	9.1361	32.2481
18.41	10.4019E-06	37.1715E-06	12.6861	44.7787
20.41	14.8953E-06	52.0245E-06	17.7552	62.6714
21.66	13.0091E-06	65.0336E-06	22.1950	78.3429
23.16	16.1791E-06	81.2127E-06	27.7167	97.8331
25.83	32.2529E-06	113.4656E-06	38.7241	136.6866
32.66	127.5880E-06	241.0536E-06	82.2680	290.3858
33.58	44.8787E-06	285.9323E-06	97.5845	344.4491
34.33	39.5999E-06	325.5322E-06	111.0993	392.1532
36.41	124.2197E-06	449.7519E-06	153.4737	541.7947
38.24	111.3061E-06	561.0580E-06	191.4808	675.8799
40.57	120.7321E-06	681.7901E-06	232.6849	821.3201
42.82	144.2618E-06	826.0519E-06	281.9194	995.1055

Table 42
Experimental Hexanal Data and Calculations for 8% Oxygen Concentration, 0.24 Water Activity, and 40°C (3.2342 grams of product)

Time (hours)	Sample Volume(ml)	Injection Vol. (microliters)	Area Response (AU)	GC Range
0	---	---	---	---
9.25	1.0	0.7	2749	4
13.75	1.0	0.7	3168	4
16.75	1.0	0.7	2649	4
20.5	1.0	0.7	3997	4
23.5	1.0	0.7	4693	4
32.75	1.0	0.7	25743	4
35.75	1.0	0.7	19292	4
41.25	1.0	0.7	41430	4
45.25	1.0	0.7	67413	4
47.5	1.0	0.7	50514	4
56	1.0	0.7	76230	4
58.25	1.0	0.7	74361	4

Time (hours)	Hexanal (grams)	Total Hexanal (grams)	Total Hexanal in Product (micrograms per gram)	Total Hexanal in Linoleic
---	---	---	---	---
9.25	6.6904E-06	6.6904E-06	2.0686	7.3018
13.75	7.7102E-06	14.4006E-06	4.4526	15.7166
16.75	6.4471E-06	20.8477E-06	6.4460	22.7528
20.5	9.7278E-06	30.5755E-06	9.4538	33.3696
23.5	11.4217E-06	41.9972E-06	12.9853	45.8350
32.75	62.6526E-06	104.6498E-06	32.3572	114.2131
35.75	46.9523E-06	151.6021E-06	46.8747	165.4560
41.25	100.8312E-06	252.4333E-06	78.0512	275.5015
45.25	164.0678E-06	416.5010E-06	128.7802	454.5623
47.5	122.9395E-06	539.4405E-06	166.7926	588.7364
56	185.5264E-06	724.9669E-06	224.1565	791.2169
58.25	180.9777E-06	905.9446E-06	280.1140	988.7329

Table 43
Experimental Hexanal Data and Calculations for 8% Oxygen Concentration, 0.062 Water Activity, and 66°C (2.1064 grams of product)

Time (hours)	Sample Volume(ml)	Injection Vol. (microliters)	Area Response (AU)	GC Range
0	---	---	---	---
2.75	1.0	0.7	16454	2
4	1.0	0.7	53685	2
5.17	1.0	0.7	125570	2
6.34	1.0	0.7	182135	2
6.84	1.0	0.7	123510	2
7.34	1.0	0.7	36057	4
7.76	1.0	0.7	37602	4
8.26	1.0	0.7	62029	4
8.76	1.0	0.7	64295	4
9.26	1.0	0.7	89639	4
9.76	1.0	0.7	85505	4
10.51	1.0	0.7	147130	4
11.01	1.0	0.7	68295	4

Time (hours)	Hexanal (grams)	Total Hexanal (grams)	Total Hexanal in Product (micrograms per gram)	Total Hexanal in Linoleic
---	---	---	---	---
2.75	10.0113E-06	10.0113E-06	4.7528	16.7441
4	32.6643E-06	42.6756E-06	20.2600	71.3758
5.17	76.4022E-06	119.079E-06	56.5320	199.1621
6.34	110.8191E-06	229.897E-06	109.1421	384.5070
6.84	75.1488E-06	305.046E-06	144.8186	510.1957
7.34	87.7545E-06	392.800E-06	186.4793	656.9660
7.76	91.5147E-06	484.315E-06	229.9255	810.0268
8.26	150.964E-06	635.279E-06	301.5947	1062.517
8.76	156.479E-06	791.758E-06	375.8821	1324.231
9.26	218.161E-06	1009.919E-06	479.4526	1689.110
9.76	208.0996E-06	1218.019E-06	578.2466	2037.161
10.51	358.081E-06	1576.100E-06	748.2433	2636.059
11.01	166.214E-06	1742.314E-06	827.1527	2914.057

Table 44
Experimental Hexanal Data and Calculations for 8% Oxygen Concentration, 0.26 Water Activity, and 66°C (2.0757 grams of product)

Time (hours)	Sample Volume(ml)	Injection Vol. (microliters)	Area Response (AU)	GC Range
0	---	---	---	---
2.67	1.0	0.7	10247	2
4.34	1.0	0.7	33045	2
5.17	1.0	0.7	7950	4
5.75	1.0	0.7	7441	4
6.25	1.0	0.7	11720	4
6.83	1.0	0.7	15213	4
7.41	1.0	0.7	17432	4
8.24	1.0	0.7	41396	4
8.66	1.0	0.7	24566	4
9.08	1.0	0.7	21333	4
9.5	1.0	0.7	39070	4

Time (hours)	Hexanal (grams)	Total Hexanal (grams)	Total Hexanal in Product (micrograms per gram)	Total Hexanal in Linoleic
---	---	---	---	---
2.67	6.2347E-06	6.2347E-06	3.0037	10.6102
4.34	20.1060E-06	26.3407E-06	12.6900	44.8266
5.17	19.3485E-06	45.6892E-06	22.0115	77.7539
5.75	18.1097E-06	63.7989E-06	30.7361	108.5731
6.25	28.5238E-06	92.3227E-06	44.4779	157.1149
6.83	37.0250E-06	129.348E-06	62.3154	220.1246
7.41	42.4255E-06	171.774E-06	82.7547	292.3252
8.24	100.748E-06	272.522E-06	131.2916	463.7783
8.66	59.7880E-06	332.546E-06	160.2091	565.9272
9.08	51.9197E-06	384.466E-06	185.2223	654.2848
9.5	95.0875E-06	479.553E-06	231.0319	816.1040

Table 45
Experimental Hexanal Data and Calculations for 1.5% Oxygen Concentration, 0.071 Water Activity, and 66°C (2.2195 grams of product)

Time (hours)	Sample Volume(ml)	Injection Vol. (microliters)	Area Response (AU)	GC Range
0	---	---	---	---
4	1.0	0.7	7791	4
6	1.0	0.7	14255	4
6.83	1.0	0.7	11876	4
7.58	1.0	0.7	11263	4
8.25	1.0	0.7	10840	4
9	1.0	0.7	21803	4
9.42	1.0	0.7	9497	4
11.42	1.0	0.7	72880	4
11.75	1.0	0.7	20570	4
12.25	1.0	0.7	34541	4

Time (hours)	Hexanal (grams)	Total Hexanal (grams)	Total Hexanal in Product (micrograms per gram)	Total Hexanal in Linoleic
---	---	---	---	---
4	18.9615E-06	18.9615E-06	8.5431	30.2054
6	34.6934E-06	53.6549E-06	24.1743	85.4713
6.83	28.9035E-06	82.5584E-06	37.1968	131.514
7.58	27.4116E-06	109.970E-06	49.5472	175.180
8.25	26.3821E-06	136.352E-06	61.4337	217.206
9	53.0635E-06	189.416E-06	85.3417	301.736
9.42	23.1135E-06	212.529E-06	95.7554	338.555
11.42	177.373E-06	389.902E-06	175.671	621.107
11.75	50.0627E-06	439.964E-06	198.227	700.855
12.25	84.0649E-06	524.030E-06	236.103	834.771

Table 46
Experimental Hexanal Data and Calculations for 1.5% Oxygen Concentration, 0.21 Water Activity, and 66°C (2.2644 grams of product)

Time (hours)	Sample Volume(ml)	Injection Vol. (microliters)	Area Response (AU)	GC Range
0	---	---	---	---
5	1.0	0.7	18964	2
7	1.0	0.7	59948	2
7.75	1.0	0.7	33680	2
8.42	1.0	0.7	40864	2
8.92	1.0	0.7	45039	2
9.42	1.0	0.7	42364	2
9.92	1.0	0.7	58678	2
10.34	1.0	0.7	64924	2
11.76	1.0	0.7	173160	2
12.26	1.0	0.7	64676	2
12.76	1.0	0.7	92312	2
13.26	1.0	0.7	115058	2
13.84	1.0	0.7	31964	4
14.42	1.0	0.7	24224	4
15	1.0	0.7	37747	4

Time (hours)	Hexanal (grams)	Total Hexanal (grams)	Total Hexanal in Product (micrograms per gram)	Total Hexanal in Linoleic
---	---	---	---	---
5	11.5385E-06	11.5385E-06	5.0956	17.9462
7	36.4749E-06	48.0134E-06	21.2036	74.6766
7.75	20.4924E-06	68.5058E-06	30.2534	106.5490
8.42	24.8632E-06	93.3692E-06	41.2335	145.2197
8.92	27.4037E-06	120.7731E-06	53.3355	187.8416
9.42	25.7761E-06	146.5490E-06	64.7187	227.9317
9.92	35.7022E-06	182.251E-06	80.4853	283.4600
10.34	39.5025E-06	221.754E-06	97.9306	344.9001
11.76	105.3538E-06	327.112E-06	144.4586	508.7663
12.26	39.3517E-06	366.464E-06	161.8371	569.9716
12.76	56.1666E-06	422.631E-06	186.6415	657.3296
13.26	70.2782E-06	492.909E-06	217.6775	766.6350
13.84	77.7931E-06	570.702E-06	252.0323	887.6285
14.42	58.9557E-06	629.658E-06	278.0684	979.3244
15	91.8676E-06	721.526E-06	318.6389	1122.209

Table 47
Experimental Hexanal Data and Calculations for 1.5% Oxygen Concentration, 0.30 Water Activity, and 66°C (3.0376 grams of product)

Time (hours)	Sample Volume(ml)	Injection Vol. (microliters)	Area Response (AU)	GC Range
0	---	---	---	---
4	1.0	0.7	9067	4
6.25	1.0	0.7	21961	4
7.25	1.0	0.7	17445	4
8	1.0	0.7	16758	4
8.5	1.0	0.7	13637	4
9.75	1.0	0.7	20614	4
10.25	1.0	0.7	20619	4
10.83	1.0	0.7	25910	4
11.33	1.0	0.7	27675	4
11.83	1.0	0.7	28782	4
12.58	1.0	0.7	35763	4
13.08	1.0	0.7	31869	4
13.41	1.0	0.7	24862	4

Time (hours)	Hexanal (grams)	Total Hexanal (grams)	Total Hexanal in Product (micrograms per gram)	Total Hexanal in Linoleic
---	---	---	---	---
4	22.0670E-06	22.0670E-06	7.2646	25.6629
6.25	53.4481E-06	75.5151E-06	24.8601	87.8204
7.25	42.4571E-06	117.972E-06	38.8372	137.196
8	40.7851E-06	158.757E-06	52.2642	184.627
8.5	33.1893E-06	191.946E-06	63.1937	223.224
9.75	50.1698E-06	242.116E-06	79.7063	281.569
10.25	50.1819E-06	292.298E-06	96.2266	339.928
10.83	63.0590E-06	355.357E-06	116.986	413.263
11.33	67.3546E-06	422.712E-06	139.160	491.594
11.83	70.0488E-06	492.761E-06	162.221	573.057
12.58	87.0390E-06	579.80E-06	190.874	674.279
13.08	77.5619E-06	657.362E-06	216.408	764.480
13.41	60.5044E-06	717.870E-06	236.328	834.848

Table 48
Experimental Hexanal Data and Calculations for 1.5% Oxygen Concentration, 0.53 Water Activity, and 66°C (2.7387 grams of product)

Time (hours)	Sample Volume(ml)	Injection Vol. (microliters)	Area Response (AU)	GC Range
0	---	---	---	---
4.5	1.0	0.7	47604	2
6.92	1.0	0.7	15744	4
7.59	1.0	0.7	12691	4
7.92	1.0	0.7	10746	4
8.34	1.0	0.7	12716	4
8.76	1.0	0.7	14149	4
9.26	1.0	0.7	21402	4
10.01	1.0	0.7	36765	4
11.76	1.0	0.7	64250	4
12.43	1.0	0.7	50409	4
12.85	1.0	0.7	38337	4

Time (hours)	Hexanal (grams)	Total Hexanal (grams)	Total Hexanal in Product (micrograms per gram)	Total Hexanal in Linoleic
---	---	---	---	---
4.5	28.9643E-06	28.9643E-06	10.5759	37.2362
6.92	38.3173E-06	67.2816E-06	24.5670	86.4965
7.59	30.8870E-06	98.1731E-06	35.8466	126.210
7.92	26.1533E-06	124.3262E-06	45.3960	159.832
8.34	30.9478E-06	155.274E-06	56.6962	199.619
8.76	34.4354E-06	189.709E-06	69.2697	243.888
9.26	52.0876E-06	241.797E-06	88.2890	310.852
10.01	89.4776E-06	331.275E-06	120.961	425.883
11.76	156.3708E-06	487.645E-06	178.057	626.911
12.43	122.6847E-06	610.329E-06	222.854	784.632
12.85	93.3035E-06	703.633E-06	256.922	904.582

APPENDIX F
Percent Recovery Data and Calculations

Table 49
Percent Recovery Data

Sample #	Grams Injected	Area Response
1a	8.34E-06	11103
1b	8.34E-06	11188
1c	8.34E-06	11291

Average Area Response= 11194
Grams of Hexanal Recovered= 6.81E-06
Percent Recovery= 81.7%

2a	16.68E-06	22698
2b	16.68E-06	21830
2c	16.68E-06	22115

Average Area Response= 22214
Grams of Hexanal Recovered= 13.52E-06
Percent Recovery= 81%

3a	3.34E-06	43167
3b	3.34E-06	40015
3c	3.34E-06	45513

Average Area Response= 4290
Grams of Hexanal Recovered=2.61E-06
Percent Recovery= 78.2%

Average Percent Recovery= 80.3%

APPENDIX G
Arrhenius Plot Data

Table 50
Activation Energy Experimental Data

a_w	Rate Constant (b)	(y-axis) ln b	T (°C)	T (°K)	(x-axis) 1/T (°K)
0.069	0.0210172	-3.8624	23	296	0.003378
0.072	0.15033	-1.8949	40	313	0.003194
0.062	0.6980611	-0.3594	66	339	0.002950

E_a =(slope * R)/1000
=(-8071.38 * 1.98 cal/deg-mole)/1000
=15.98 Kcal/mole

Correlation Coefficient =0.977

a_w	Rate Constant (b)	(y-axis) ln b	T (°C)	T (°K)	(x-axis) 1/T (°K)
0.20	0.0183784	-3.9966	23	296	0.003378
0.24	0.112189	-2.1876	40	313	0.003194
0.26	0.6885132	-0.3732	66	339	0.002950

E_a =(slope * R)/1000
=(-8407.59 * 1.98 cal/deg-mole)/1000
=16.65 Kcal/mole

Correlation Coefficient =0.993

LIST OF REFERENCES

1. Aluyah, A.O., Fenton, T.W., Hardin, R.T., and Sim, J.S. (1993). Measuring Lipid Oxidation Volatiles in Meats. J. Food Sci. 58:270.

2. Almeida-Dominguez, N.G., Higuera-Ciapara, I., Goycoolea, F.M., Valencia, M.E. (1992). Package, Temperature and TBHQ Effects on Oxidative Deterioration of Corn-Based Snacks. J. Food Sci. 57:112.

3. Bigalli, G. (1977). Determination of Pentane Formed During Autoxidation of Oils Contained in Solid Samples. J. Amer. Oil Chem. Soc. 54:229.

4. Buckholz, Withcombe, D.A., and Henayk, D. (1980). Application and Characteristics of Polymer Adsorption Method Used to Analyze Flavor Volatiles from Peanuts. J. Agric. Food Chem. 28:760-765.

5. Dokhani, S. (1975). Michigan State University, Department of Food Science and Human Nutrition, M.S. Thesis.

6. Duckworth, R.B. (1981). Solute Mobility in Relation to Water Content and Water Activity, in "Water Activity: Influences on Food Quality" (L.B. Rockland and G.F. Stewart Eds.), Academic Press, New York, pg 295.

7. Duxbury, Dean, (1990). Shelf-life of Snack Foods Optimized by Natural Antioxidant Systems. J. Food Processing 106:51.

8. Fennema, O.R. (1985). "Food Chemistry." Marcel Dekker, Inc., New York, pp 23-68.

9. Fritsch, C.W. and Gale, J.A. (1977). Hexanal as a Measure of Rancidity in Low-Fat Foods. J. Amer. Oil Chem. Soc. 54:225-228.

10. Galt, A.M. and MacLeod, G. (1984). Headspace Sampling of Cooked Beef Aroma Using Tenax GC. J. Agric. Food Chem. 32:59-64.

11. Hall, Anderson, Lingnert and Olofsson (1985). Flavor Changes During Storage: Kinetics of the Formation of Volatile Fat Oxidation Products and Other Volatile Compounds. J. Food Quality 7:153.

12. Hallberg, M.L. and Lingnert, H. (1991). Lipid Oxidation in Potato Slices Under Conditions Simulating the Production of Potato Granules. J. Amer. Oil Chem. Soc. 68:167-170.

13. Jeon, I.S., Bassette, R. (1984). Analysis of n-Pentanal and Hexanal as Indices of Potato Chip Shelf-Life. J. Food Quality 7:97-105.

14. Karel, M. and Yong, S. (1981). Autoxidation-Initiated Reactions in Foods, in "Water Activity: Influences on Food Quality" (L.B. Rockland and G.F. Stewart Eds.), Academic Press, New York, pg 511.

15. Kirk, J. (1981). Influence of Water Activity on Stability of Vitamins in Dehydrated Foods, in "Water Activity: Influences on Food Quality" (L.B. Rockland and G.F. Stewart Eds.), Academic Press, New York, pg 531.

16. Kirloskar, M. (1991). Shelf-Life Prediction of a Packaged Moisture Sensitive Solid Drug Product Over a Range of Temperature and Relative Humidity Values. Michigan State University, School of Packaging, M.S. Thesis.

17. Koelsch, C.M. (1989). A System for the Measurement of the Rate of Lipid Oxidation at Constant Oxygen Concentrations and Relative Humidity. Michigan State University, School of Packaging, M.S. Thesis.

18. Kumor, E.A. (1986). The Characterization and Stability of the Lipids in Oat Cereal. Michigan State University, Dept. of Food Science and Human Nutrition, M.S. Thesis.

19. Labuza, T.P. (1971). Kinetics of Lipid Oxidation. CRC Crit. Reviews in Food Tech. 2:355.

20. Labuza, T.P., Maloney, J.F. and Karel, M. (1966). Autoxidation of Methyl Linoleate in Freeze-Dried Model Systems. 2. Effect of Water on Cobalt-Catalyzed Oxidation. J. Food Sci. 31:885.

21. Labuza, T.P., McNally, L., Gallagher, D., Hawkes, J. and Hurtado, F. (1972). Stability of Intermediate Moisture Foods. 1. Lipid Oxidation. J. Food Sci. 37:154.

22. Labuza, T.P., Heidelbaugh, N.D., Silver, M. and Karel, M. (1971). Oxidation at Intermediate Moisture Contents. J. Amer. Oil Chem. Soc. 48:86.

23. Labuza, T.P., Tannenbaum, S.R. and Karel, M. (1970). Water Content and Stability of Low-Moisture and Intermediate-Moisture Foods. Food Tech. 24:543.

24. Nawar, W.W. (1985). Lipids. In "Food Chemistry" (O.R. Fennema Ed.), Marcell Dekker, New York, pp 139-244.

25. Olafspottir, G., Steinke, J.A., Lindsay, R.C. (1985). Quantitative Performance of a Simple Tenax GC Adsorption Method for Use in the Analysis of Aroma Volatiles. J. Food Sci. 50:1432.

26. Park, P. (1993). Loss of Volatile Lipid Oxidation Products During Thermal Desorption in Dynamic Headspace-Capillary Gas Chromatography. J. Food Sci. 58:220-222.

27. Quast, D. and Karel, M. (1972). Effects of Environmental Factors on the Oxidation of Potato Chips. J. Food Sci. 37:584.

28. Sapers, G.M., Panasuik, Talley, Osman (1972). Flavor Quality and Stability of Potato Flakes (Volatile Components Associated with Storage Changes). J. Food Sci. 37:579.

29. Scholz, R.G. and Ptak, L.R. (1966). A Gas Chromatographic Method for Measuring Rancidity in Vegetable Oils. J. Amer. Oil Chem. Soc. 43:596.

30. Strasburg, G. (1992). Personal Communication.

31. Sugisawa, H. (1981). Sample Preparation: Isolation and Concentration. In "Flavor Research" (K. Teranishi, R.A. Flath and H. Sugisawa Eds.) Marcell Dekker, New York, pg 11.

32. van den Berg, C. and Bruin, S. (1981). Water Activity and Its Estimation in Food Systems: Theoretical Aspects. In "Water Activity: Influences on Food Quality" (L.B. Rockland and G.F. Stewart Eds.), Academic Press, New York, pg 1.

33. Waltking, A.E. and Goetz, A.G. (1990). Instrumental Determination of Flavor Stability of Fats and Fatty Foods and Its Correlation With Sensory Flavor Responses. CRC Critical Reviews in Food Sci. and Nutrition 19(2):99.